

# Synthesis and Stereochemistry of New Naphthoxazine Derivatives

PhD Thesis

Diána Tóth

Supervisor  
Prof. Dr. Ferenc Fülöp



Institute of Pharmaceutical Chemistry, University of Szeged  
Szeged, Hungary  
2010

*Organic chemistry is the child of medicine, and however far it may go  
on its way, with its most important achievements,  
it always returns to its parent.*

**By J.L.W. Thudichum**  
*Journal of the Royal Society of Arts*  
On the Discoveries and Philosophy of Leibig  
Volume 24, 1876 (p. 141)

# CONTENTS

<b>CONTENTS.....</b>	<b>3</b>
<b>PUBLICATIONS .....</b>	<b>4</b>
<b>1. INTRODUCTION AND AIMS.....</b>	<b>6</b>
<b>2. LITERATURE</b>	
<b>Syntheses of aminoquinolinol and aminoisoquinolinol derivatives .....</b>	<b>9</b>
<i>2.1. Syntheses by using aliphatic aldehydes .....</i>	<i>9</i>
<i>2.2. Syntheses by using aromatic aldehydes.....</i>	<i>11</i>
2.2.1. Syntheses by using aromatic aldehydes and ammonia.....	11
2.2.2. Syntheses by using aromatic aldehydes and aliphatic amines.....	12
2.2.3. Syntheses by using aromatic aldehydes and aromatic amines .....	13
2.2.4. Syntheses by using aromatic aldehydes and amides or carbamates .....	17
<b>3. RESULTS AND DISCUSSION .....</b>	<b>19</b>
<i>3.1. Syntheses and ring-chain tautomerism of 1,3-diarylnaphth[1,2-e][1,3]oxazines .....</i>	<i>19</i>
3.1.1. Syntheses of the model compounds .....	19
3.1.2. Study of the ring-chain tautomeric equilibria of 1-alkyl-3-aryl-2,3-dihydro-1H-naphth[1,2-e][1,3]oxazines .....	20
3.1.2.1. Geometry optimalization.....	23
3.1.2.2. Natural bond orbital (NBO) analysis.....	25
3.1.2.3. Shifted carbon chemical shift (SCS) analysis .....	28
<i>3.2. Synthesis and conformational analysis of naphthyl-naphthoxazine derivatives.....</i>	<i>30</i>
3.2.1. Syntheses of the naphthyl-naphthoxazine model system.....	30
3.2.2. Conformational analysis.....	34
3.2.2.1. Compounds with $sp^3$ C-2 or C-3 atoms.....	34
3.2.2.2. Compounds with $sp^2$ C-2 or C-3 atoms.....	37
<i>3.3. Methods .....</i>	<i>39</i>
<b>4. SUMMARY .....</b>	<b>40</b>
<b>5. ACKNOWLEDGEMENTS.....</b>	<b>42</b>
<b>6. REFERENCES.....</b>	<b>43</b>

## PUBLICATIONS

### *Papers related to the thesis*

- I. Diána Tóth, István Szatmári, Ferenc Fülöp  
Substituent Effects in the Ring-Chain Tautomerism of 1-Alkyl-3-arylnaphth-[1,2-*e*][1,3]oxazines  
*Eur. J. Org. Chem.* **2006**, 4664-4669.
- II. István Szatmári, Diána Tóth, Andreas Koch, Matthias Heydenreich, Erich Kleinpeter, Ferenc Fülöp  
Study of the Substituent-influenced Anomeric Effect in the Ring-Chain Tautomerism of 1-Alkyl-3-aryl-naphth[1,2-*e*][1,3]oxazines  
*Eur. J. Org. Chem.* **2006**, 4670-4675.
- III. Diána Tóth, István Szatmári, Andreas Koch, Matthias Heydenreich, Erich Kleinpeter, Ferenc Fülöp  
Synthesis and Conformational Analysis of Naphthoxazine Derivatives  
*J. Mol. Struct.* **2009**, 929, 58-66.

### *Other publications*

- IV. Anita Sztojkov-Ivanov, Diána Tóth, István Szatmári, Ferenc Fülöp, Antal Péter  
High-performance Liquid Chromatographic Enantioseparation of 1-(Aminoalkyl)-2-naphthol Analogs on Polysaccharide-based Chiral Stationary Phases  
*Chirality* **2007**, 374-379.
- V. Attila Papp, Diána Tóth, Árpád Molnár  
Suzuki-Miyaura Coupling on Heterogeneous Palladium Catalysts  
*React. Kinet. Catal. Lett.* **2006**, 87, 335-342.

---

*Conference lectures*

- VI. Diána Tóth, István Szatmári, Ferenc Fülöp  
Substituent Effect in the Ring-Chain Tautomerism of 1-Alkyl-3-aryl-naphth[1,2-*e*]-[1,3]oxazines  
*1<sup>st</sup> BBBB Conference on Pharmaceutical Sciences*  
September 26-28. 2005. Siófok, Book of Abstracts P-52
- VII. Diána Tóth, István Szatmári, Ferenc Fülöp  
Substituent Effect in the Ring-Chain Tautomerism of 1-Alkyl-3-aryl-naphth[1,2-*e*]-[1,3]oxazines  
*13<sup>th</sup> FECHM Conference on Heterocycles in Bioorganic Chemistry*  
May 28-31, 2006. Sopron, Book of Abstracts PO-39
- VIII. Tóth Diána  
Szubsztituenshatás vizsgálata 1-alkil-3-aril-naft[1,2-*e*][1,3]oxazinok gyűrű-lánc tautomériájában  
*A Szegedi Ifjú Kémikusokért Alapítvány Előadóülése*  
Szeged, 2006. január 17.
- IX. Szatmári István, Tóth Diána, Gyémánt Nóra, Molnár József, Peter de Witte, Fülöp Ferenc  
Betti-reakció alkalmazása új, MDR aktív vegyületek szintézisére  
*Gyógyszerkémia és Gyógyszertechnológiai Szimpózium 2006*  
Eger, 2006. szeptember 18-19.
- X. Tóth Diána  
Szubsztituens-indukált anomer hatás tanulmányozása az 1-alkil-3-aril-naft[1,2-*e*]-[1,3]oxazinok gyűrű-lánc tautomériájában  
XXIX. Kémiai Előadói Napok  
Szeged, 2006. október 31.

## 1. INTRODUCTION AND AIMS

The Mannich reaction is one of the most frequently applied multicomponent reactions in organic chemistry.<sup>1,2</sup> One of its special variants is the modified three-component Mannich reaction, in which the electron-rich aromatic compounds are 1- or 2-naphthol. In this recent reaction, the order of the nitrogen sources used (ammonia or amine) largely determines the reaction conditions and the method of isolation of the synthesized Mannich product.<sup>3</sup> One hundred years ago, Mario Betti reported the straightforward synthesis of 1,3-diphenylnaphthoxazine from methanolic ammonia as nitrogen source, benzaldehyde and 2-naphthol in methanol. Acidic hydrolysis of the ring compound produced led to 1-aminobenzyl-2-naphthol. This aminonaphthol became known in the literature as the Betti base, and the protocol as the Betti reaction.<sup>4-6</sup> On the other hand, the use of non-racemic amines has opened up a new area of application of these enantiopure aminonaphthols as chiral catalysts in enantioselective transformations.<sup>3</sup>

The structures and reactivities of numerous five- and six-membered, saturated 1,3-*X,N*-heterocycles (*X* = *O*, *S*, *NR*) can be characterized by the ring-chain tautomeric equilibria of the 1,3-*X,N*-heterocycles and the corresponding Schiff bases. The oxazolidines and tetrahydro-1,3-oxazines are the saturated 1,3-*X,N*-heterocycles whose ring-chain tautomerism has been studied most thoroughly. From quantitative studies on the tautomeric equilibria, it has been concluded that the tautomeric ratios for oxazolidines and tetrahydro-1,3-oxazines bearing a substituted phenyl group at position 2 can be characterized by an aromatic substituent dependence:<sup>7</sup>

$$\log K_X = \rho\sigma^\dagger + \log K_{X=H} \quad (1)$$

where  $K_X$  is the [ring]/[chain] ratio and  $\sigma^\dagger$  is the Hammett–Brown parameter (electronic character) of substituent *X* on the 2-phenyl group.<sup>8</sup>

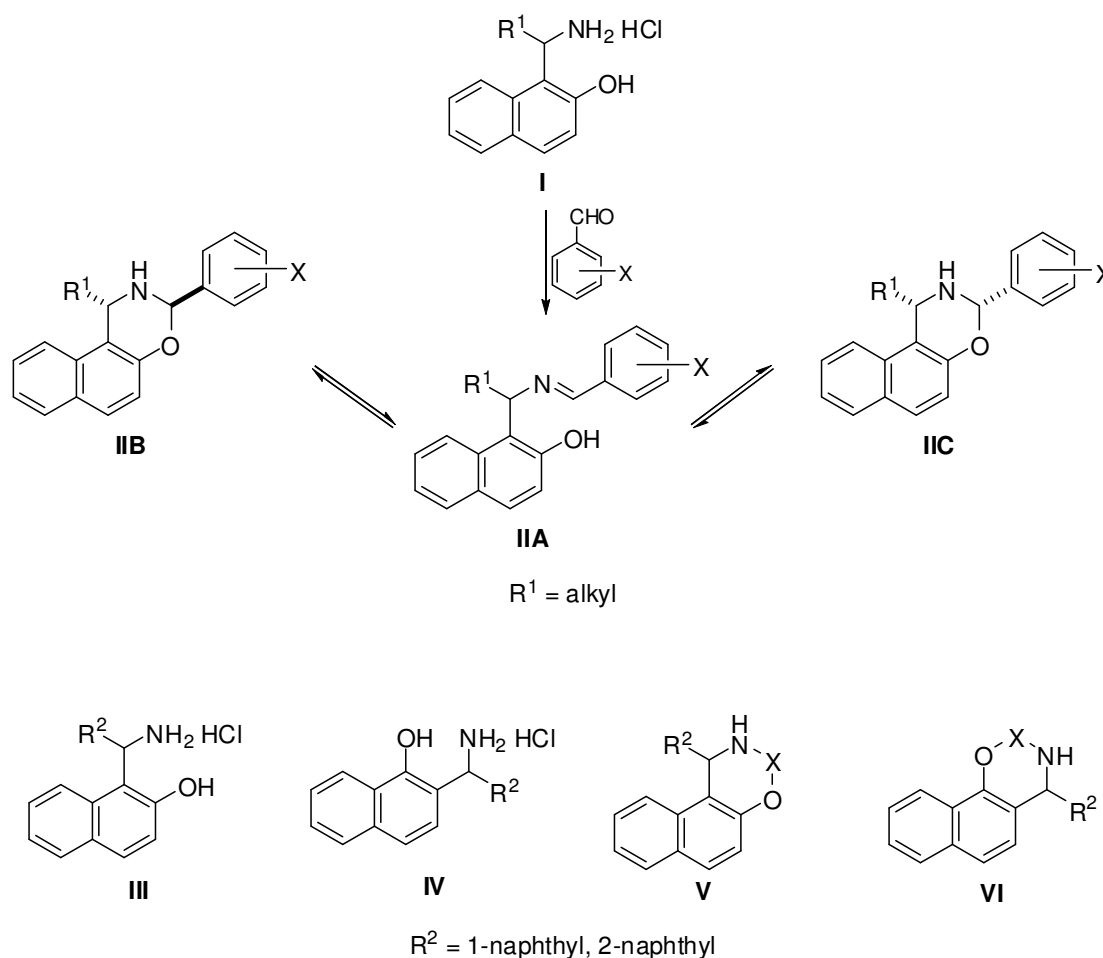
The scope and limitations of Eq. 1 have been thoroughly studied from the aspects of the applicability of this equation in the case of complex tautomeric mixtures containing several types of open and/or cyclic forms, and the influence of the steric and/or electronic effects of substituents at positions other than 2 on the parameters in Eq. 1.<sup>7</sup>

Quantitative investigations on the ring-chain tautomeric equilibria of 1,3-diaryl-2,3-dihydro-1*H*-naphth[1,2-*e*][1,3]oxazines, 2,4-diaryl-2,3-dihydro-1*H*-naphth[2,1-*e*][1,3]oxazines and 3-alkyl,1-aryl-2,3-dihydro-1*H*-naphth[1,2-*e*][1,3]oxazines led to the first precise mathematical formulae with which to characterize the effects of substituents situated other than between the heteroatoms. The additional stabilization effect was explained with the aid of a

substituent-influenced anomeric effect related to the relative configurations of C-1 and C-3<sup>9,10</sup> or C-2 and C-4.<sup>11</sup>

The stereoelectronic effect relating to the relative configurations of C-1 and C-3 or C-2 and C-4 could originate from the aryl substituent at position 1 or 4. There appear to be no published examples of the study of such effects of an alkyl group at the same position of the naphthoxazine model system.

My PhD work focused on the syntheses of 1- $\alpha$ -aminoalkyl-2-naphthol derivatives (**I**) and, by transformation to different substituted 1-alkyl,3-arylnaphthoxazines (**II**), study of the double substituent effects on the ring-chain tautomeric equilibria.



In the literature on the modified Mannich reaction, only a few examples can be found where benzaldehyde is replaced by other aromatic aldehydes. We therefore set out to prepare new primary aminonaphthols from 1- or 2-naphthol and 1- or 2-naphthaldehyde (**III** and **IV**).

While primary aminonaphthols can be easily transformed to heterocyclic compounds,<sup>12,13</sup> our aim was to examine the synthetic applicability of these compounds through simple ring-closure reactions leading to **V** and **VI**. Study of the influence of the substituents newly inserted at

---

position 3 or 2 and the effect of the connecting position of the naphthalene ring on the conformation of **V** and **VI** was also planned.

The synthesis, transformations and applications of aminonaphthol derivatives were earlier reviewed up to 2004.<sup>3</sup> Some technical modifications concerning the chemistry of this type of compounds were recently published, but the variant of the reaction starting from *N*-containing naphthol analogues has not been reviewed. Accordingly, my supervisor advised me to analyse and to review the chemistry of aminoquinolinol and aminoisoquinolinol derivatives, including the syntheses, applications and biological effects.



## 2. LITERATURE

### Syntheses of aminoquinolinol and aminoisoquinolinol derivatives

The quinoline and isoquinoline nuclei are the backbones of numerous natural products and pharmacologically significant compounds displaying a broad range of biological activity.<sup>14,15</sup> Many functionalized quinolines and isoquinolines are widely used as antimalarial, antiasthmatic, or anti-inflammatory agents or antibacterial, antihypertensive and tyrosine kinase PDGF-RTK-inhibiting agents.<sup>16-18</sup> Their analogues containing a hydroxygroup can participate in modified three-component Mannich reactions<sup>19-22</sup> and, as a result of an integrated, virtual database screening, 7-[anilino(phenyl)methyl]-2-methyl-8-quinolinol was found to represent a promising new class of non-peptide inhibitors of the MDM2-p53 interaction.<sup>23</sup>

Naphthoxazinone derivatives have received considerable attention due to the interesting pharmacological properties associated with this heterocyclic scaffold.<sup>24-27</sup> It has been reported that they act as antibacterial agents,<sup>28</sup> while (*S*)-6-chloro-4-cyclopropylethynyl-1,4-dihydro-4-trifluoromethyl-2*H*-[3,1]benzoxazin-2-one (Efavirenz Sustiva), or a benzoxazinone derivative, is a non-nucleoside reverse transcriptase inhibitor that was approved by the FDA in 1998 and is currently in clinical use for the treatment of AIDS.<sup>29</sup>

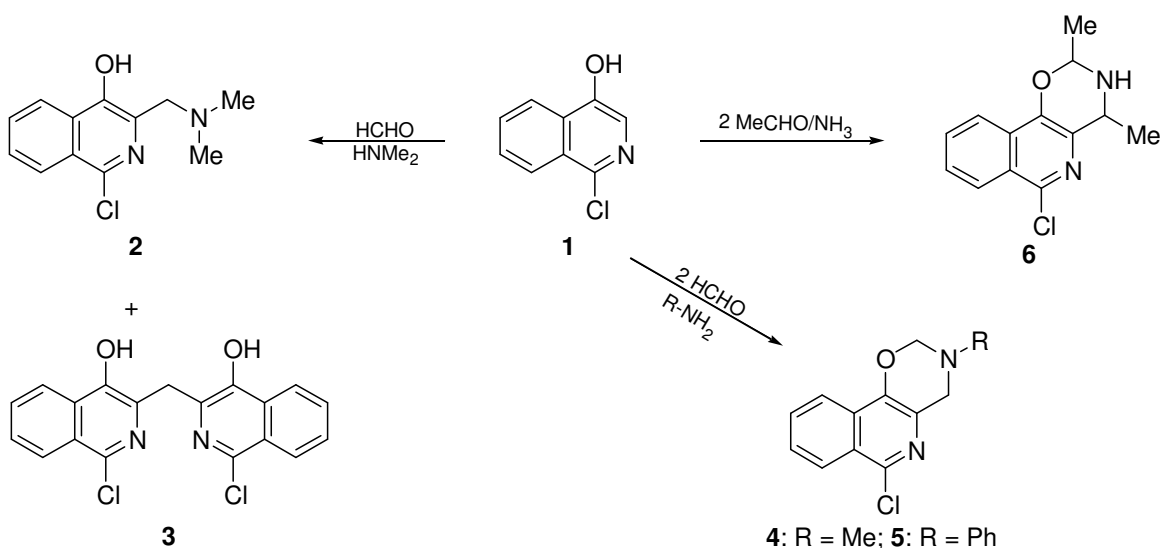
In this framework, the literature on the synthesis and transformations of aminoquinolinol and aminoisoquinolinol derivatives will be reviewed. The topics will be divided with regard to the type of aldehyde (aliphatic and aromatic) and then to the nitrogen sources used.

#### 2.1. Syntheses by using aliphatic aldehydes

The reaction of **1** with dimethylamine in the presence of formaldehyde led to the Mannich base **2**, together with the by-product **3**. The results and the analytical data demonstrated that **3** is 1,1'-dichloro-3,3'-methylenedi-4-isoquinolinol.

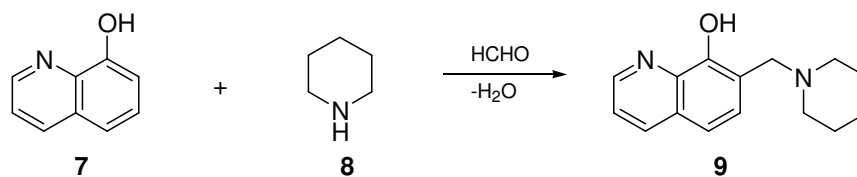
On the use of primary amines with two equivalents of formaldehyde, the Mannich bases formed underwent cyclization, leading to **4** and **5**.

The reaction of **1** with 2 equivalents of acetaldehyde and ammonia in benzene under reflux led to the formation of a colourless product, 6-chloro-3,4-dihydro-2,4-dimethyl-2*H*-1,3-oxazino[5,6-*c*]isoquinoline (**7**) in good yield.<sup>30</sup>



Scheme 1

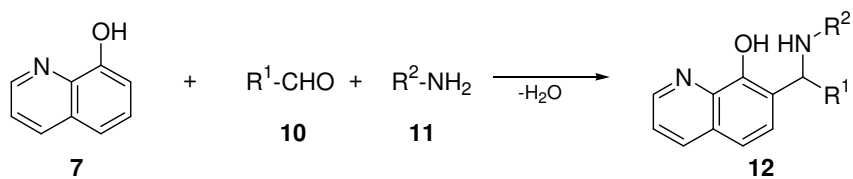
Möhrle *et al.* successfully applied this modified three-component Mannich reaction to prepare **9** (Scheme 2) from 8-quinolinol (**7**), formaldehyde and piperidine (**8**) as a cyclic secondary amine.<sup>31</sup>



Scheme 2

The Mannich reactions of substituted anilines, benzaldehyde and 8-quinolinol yielded 7- $\alpha$ -anilinobenzyl-8-quinolinol derivatives.<sup>32,33</sup> The simplicity of this three-component reaction led to the combination of aliphatic aldehydes (**10**) and aromatic amines (**11**) to obtain 7-anilinoalkyl-8-quinolinols (Scheme 3; **12a,b**).<sup>20,34,35</sup>

Goyal *et al.* extended the Mannich aminoalkylation of 8-quinolinol by using sulphonamides,<sup>36</sup> which are drugs of established therapeutic importance. The reactions of **7** with substituted sulphonamides (**11**) in the presence of acetaldehyde led to 7-substituted-8-hydroxyquinolines (Scheme 3; **12c-f**).<sup>37</sup>



Compounds	$R^1$	$R^2$	References
<b>12a</b>	$n\text{-C}_6\text{H}_{13}$		35
<b>12b</b>	$n\text{Pr}$		34
<b>12c</b>	Me		37
<b>12d</b>	Me		37
<b>12e</b>	Me		37
<b>12f</b>	Me		37

Scheme 3

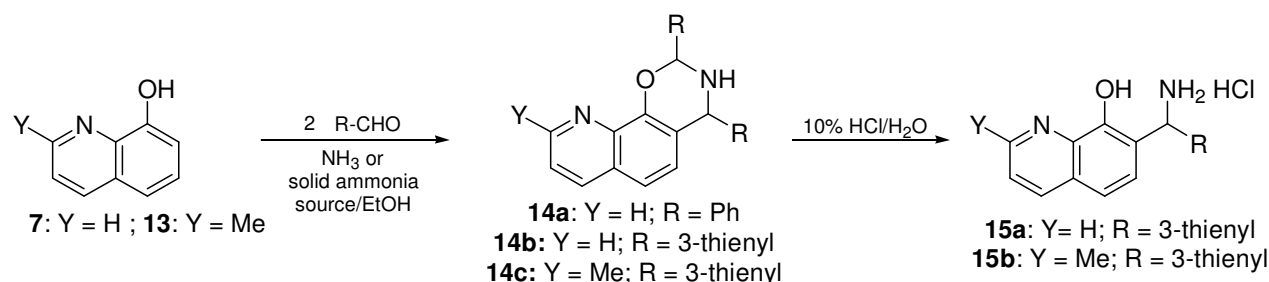
## 2.2. Syntheses by using aromatic aldehydes

Due to the relatively high diversity of this topic, this section will be organized with regard to the order of the nitrogen source.

### 2.2.1. Syntheses by using aromatic aldehydes and ammonia

The application of ammonia as nitrogen source with benzaldehyde and 2-naphthol to prepare 1- $\alpha$ -aminobenzyl-2-naphthol (the Betti base) was first introduced by Betti. When this classical procedure was applied for the aminoalkylation of **7**, **14a** was prepared (Scheme 4).<sup>38</sup>

As a new approach, ammonium acetate was tested as a green solid ammonium source and as a possible replacement for ethanolic ammonia solution (Scheme 4). The reactants were *N*-containing naphthol analogues (**7** and **13**), 3-thiophenecarboxaldehyde and solid ammonia sources. The ammonia sources yielded **15**, but the isolation of **14** required an aqueous work-up, which destroyed the rapidity and one-pot handling of the reaction. Similar reaction results were obtained with several equivalents of ammonium carbamate (Scheme 4).<sup>39</sup>

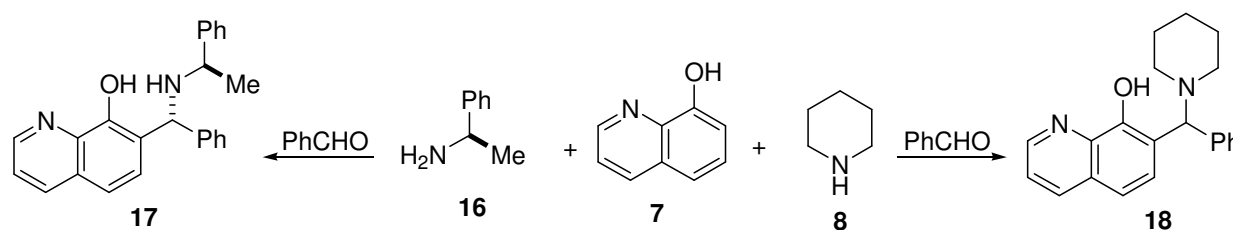


**Scheme 4**

### 2.2.2. Syntheses by using aromatic aldehydes and aliphatic amines

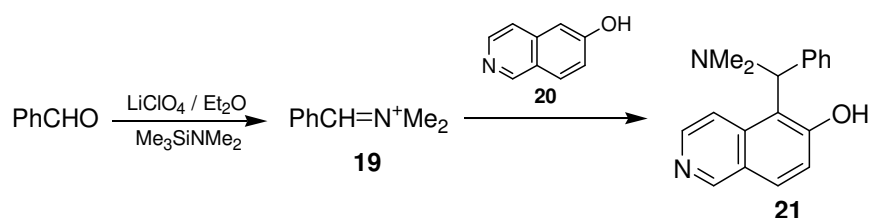
Electron-rich aromatic compounds such as 2-naphthol undergo 1-aminoalkylation in high yields (93%) with high diastereomeric ratios (d.r. = 99) when treated with (*R*)-1-phenylethylamine (**16**) and aromatic aldehydes.<sup>40</sup> The less reactive 8-quinolinol (**7**) gave **17** in moderate yield (44%) and with poor d.r. (1.4). The reaction was performed under solvent-free conditions: a mixture of 8-quinolinol, (*R*)-1-phenylethylamine and benzaldehyde, in a molar ratio of 1.0:1.05:1.2, was stirred and heated at 60 °C for the time required, under an inert atmosphere (Scheme 5).<sup>40</sup>

8-Quinolinol (**7**) has been reacted with piperidine as cyclic secondary amine in the presence of benzaldehyde, leading to **18** in good yield (Scheme 5).<sup>31</sup>



**Scheme 5**

The aminomethylation of electron-rich aromatic compounds under solvent-free conditions and the lithium perchlorate-mediated, one-pot, three-component aminoalkylation of aldehydes have been reported for the preparation of a variety of amines and aminoesters, and also functionalized alkylamines.<sup>41-44</sup> The preparation and purification of iminium salts in a separate step, and their hygroscopicity and susceptibility to hydrolysis (with the exception of Eschenmoser's salts),<sup>45</sup> led to the development of an alternative method for the aminoalkylation of electron-rich aromatic compounds. In continuation of the work on the lithium perchlorate-mediated aminoalkylation reaction,<sup>46-48</sup> Naimi-Jamal *et al.* described an efficient three-component and one-pot method for the aminoalkylation of electron-rich aromatic compounds, using aldehydes and (trimethylsilyl)dialkylamines. Among such compounds ( $\alpha$ - or  $\beta$ -naphthol, indole, *N*-methylindole and coumarin), 6-hydroxyisoquinoline, at room temperature in a concentrated solution of lithium perchlorate in diethyl ether, gave **21** in good yield (Scheme 6).<sup>49</sup>



**Scheme 6**

### 2.2.3. Syntheses by using aromatic aldehydes and aromatic amines

The Mannich aminoalkylation of 8-quinolinol (**7**) with aniline and benzaldehyde, yielding 7- $\alpha$ -anilinobenzyl-8-quinolinol (Scheme 7, Entry 1), was reported by Betti.<sup>32,33</sup> The reaction was extended to substituted aniline derivatives and to aromatic aldehydes, as depicted in Scheme 7, Entries 2-27.<sup>35,50-52</sup>

Hamachi *et al.* carried out the addition of 8-quinolinol to the Schiff base formed from 2-pyridinecarboxaldehyde and different substituted aniline derivatives (Scheme 7, Entries 28-36). The procedure is very simple: an ethanolic solution of equivalent amounts of Schiff base and 8-quinolinol is allowed to stand at room temperature, leading to the desired 7-substituted quinolinol in good to excellent yield.<sup>53</sup>

8-Quinolinol (**7**) and its derivative **13** have been reported to be bactericides<sup>54</sup> and fungicides.<sup>55</sup> Esters of *p*-aminobenzoic acid are also known for their antibacterial activity.<sup>56</sup> On this basis, three new 7-( $\alpha$ -anilinobenzyl)-8-quinolinol derivatives (Scheme 7, Entries 37-39)

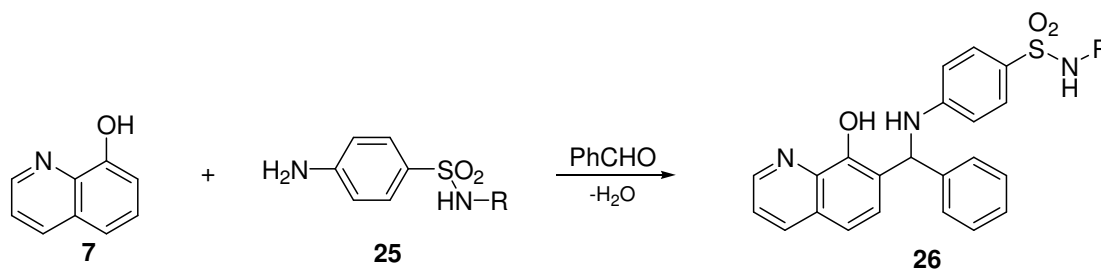
have been synthesized from 8-quinolinol, benzaldehyde and anthranilic acid or ethyl anthranilate.<sup>50</sup> The reaction was extended by Thaker *et al.* by using a series of anthranilic acid esters substituted aromatic aldehydes (Scheme 7, Entries 40-53).<sup>57</sup>

<p>7: Y = H; 13: Y = Me      22      23      24</p>				
Entry	Y	R <sup>1</sup>	R <sup>2</sup>	References
1	H	H	Ph	32-34, 50, 51
2	H	4-Cl	Ph	35
3	H	3-Et	Ph	35
4	H	2-Cl	Ph	35
5	H	3-NO <sub>2</sub>	Ph	35
6	H	H	4- <i>i</i> Pr-Ph	51
7	H	4-NO <sub>2</sub>	3-OH-Ph	35
8	H	2-Cl	3-OH-Ph	35
9	H	3-Cl	3-OH-Ph	35
10	H	2-CH <sub>3</sub>	3-OH-Ph	35
11	H	4-NO <sub>2</sub>	6-Br-3-OH-Ph	35
12	H	4-Cl-2-NO <sub>2</sub>	2-OH-Ph	35
13	Me	H	Ph	51
14	Me	2-COOEt	Ph	51
15	H	H	4-MeO-Ph	34
16	H	2-Me	Ph	34
17	H	4-Me	Ph	34
18	H	2-OMe	Ph	34
19	H	3-Cl	Ph	34
20	H	2-NO <sub>2</sub>	Ph	34
21	H	4-NO <sub>2</sub>	Ph	34
22	Me	4-NO <sub>2</sub>	Ph	34, 52
23	H	4-NO <sub>2</sub>	2-furyl	34
24	Me	2-OMe	Ph	52
25	Me	4-NO <sub>2</sub>	3-OH-Ph	52
26	Me	4-NO <sub>2</sub>	2-furyl	52
27	H	3-NO <sub>2</sub>	2-furyl	52
28	H	H	2-Py	53
29	H	2-Me	2-Py	53
30	H	4-Me	2-Py	53
31	H	2-OMe	2-Py	53
32	H	4-OMe	2-Py	53
33	H	2-OEt	2-Py	53
34	H	4-OEt	2-Py	53
35	H	2-Cl	2-Py	53
36	H	4-Cl	2-Py	53
37	H	2-COOH	Ph	50
38	H	2-COOEt	Ph	50

39	H	4-COOH	Ph	50
40	H	4-COOEt	Ph	57
41	H	4-COO- <i>n</i> Pr	Ph	57
42	H	4-COO- <i>n</i> Bu	Ph	57
43	H	4-COOEt	4-MeO-Ph	57
44	H	4-COO- <i>n</i> Pr	4-MeO-Ph	57
45	H	4-COOEt	3-NO <sub>2</sub> -Ph	57
46	H	4-COO- <i>n</i> Pr	3-NO <sub>2</sub> -Ph	57
47	H	4-COOEt	3-MeO-4-OH-Ph	57
48	H	4-COO- <i>n</i> Pr	3-MeO-4-OH-Ph	57
49	H	4-COO- <i>n</i> Bu	3-MeO-4-OH-Ph	57
50	H	4-COOEt	5-Br-3-MeO-4-OH-Ph	57
51	H	4-COOEt	3-furyl	57
52	H	4-COO- <i>n</i> Pr	3-furyl	57
53	H	4-COO- <i>n</i> Bu	3-furyl	57

Scheme 7

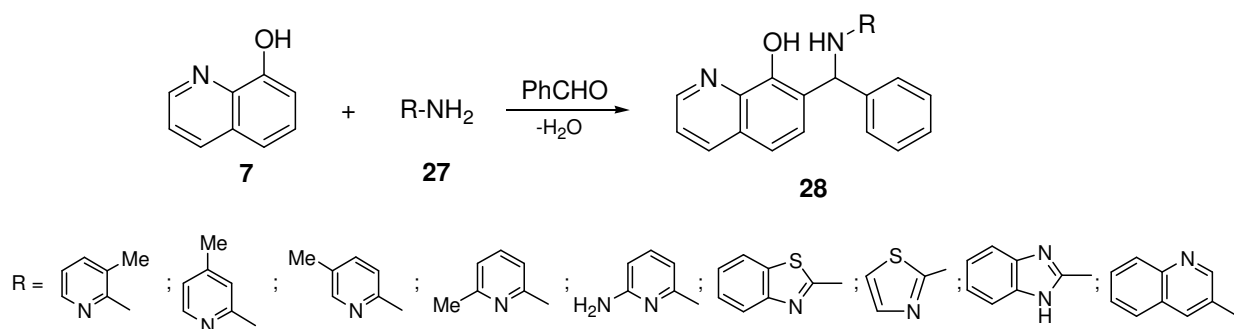
Sulphonamides **25** are special substituted aniline derivatives of established therapeutic importance. When they react with 8-quinolinol in the presence of benzaldehyde, 7-substituted-8-hydroxyquinolines (**26**) are obtained (Scheme 8). The *in vitro* efficacy of the compounds produced (**12c-f** and **26**) against *Escherichia coli*, *Vibria cholerae*, *Achromobacter hydrophilis*, *Proteus mirabilis*, *Klebsiella pneumoniae*, *Salmonella typhi*, *Plesiomonas schigellaides*, *Proteus vulgaris*, *Citrobacter* and *C. ovis* has been studied.<sup>37</sup>



R = 2-pyrimidinyl, 2,6-di-OMe-4-pyrimidinyl, 4,6-di-Me-2-pyrimidinyl, 2,6-di-Me-4-pyrimidinyl

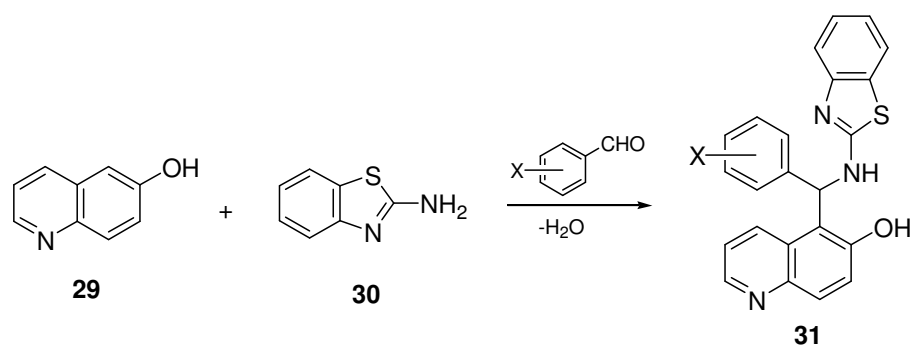
Scheme 8

The reaction of **7**, benzaldehyde and aniline has been extended to other aromatic amines,<sup>34</sup> such as 2-amino-3-methylpyridine, 2-amino-4-methylpyridine, 2-amino-5-methylpyridine, 2-amino-6-methylpyridine, 2,6-diaminopyridine, 2-aminobenzothiazole, 2-aminothiazole, 2-aminobenzimidazole and 3-aminoquinoline, leading to **28** (Scheme 9). It is interesting to note that 2,6-diaminopyridine appeared to react at only one amino group.<sup>20</sup> The compounds were synthesized for their potential usefulness as analytical reagents and for possible amoebicidal activity.



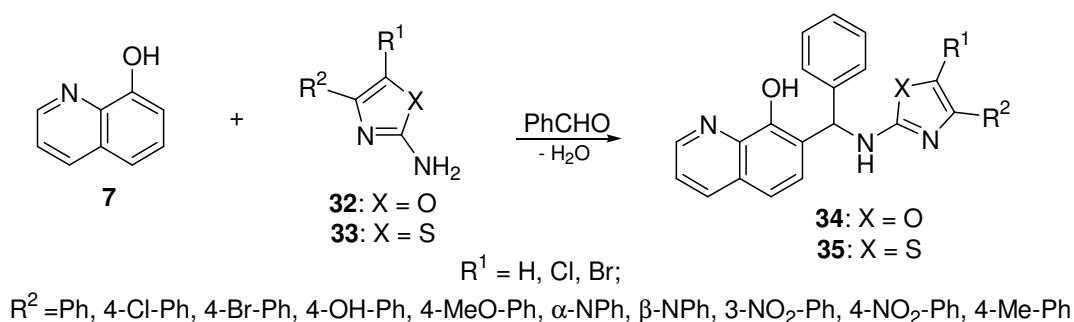
Scheme 9

Shaabani *et al.* reported an efficient and environmentally friendly approach for the synthesis of 5-(2'-aminobenzothiazolomethyl)-6-hydroxyquinolines (Scheme 10; **31**) via the condensation of a substituted benzaldehyde, 6-quinolinol (**29**) and 2-aminobenzothiazole (**30**), with water as the solvent. On the use of ionic solutes such as LiCl, NaCl, NaNO<sub>3</sub>, Na<sub>2</sub>SO<sub>4</sub>, LiNO<sub>3</sub> or LiSO<sub>4</sub>, the yield of the reaction improved.<sup>58</sup>



Scheme 10

The reactions of **8** with different substituted oxazole (**32**) and thiazole (**33**) derivatives in the presence of benzaldehyde led to the Mannich bases **34** and **35**, as depicted in Scheme 11.<sup>21</sup> Compounds **34** and **35** were screened for their fungicidal activity against *Pyricularia oryzae* (Cav) and for antibacterial activity against *Esch. coli* and *Staph. aureus* by usual methods.<sup>21</sup>

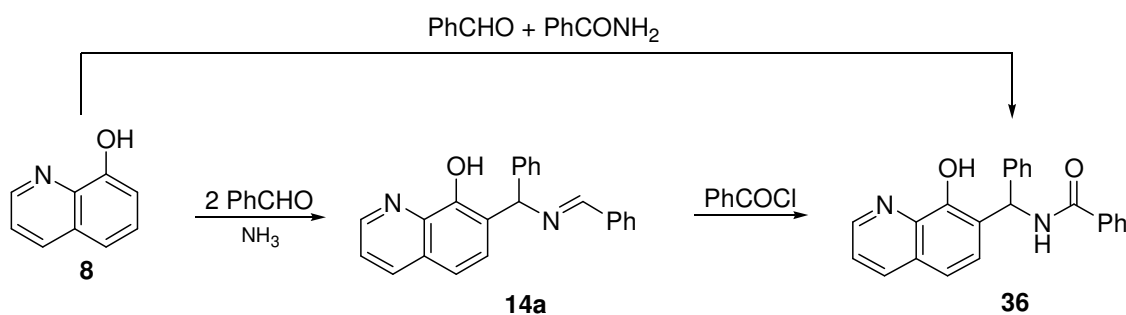


Scheme 11



Almost all the compounds displayed promising antifungal and antibacterial activities. It has been observed that the introduction of a halogen atom on C-5 of either a thiazole or an oxazole moiety augments the activity. Chloro derivatives were found to be more active than bromo derivatives. Substituents on C-4 of the thiazole or oxazole nucleus contributed towards the fungicidal activity in the following sequence: chlorophenyl  $\geq$  bromophenyl > naphthyl > nitrophenyl. Both pathogenic bacteria proved equally sensitive towards the compounds at 100 ppm. It has also been observed that, in general, substituted thiazolyl compounds are slightly more active than substituted oxazolyl ones.<sup>21</sup>

#### 2.2.4. Syntheses by using aromatic aldehydes and amides or carbamates



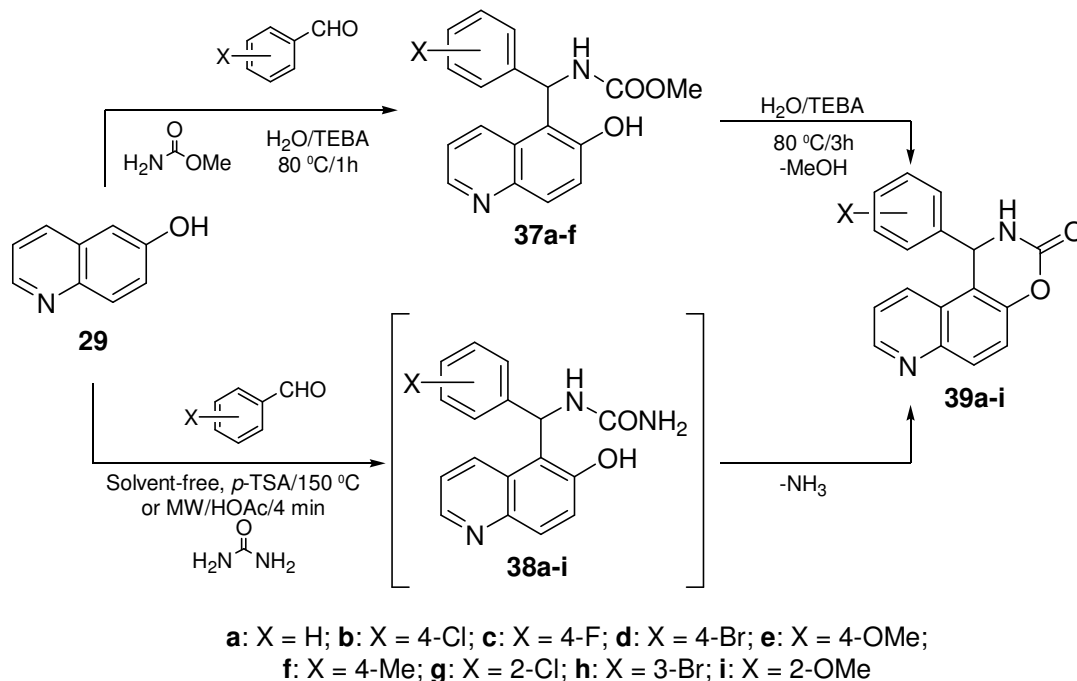
Scheme 12

The Möhrle research group introduced an amide instead of ammonia as nitrogen source to synthesize **36** from **7**, benzaldehyde and benzamide. It is interesting to note that milder reaction conditions were needed for the synthesis of **36** through acylation of the intermediate Schiff base **14a** (Scheme 12).<sup>38</sup> It is known from the literature that the  $\alpha$ -naphthol analogue of **14a** in CDCl<sub>3</sub> at 300 K contained the two epimeric forms (*trans* and *cis*) in a quality of ~ 22-22% besides the Schiff base in 56%.<sup>11</sup> In contrast with this, the structure of **14a** (Scheme 12) was described by Möhrle as the Schiff base, based on the <sup>1</sup>H NMR spectra.

Mosslemin *et al.* reported an efficient one-pot synthesis for the preparation of 1,2-dihydro-1-aryl[1,3]oxazino[5,6-*f*]quinolin-3-one derivatives (**39a-f**) in three-component cyclocondensation reactions of 6-quinolinol (**29**), aromatic aldehydes and methyl carbamate in aqueous media. In the case X = H (**39a**), the intermediate carbamatonaphthol **37a** was isolated, characterized and transformed by further heating to **39a** (Scheme 13).<sup>59</sup>

The syntheses of **39a-i** from **29**, aryl aldehyde and urea were achieved by Bazgir *et al.* It was proposed that **39a-i** were formed from the intermediate carbamatisoquinolinol **38a-i**

following the loss of one mole of ammonia. The reactions were carried out with a catalytic amount of *p*-toluenesulphonic acid (*p*-TSA) at 150 °C under solvent-free conditions or by microwave (MW) irradiation (Scheme 13).<sup>60</sup>



**Scheme 13**

Comparison the reactivities of quinolinols or isoquinolinols with those of the corresponding  $\alpha$ - or  $\beta$ -naphthol analogs with regard to the reaction conditions and yields allows the conclusion that quinolinols and isoquinolinols are weaker C-H acids than naphthols.

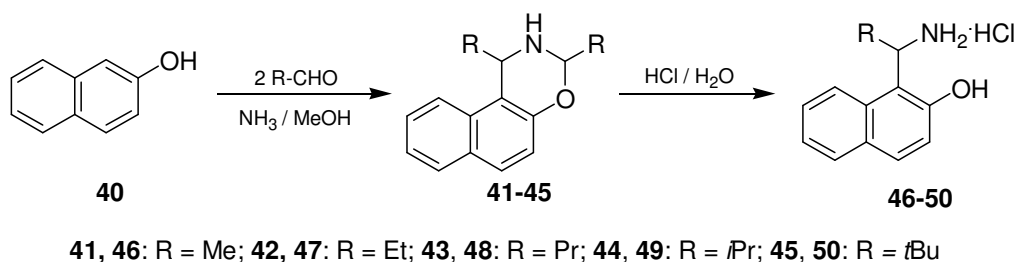
The reaction product of a primary aminonaphthol analog and benzaldehyde in CDCl<sub>3</sub> at 300 K has been reported to be a three-component tautomeric mixture containing the two epimeric naphthoxazine forms (*trans* and *cis*) besides the Schiff base. In contrast with this, the structure of its *N*-containing analogue has been described as the Schiff base, based on the <sup>1</sup>H NMR spectra.

### 3. RESULTS AND DISCUSSION

#### 3.1. Syntheses and ring-chain tautomerism of 1,3-diarylnaphth[1,2-e][1,3]oxazines

##### 3.1.1. Syntheses of the model compounds

In our experiments, naphthoxazines **41-45** were formed by the condensation of 2-naphthol **40** and the corresponding aliphatic aldehyde in the presence of methanolic ammonia solution in absolute methanol at 60 °C for 6–72 h (Scheme 14). The acidic hydrolysis of **41-45** led to the desired aminonaphthol hydrochlorides **46-50** in low yields in a two-step process. The overall yield was improved considerably when the solvent was evaporated off after the formation of the intermediate naphthoxazines **41-45** and the residue was directly hydrolysed with hydrochloric acid (*e.g.* for **46** the overall yield could be increased from 15% to 95%).

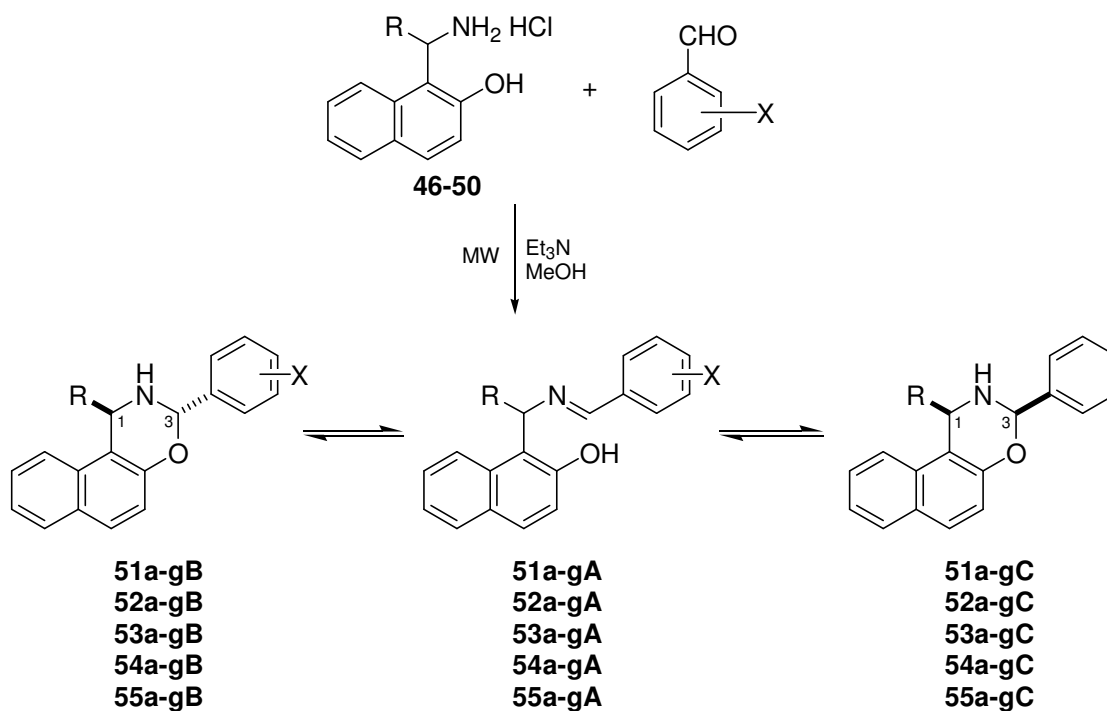


Scheme 14

Because of the instability of **46-50**, they were isolated as hydrochlorides, which in subsequent transformations were basified *in situ* with triethylamine. The condensation of aminonaphthols **46-50** with one equivalent of aromatic aldehyde in absolute methanol in the presence of triethylamine at ambient temperature did not lead to the formation of the desired naphthoxazines. By heating under microwave conditions,<sup>61</sup> **51-55** were successfully prepared. The isolation protocol involved the use of controlled microwave agitation (CEM microwave reactor, 10 min at 80 °C), after which the mixture was left to stand at room temperature until crystals had formed.

### 3.1.2. Study of the ring-chain tautomeric equilibria of 1-alkyl-3-aryl-2,3-dihydro-1H-naphth[1,2-e][1,3]oxazines

The  $^1\text{H}$  NMR spectra of **51-54** revealed that, in  $\text{CDCl}_3$  solution at 300 K, the members **a-g** of each set of compounds **51-54** existed in three-component ring-chain tautomeric mixtures, containing the C-3 epimeric naphthoxazines (**B** and **C**) and also the open tautomer (**A**). The proportion of the ring forms decreased as the alkyl substituent at position 1 became more bulky. Accordingly, for some 1-*i*-propyl-3-arylnaphthoxazine derivatives **54**, the proportions of the ring forms (**B** and **C**) were comparable with the limiting error and in the case of **55**, only the derivatives **55a**, **55e** and **55f** were synthesized. As expected, ring forms **B** and **C** of compounds **55** were not found at all in the tautomeric mixture. In order to acquire reliable results, more sample data were needed and the series of compounds was therefore expanded to include naphthoxazines **57**. The tautomeric behaviour of analogues **57a**, **d-g** was known from the literature, but compounds **57b**, **d-g** were absent and were synthesized according to Scheme 16.<sup>9</sup>



46, 51: R = Me; 47, 52: R = Et; 48, 53: R = Pr; 49, 54: R = *i*Pr; 50, 55: R = *t*Bu  
 a: X = *p*-NO<sub>2</sub>; b: X = *m*-Cl; c: X = *p*-Br; d: X = *p*-Cl; e: X = H; f: X = *p*-Me; g: X = *p*-OMe

**Scheme 15**

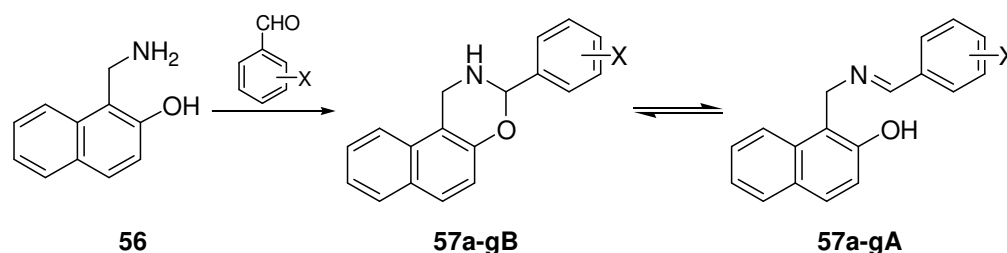
Table 1 shows the proportions of the diastereomeric ring forms (**B** and **C**) from the tautomeric equilibria of **51-55** and **57**, which were determined by integration of the well-

separated O-CHAr-N (ring) and N=CHAr (chain) proton signals in the  $^1\text{H}$  NMR spectra. As a consequence of the very similar NMR spectroscopic characteristics of 1-alkyl-3-aryl-2,3-dihydro-1H-naphth[1,2-e][1,3]oxazines **51-55**), only the data for **51** were chosen to illustrate the  $^1\text{H}$  NMR spectra of the prepared tautomeric compounds.

To study the double substituent dependence of  $\log K_B$  and  $\log K_C$ , the following Hansch-type quantitative structure-properties relationship model equation (Eq. 2) was set up:

$$\log K_{B \text{ or } C} = k + \rho^R P^R + \rho^X \sigma^{\pm X} \quad (2)$$

where  $K_B = [B]/[A]$ ,  $K_C = [C]/[A]$ ,  $P^R$  is an alkyl substituent parameter and  $\sigma^{\pm X}$  is the Hammett-Brown parameter of the aryl substituent at position 3. In order to find the accurate dependence of  $\log K_{B \text{ or } C}$ , three different alkyl substituent parameters were studied:  $E_s$  (calculated from the hydrolysis or aminolysis of esters)<sup>62</sup> and two other steric parameters independent of any kinetic data:  $\nu$ , derived from the van der Waals radii,<sup>63,64</sup> and  $V^a$ , the volume of the portion of the substituent that is within 0.3 nm of the reaction centre.<sup>65</sup>



**Scheme 16**

**Table 1.** Proportions (%) of the ring-closed tautomeric forms (**B** and **C**) in tautomeric equilibria for **51-54** and **57** ( $\text{CDCl}_3$ , 300 K)

Comp.	X	$\sigma^{\pm}$	<b>57</b>		<b>51</b>		<b>52</b>		<b>53</b>		<b>54</b>		<b>55</b>	
			R	$V^a$	H	Me	Et		Pr		<i>i</i> Pr		<i>t</i> Bu	
					0	2.84	4.31		4.78		5.74		7.16	
			<b>B</b>	<b>B</b>	<b>C</b>	<b>B</b>	<b>C</b>	<b>B</b>	<b>C</b>	<b>B</b>	<b>C</b>	<b>B</b>	<b>C</b>	<b>C</b>
<b>A</b>	<i>p</i> -NO <sub>2</sub>	0.79	95.2	70.3	10.0	59.4	4.8	60.3	4.4	8.9	~0	~0	~0	
<b>B</b>	<i>m</i> -Cl	0.40	86.5	52.8	7.7	21.3	6.8	25.3	2.6	3.5	2.5	–	–	
<b>C</b>	<i>p</i> -Br	0.15	81.1	39.5	6.0	26.5	2.7	23.4	1.5	1.2	0.7	–	–	
<b>D</b>	<i>p</i> -Cl	0.11	79.4	39.4	6.3	25.2	2.2	24.8	1.5	1.8	1.1	–	–	
<b>E</b>	H	0	72.3	30.4	5.2	18.4	1.9	12.8	~0	~0	~0	~0	~0	
<b>F</b>	<i>p</i> -Me	–0.31	58.3	18.0	2.5	11.6	~0	9.1	~0	~0	~0	~0	~0	
<b>G</b>	<i>p</i> -OMe	–0.78	45.4	10.9	1.7	3.5	~0	3.9	~0	~0	~0	–	–	

Multiple linear regression analysis of Eq. 2 was performed by using the SPSS statistical software, and a value of 0.05 was chosen as the significance level.<sup>66</sup> Good correlations were found for all three alkyl substituent parameters. The linear regression analysis data for the series **51-54** and **57** are given in Table 2. The best correlations were observed for the Meyer parameter ( $V^a$ ) of the alkyl substituents, and this was used for the further examinations.

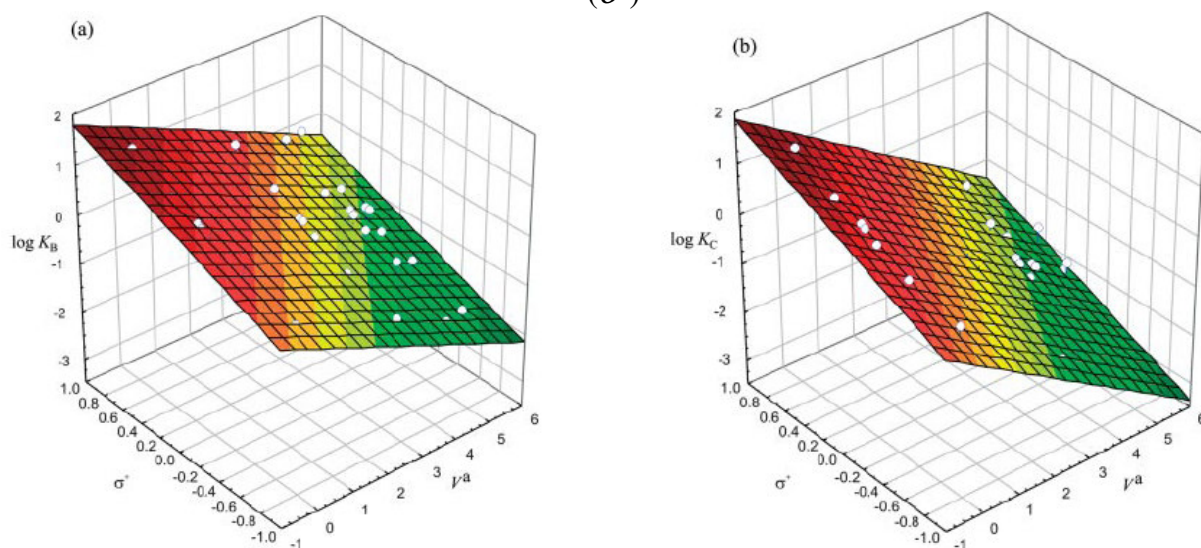
The parameters given in Table 2 indicate that the tautomeric interconversion (*e.g.*  $\log K_B$  and  $\log K_C$  values) could be described by using two substituent parameters ( $V^a$  and  $\sigma^+$ ), which means that, when  $\log K_B$  or  $\log K_C$  was plotted vs the Meyer parameter ( $V^a$ ) and the Hammett-Brown parameter ( $\sigma^+$ ), a plane could be fitted to the data points (Fig. 1).

**Table 2.** Multiple linear regression analysis of  $\log K_B$  and  $\log K_C$  values for **51-54** and **57**

		$K$	$\rho^R$	$\rho^X$	$R$
$P^R = V^a$	<b>51-54, 57B</b> $\rightleftharpoons$ <b>51-54, 57A</b>	0.605	-320	0.848	0.965
	<b>51-54, 57C</b> $\rightleftharpoons$ <b>51-54, 57A</b>	0.413	-464	0.978	0.994
$P^R = Es$	<b>51-54, 57B</b> $\rightleftharpoons$ <b>51-54, 57A</b>	0.609	0.948	0.809	0.938
	<b>51-54, 57C</b> $\rightleftharpoons$ <b>51-54, 57A</b>	0.524	1.442	0.881	0.992
$P^R = \nu$	<b>51-54, 57B</b> $\rightleftharpoons$ <b>51-54, 57A</b>	0.624	-2.250	0.822	0.946
	<b>51-54, 57C</b> $\rightleftharpoons$ <b>51-54, 57A</b>	0.516	-3.356	0.886	0.994

The slopes of the alkyl substituent parameters ( $\rho^R$ ) for the equilibria **B**  $\rightleftharpoons$  **A** and **C**  $\rightleftharpoons$  **A** exhibited a significant difference (-0.320 vs -0.464). This difference can be explained by an additional stabilization effect caused by the alkyl substituents.

**Figure 1.** (a) Plots of  $\log K_B$  for **51-54B** and **57B** vs Meyer ( $V^a$ ) and Hammett-Brown parameters ( $\sigma^+$ ). (b) Plots of  $\log K_C$  for **51-54C** and **57C** vs Meyer ( $V^a$ ) and Hammett-Brown parameters ( $\sigma^+$ )



### 3.1.2.1. Geometry optimization

We set out to extend the application of the concept of the anomeric effect by using the tautomeric equilibrium of 1-alkyl-3-aryl-2,3-dihydro-1*H*-naphth[1,2-*e*][1,3]oxazines (**51-55**, Scheme 15) as model system. We also hoped to demonstrate that the significant difference between the slopes of the  $V^a$  values for ring<sup>trans</sup>-chain (Eq. 3) and ring<sup>cis</sup>-chain (Eq. 4) equilibria (-0.32 vs -0.46) can be explained by a consideration of substituent-dependent stereoelectronic stabilization effects<sup>65</sup>. The syntheses of the model compounds 1-alkyl-3-aryl-naphth[1,2-*e*][1,3]oxazines (**51-55** Scheme 15) were described previously.<sup>65</sup>

$$\log K_B = 0.61 - 0.32V^a + 0.85\sigma^+ \quad (3)$$

$$\log K_C = 0.41 - 0.46V^a + 0.98\sigma^+ \quad (4)$$

Since stereoelectronic interactions are highly dependent on the geometry of the studied molecules, a thorough conformational analysis was performed. Our goal was to determine the predominant geometry for all of the models.

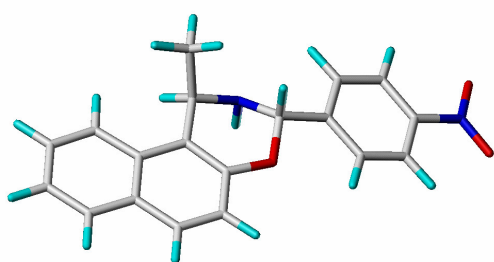
The relevant calculated conformations that can be attributed to nitrogen–ring inversions of **52aB** and **52aC**, as examples, are shown in Figure 2. Chemical shifts and coupling constants were calculated at the same level of theory; selected bond lengths (for comparison with NOE measurements) and NMR parameters are given in Table 3 (Scheme 15).

**Table 3.** Some measured (NMR) and calculated parameters for **52a**

Entry	Parameters	<b>52aB</b> <sup>a</sup>	<b>52aB</b> <sub>1</sub> <sup>b</sup>	<b>52aB</b> <sub>2</sub> <sup>b</sup>	<b>52aB</b> <sub>3</sub> <sup>b</sup>	<b>52aB</b> <sub>4</sub> <sup>b</sup>	<b>52aC</b> <sup>a</sup>	<b>52aC</b> <sub>1</sub> <sup>b</sup>	<b>52aC</b> <sub>2</sub> <sup>b</sup>	<b>52aC</b> <sub>3</sub> <sup>b</sup>	<b>52aC</b> <sub>4</sub> <sup>b</sup>
1	$d_{C1-Me-C3H}$ <sup>c</sup>	yes	2.78	4.39	2.83	4.43	-	-	-	-	-
2	$d_{C1-H-C3H}$ <sup>c</sup>	-	-	-	-	-	yes	2.77	4.04	2.81	4.07
3	$J_{C1-H-NH}$	4.6 <sup>d</sup>	4.80	7.77	1.01	3.42	8.8 <sup>d</sup>	7.37	4.98	5.13	1.22
4	$J_{C3-H-NH}$	14.2 <sup>d</sup>	12.84	4.84	0.58	2.53	14.0 <sup>d</sup>	12.85	6.53	0.83	1.24
5	$\delta_{C1-H}$	4.65	4.51	4.53	4.71	4.66	5.01	5.02	4.33	4.98	4.58
6	$\delta_{C3-H}$	6.06	6.15	5.85	5.93	5.81	5.66	5.60	6.04	5.43	6.09
7	$\delta_{C1}$	45.8	48.3	44.0	48.9	44.7	47.9	48.9	46.8	50.8	46.6
8	$\delta_{C3}$	80.7	78.5	83.7	81.6	82.2	85.5	84.1	82.9	85.7	81.8

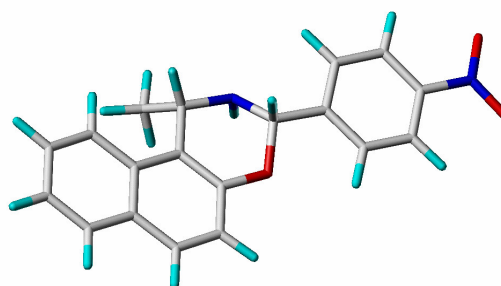
<sup>a</sup> Measured NMR parameters. <sup>b</sup> Calculated NMR parameters. <sup>c</sup> Observed NOE interaction/calculated distances. <sup>d</sup> The coupling constants were measured in CD<sub>2</sub>Cl<sub>2</sub> at 173 K

**Figure 2.** Calculated global energy minimum conformations for **52a**



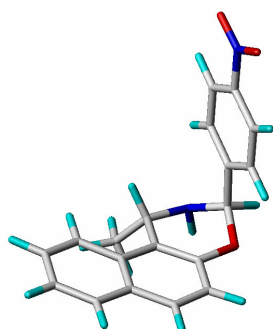
$\Delta E = 0.0$  kcal/mol

**52aB<sub>1</sub>**



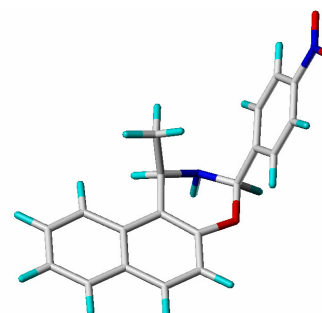
$\Delta E = 0.0$  kcal/mol

**52aC<sub>1</sub>**



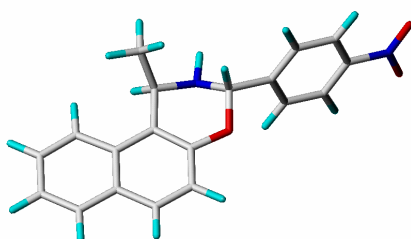
$\Delta E = 2.8$  kcal/mol

**52aB<sub>2</sub>**



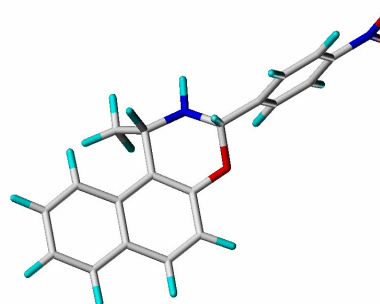
$\Delta E = 2.2$  kcal/mol

**52aC<sub>2</sub>**



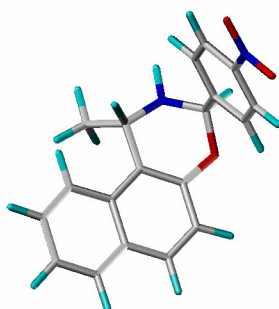
$\Delta E = 3.9$  kcal/mol

**52aB<sub>3</sub>**



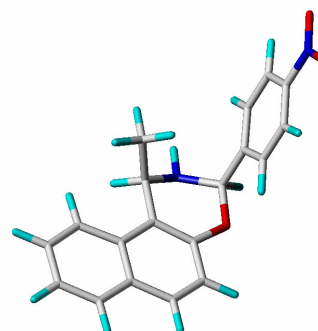
$\Delta E = 3.8$  kcal/mol

**52aC<sub>3</sub>**



$\Delta E = 8.1$  kcal/mol

**52aB<sub>4</sub>**



$\Delta E = 7.6$  kcal/mol

**52aC<sub>4</sub>**



In the analysis of **52a**, the strong NOE interaction between the C1-*Me* protons and C3-*H* (for **B**) or between C1-*H* and C3-*H* (for **C**) predicted the presence of **B**<sub>1</sub> and **B**<sub>3</sub>, or **C**<sub>1</sub> and **C**<sub>3</sub> geometries, respectively (Table 3, Entries 1 and 2). The only difference between **B**<sub>1</sub> and **B**<sub>3</sub>, or **C**<sub>1</sub> and **C**<sub>3</sub> is a nitrogen inversion. To decide between the **B**<sub>1</sub> and **B**<sub>3</sub>, or **C**<sub>1</sub> and **C**<sub>3</sub> geometries, the coupling constants <sup>3</sup>*J* observed between N-*H* and C1-3-*H* of **52a** with low-temperature <sup>1</sup>H NMR techniques (CD<sub>2</sub>Cl<sub>2</sub>, 173 K) should be taken into account. These values (Table 3, Entries 3 and 4) were in very good agreement with the coupling constants calculated for conformers **B**<sub>1</sub> and **C**<sub>1</sub>. This finding, together with the comparison of the energy values (the data were calculated for the full set of compounds, but are shown only for **52a**; Figure 2) allows the conclusion that, for all of our model compounds, **B**<sub>1</sub> and **C**<sub>1</sub> are the global minimum conformers.

The NMR calculations were performed at the B3LYP/6-31G\* level, with geometries optimized at the same level. Table 3 (Entries 5-8) summarizes the measured and calculated <sup>1</sup>H NMR (C1-*H* and C3-*H*) and <sup>13</sup>C NMR (C1 and C3) chemical shifts for **52a**.

#### 3.1.2.2. Natural bond orbital (NBO) analysis

The extra stabilization effects of the conformers that is observed with alkyl substituents at position 1 of the *trans* ring form, indicated by the slopes (-0.32 vs -0.46), may originate from a substituent-dependent stereoelectronic effect. Analysis of the delocalization energy contributions to this effect is a complex problem which can be tackled through a second-order perturbative analysis of the elements of the Fock matrix elements in the frame of the DFT hybrid method in the NBO basis.

The NBO<sup>67</sup> calculations were performed at the B3LYP/6-31G\* level, with geometries optimized at the same level. The solvent effect can be taken into account with a self-consistent reaction field method. The self-consistent isodensity polarized continuum model (SCIPCM)<sup>68</sup> used the isodensity surface of the electron density, which was influenced consistently by a dielectric continuum outside the molecule. The solvent effect was checked for series of compounds **52** (data not included). A dielectric constant  $\epsilon = 4.81$  (chloroform) and a value of 0.0004 a.u. for the isodensity surface were used in the calculations. The difference between the epimerization energy without a solvent effect ( $\Delta E_{\text{B-C}} = 1.12$  kcal/mol) and that including a solvent effect ( $\Delta E_{\text{B-C}} = 1.21$  kcal/mol) was found to be 0.09 kcal/mol for the most polar compound **52a**; in the further calculations, the effect of the solvent was neglected.

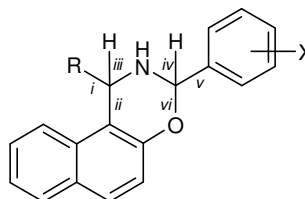
We were interested in the substituent dependence of the calculated NBO parameters. The calculated occupancy values (Table S1) and the energies for the overlap (Tables S2-S4) for the lone pairs of electrons on the nitrogen and oxygen atoms are given in the Supporting Information. Accordingly, multiple linear regression analysis of these values as dependent variable (DV), with  $V^a$  and  $\sigma^+$  as independent variables, was performed with SPSS statistical software according to Eq. (5). A value of 0.05 was chosen to denote the level of significance.<sup>69</sup>

$$DV = k + \rho^1 V^a + \rho^2 \sigma^+ \quad (5)$$

The calculated occupancy values indicate the level of overlap (%) with different antibonding orbitals. Comparison of the results of the regression analysis of the level of overlap of the lone pair of electrons ( $n$ ) on the nitrogen atom (Table 4, Entry 1) for the *trans* (**B**) and *cis* (**C**) ring forms revealed a somewhat higher slope for the **B** form (0.12 vs 0.04) as compared with that for **C**. This was in accordance with our experimental findings. It was also concluded that the extra stabilization energy could result from a complex stereoelectronic interaction between  $n_N$  and the vicinal antibonding orbitals. Hence, regression analysis of the overlapping energies (kcal/mol) was performed for the six possible vicinal antibonding orbitals (three around C-1 and three around C-3). The results showed that the overlap of  $n_N$  and the antibonding orbital of the C-1-R bond ( $\sigma^*_{i1}$ ) in **B** or the C-1-H bond ( $\sigma^*_{iii1}$ ) in **C** had relatively similar intensities (around 2.6 kcal/mol; Table 4, Entry 2). The opposite slope can be explained by the change in the relative configuration of C-1 and is in accordance with the experimental findings. The overlap of  $n_N$  and  $\sigma^*_{ii1}$  in **B** and the corresponding overlap in **C** (Table 4, Entry 3) showed similar intensities and similar tendencies.

The low intercept **C** (0.79 and 0.87 respectively: Table 4, Entries 5 and 6) and slope (around 0) indicate that, around C-3, the most important and the strongest overlap occurs in the direction of the most polar C-O ( $\nu_i$ ) bond (Table 4, Entry 7). No comparable difference was observed between ring forms **B** and **C** either in the slope of  $V^a$  or in the slope of  $\sigma^+$ . The value of 0.1 for  $V^a$  can be explained by the small inductive influence of the alkyl substituents. The slope of  $\sigma^+$ , which is double the expected value, can be a result of the polarization of bond  $\nu_i$ , induced by substituent X.

**Table 4.** Multiple linear regression analysis of the occupancy and overlapping energy values of the lone pairs of electrons on the nitrogen atoms as dependent variables according to equation (5) for **51-55**



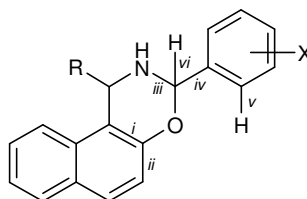
Entry	Dependent variable (DV)	B				C			
		$k$	$\rho^1$	$\rho^2$	$r$	$k$	$\rho^1$	$\rho^2$	$R$
1	Occupancy <sup>a</sup>	10.47	0.12	-0.12	0.906	10.51	0.04	-0.11	0.774
2	$n_N \rightarrow \sigma^*_{i}$	2.57	-0.13	- <sup>b</sup>	0.702	-	-	-	-
3	$n_N \rightarrow \sigma^*_{ii}$	6.92	-0.13	-0.11	0.949	6.75	-0.20	- <sup>b</sup>	0.953
4	$n_N \rightarrow \sigma^*_{iii}$	-	-	-	-	2.60	0.15	- <sup>b</sup>	0.905
5	$n_N \rightarrow \sigma^*_{iv}$	0.79	0.09	- <sup>b</sup>	0.746	0.79	-0.01	0.05	0.751
6	$n_N \rightarrow \sigma^*_{v}$	0.78	-0.03	0.05	0.946	0.87	0.03	- <sup>b</sup>	0.764
7	$n_N \rightarrow \sigma^*_{vi}$	15.93	0.10	-0.18	0.781	16.00	0.07	-0.19	0.795

<sup>a</sup> For regression analysis, the ratios of the occupancy values in % were used. <sup>b</sup> Insignificant (significance value > 0.05)

From the analysis of the overlapping behaviour of  $n_N$ , the additional stabilization of the conformers that is observed when alkyl substituents are at position 1 can be nicely explained, but in order to map the summed influence of the alkyl and aryl substituents, an analysis of the overlapping behaviour of the oxygen lone pairs ( $n_{O1}$  and  $n_{O2}$ ) was also necessary.

A comparison of the overlapping levels of  $n_{O1}$  and  $n_{O2}$  (Table 5, Entries 1 and 7, respectively) leads to the conclusion that  $n_{O2}$  ( $\pi$ -like lone pair) participates in overlapping interactions to a greater extent than  $n_{O1}$  does (see intercepts, Table 5, Entries 1 and 7), and because of the low slope values (Table 5, Entry 1), the substituent dependence on the overlapping level of  $n_{O1}$  can be neglected. The occupancy level of  $n_{O2}$  is strongly influenced by the aryl substituent at position 3 (-0.38 and -0.34, respectively, Table 5, Entry 7). The comparison of the slopes of  $V^a$  for the ring forms yielded low values, but the different tendencies (0.08 vs -0.07, Table 5, Entry 7) indicate that there is some influence of the alkyl substituent at position 1. Because of the large difference between the interaction of the alkyl substituent with  $n_{O2}$  and the pure electronic character of an alkyl substituent alone, this dependence can be explained only in terms of an alkyl substituent-controlled quantitative change in the torsion angle between  $n_{O2}$  and the corresponding antibonding orbital (e.g. by an alkyl substituent-dependent conformational change).

**Table 5.** Multiple linear regression analysis of the occupancy and overlapping energy values of the lone pairs of electrons on the oxygen atoms as dependent variables according to Eq. (5) for **51-55**



Entry	Dependent variable (DV)	B				C			
		<i>k</i>	$\rho^1$	$\rho^2$	<i>r</i>	<i>k</i>	$\rho^1$	$\rho^2$	<i>R</i>
1	Occupancy ( $n_{O1}$ ) <sup>a</sup>	4.05	0.03	- <sup>b</sup>	0.897	4.04	-0.01	0.02	0.834
2	$n_{O1} \rightarrow \sigma^*_i$	6.58	0.07	-0.16	0.880	6.55	-0.05	-0.15	0.937
3	$n_{O1} \rightarrow \sigma^*_{ii}$	0.50	0.02	- <sup>b</sup>	0.857	-	-	-	-
4	$n_{O1} \rightarrow \sigma^*_{iii}$	2.62	0.21	- <sup>b</sup>	0.785	2.66	-0.12	- <sup>b</sup>	0.914
5	$n_{O1} \rightarrow \sigma^*_{iv}$	1.09	-0.03	- <sup>b</sup>	0.645	1.05	-0.01	0.06	0.940
6	$n_{O1} \rightarrow \sigma^*_{v}$	0.58	0.01	0.01	0.799	0.57	-0.01	0.03	0.681
7	Occupancy ( $n_{O2}$ ) <sup>a</sup>	15.21	0.08	-0.38	0.907	15.15	-0.07	-0.34	0.928
8	$n_{O2} \rightarrow \pi^*_i$	28.17	0.28	-0.93	0.896	27.79	-0.46	-0.82	0.935
9	$n_{O2} \rightarrow \sigma^*_{iii}$	5.13	-0.41	- <sup>b</sup>	0.720	4.93	0.15	0.20	0.904
10	$n_{O2} \rightarrow \sigma^*_{vi}$	5.51	-0.08	0.21	0.599	5.34	-0.06	0.20	0.945

<sup>a</sup> For regression analysis, the ratios of the occupancy values in % were used. <sup>b</sup> Insignificant (significance value > 0.05)

The NBO analyses demonstrated that negative hyperconjugation ( $n \rightarrow \sigma^*$ ) and conjugation ( $n \rightarrow \pi^*$ ) play important roles in the ring-chain tautomeric interconversion of **51-55**. The results also indicate that these conjugative interactions, which result from substituent-dependent conformational changes, explain the relative stability differences between ring forms **B** and **C**.

### 3.1.2.3. Shifted carbon chemical shift (SCS) analysis

The changes in the  $^{13}\text{C}$  NMR chemical shift values that are induced by phenyl substituents (SCS) on C-2 have been analysed by various dual substituent parameter approaches.<sup>70-72</sup> The best correlation was obtained with the equation  $\text{SCS} = \rho_{\text{F}}\sigma_{\text{F}} + \rho_{\text{R}}\sigma_{\text{R}}$ , where  $\sigma_{\text{F}}$  characterizes the inductive effect, and  $\sigma_{\text{R}}$  the resonance effect of the aryl substituent. In a previous study on the ring-chain tautomerism of 1,3-diaryl-2,3-dihydro-1H-naphth[1,2-*e*][1,3]oxazines, by means of a dual substituent parameter treatment of SCS, the difference in the stabilities of ring forms **B** and **C** was explained by the changes in the  $sp^2$  and  $sp^3$  hybridized character of the carbon atom, which is influenced the aryl substituents on C-1 and C-3.<sup>10</sup>

The low concentrations of the minor forms of **B** and **C** in the tautomeric mixtures did not allow measurement of the  $^{13}\text{C}$  NMR chemical shifts of C-1 and C-3. They were therefore calculated for all compounds at the B3LYP/6-31G\* level with geometries optimized at the same level; they are listed in Table S5. The chemical shift changes induced by the alkyl substituent at position 1 and by the aryl substituent at position 3 (SCS) for a given compound were calculated as the differences in the calculated  $^{13}\text{C}$  NMR chemical shifts values for the substituted relative to the unsubstituted ( $\text{R} = \text{H}$ ,  $\text{X} = \text{H}$ ) compound. The multiple regression analysis<sup>69</sup> data obtained from Eq. (6) for C-1 and C-3 are presented in Table 6.

$$\text{DV} = \rho^1 V^a + \rho^2 \sigma_{\text{F}} + \rho^3 \sigma_{\text{R}} \quad (6)$$

**Table 6.** Multiple linear regression analysis of the calculated SCS values for C-1 and C-3 according to Eq. (6) for **51-55**

Dependent variable (DV)	<b>B</b>				<b>C</b>			
	$\rho^1$	$\rho^2$	$\rho^3$	$r$	$\rho^1$	$\rho^2$	$\rho^3$	$R$
SCS <sub>C1</sub>	2.22	- <sup>a</sup>	- <sup>a</sup>	0.996	2.34	- <sup>a</sup>	- <sup>a</sup>	0.997
SCS <sub>C3</sub>	-0.98	-1.79	- <sup>a</sup>	0.967	0.09	-1.02	- <sup>a</sup>	0.931

<sup>a</sup> Insignificant (significance value > 0.05).

Table 6 shows that the calculated  $^{13}\text{C}$  NMR chemical shifts for C-1 are influenced only by the alkyl substituents at position 1. The small difference in slope between ring forms **B** and **C** indicates that the behaviour of the alkyl substituent at position 1 in relation to the conformational changes around C-1 is similar in the two ring forms.

The calculated  $^{13}\text{C}$  NMR chemical shifts for C-3 seem to depend much more on the changes in the relative configurations. In comparison, the influence of an alkyl substituent at position 1 (-0.98 vs 0.09, Table 4) on the SCS values for C-3 was found to be strongly dependent on the relative configurations of C-1 and C-3. This provides further evidence for the theory that alkyl substituents stabilize the *trans* (**B**) ring form, which can be explained in terms of an alkyl substituent-induced stereoelectronic effect. This results in small alkyl substituent-induced conformational changes in **B**.

The reverse trend in the inductive substituent effect ( $\sigma_{\text{F}}$ ) for unsaturated carbon is well-documented.<sup>72-76</sup> The negative slope of  $\sigma_{\text{F}}$  for saturated carbon centres such as those situated between the two heteroatoms in 1,3-*O,N*-heterocycles was explained by Neuvonen *et al.* to be due to the substituent-sensitive polarization of the N–C–O system.<sup>70</sup> The *trans* and *cis* series in the present work offered an interesting opportunity for study of this type of reverse trend in the

substituent effect ( $\sigma_F$ ) on the calculated SCS values. Table 6 shows that negative slopes of  $\sigma_F$  (-1.79 vs -1.02) were obtained for both series **B** and **C**, which is in accordance with the concept found for similar carbon centres.<sup>10,82</sup> The difference between the slopes is a further consequence of the stronger substituent-induced stereoelectronic effect in the *trans* (**B**) ring form.

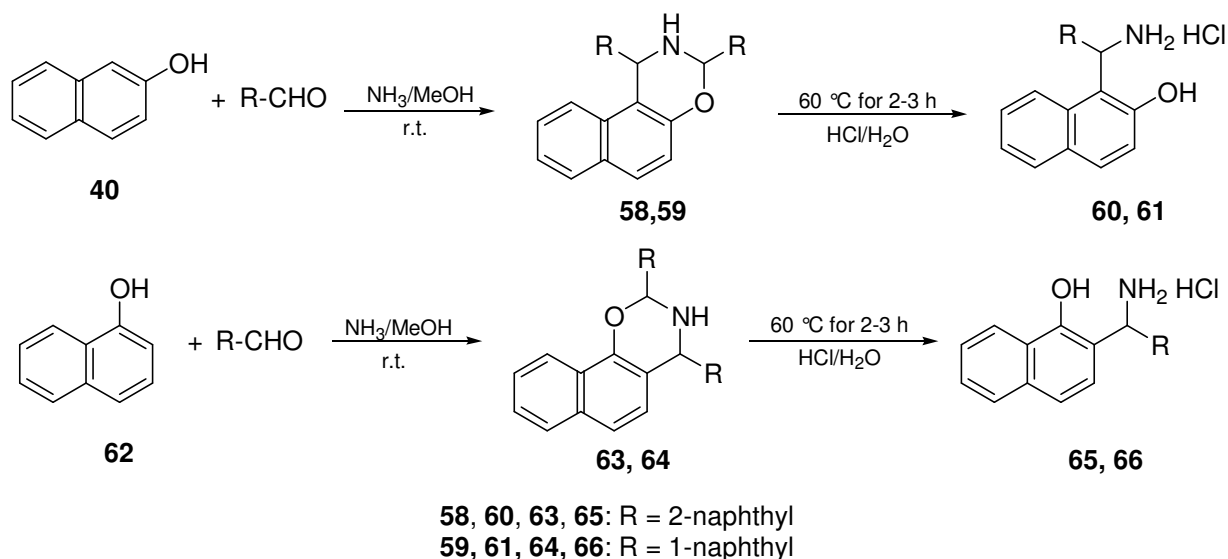
### 3.2. Synthesis and conformational analysis of naphthyl-naphthoxazine derivatives

Interest in the synthesis of primary aminonaphthols has increased greatly during the past few years following an evaluation of the hypotensive and bradycardiac effects of 1-aminomethyl-2-naphthol derivatives,<sup>77</sup> and the syntheses of a wide variety of such compounds were recently achieved through the hydrolysis of 1-amidomethyl-2-naphthols.<sup>78-80</sup> Through the use of aliphatic aldehydes, *e.g.* formaldehyde,<sup>81</sup> acetaldehyde, propionaldehyde, butyraldehyde, isobutyraldehyde and pivalaldehyde, 1-(1-aminoalkyl)-2-naphthols have been synthesized, while from heteroaromatic aldehydes primary aminonaphthols have been prepared and their ring-chain tautomeric behaviour has been studied.<sup>82</sup>

Our present aim was to prepare new primary aminonaphthols from 1- or 2-naphthol and 1- or 2-naphthaldehyde and to extend the applicability of these compounds for the preparation of new heterocyclic derivatives by simple ring-closure reactions with paraformaldehyde, 4-nitrobenzaldehyde, phosgene or 4-chlorophenyl isothiocyanate. We additionally investigated the influence of the substituent at position 3 or 2 and the connecting position of the naphthalene ring on the conformation.

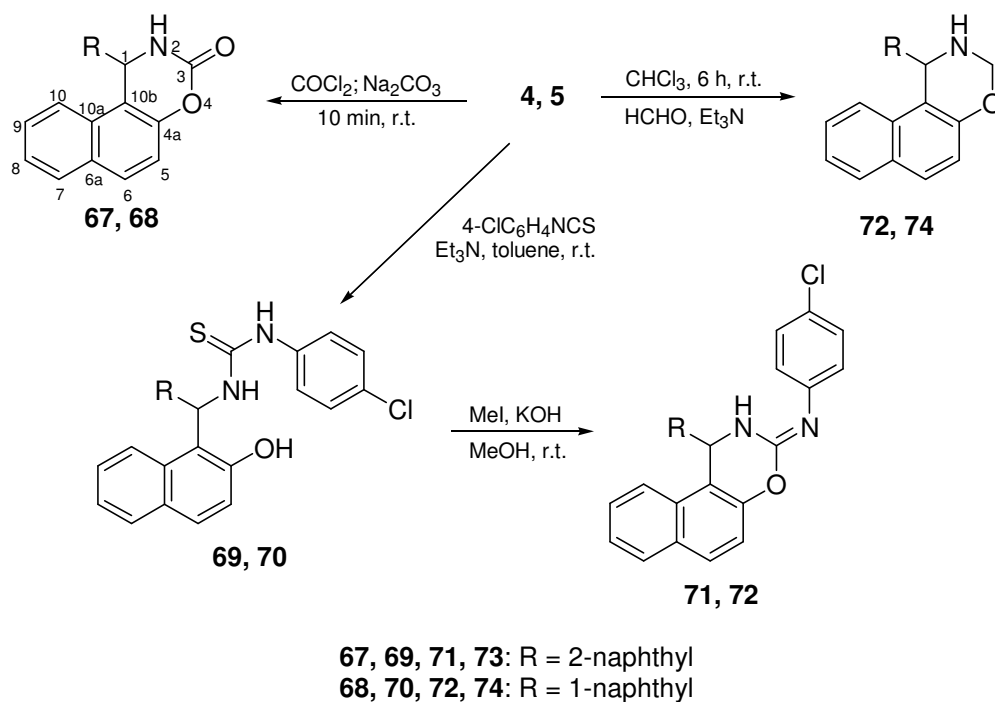
#### 3.2.1. Syntheses of the naphthyl-naphthoxazine model system

The aminonaphthols **60**, **61**, **65** and **66** were prepared via the reactions of the corresponding 1- or 2-naphthol with 1- or 2-naphthaldehyde in the presence of methanolic ammonia solution in absolute methanol at room temperature for 24 h. This led to the naphthoxazines **58**, **60**, **63** and **64** (Scheme 17), acidic hydrolysis of which gave the desired aminonaphthol hydrochlorides **60**, **61**, **65** and **66** (Scheme 17). Because of the instability of the aminonaphthyl naphthol derivatives, **60**, **61**, **65** and **66** were isolated as their hydrochlorides, in moderate to good yields (28-87%).



Scheme 17

In the first stage of the transformations of **60**, **61**, **65** and **66** to heterocyclic derivatives, an  $sp^2$  carbon (C-3 or C-2) was inserted between the hydroxy and amino groups (Schemes 18 and 19).



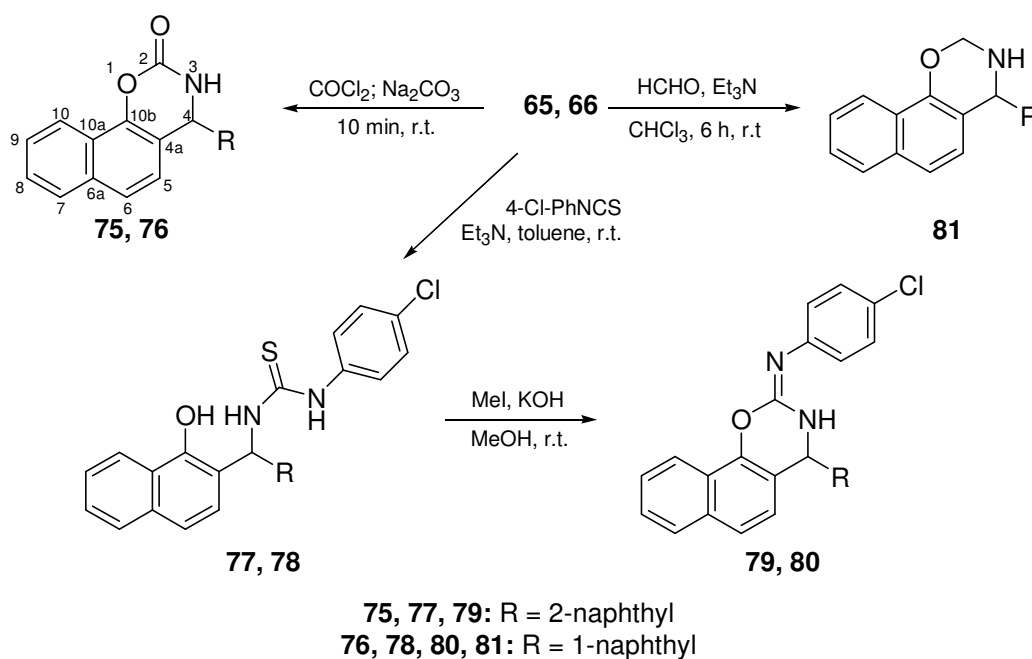
Scheme 18

When aminonaphthols **60**, **61**, **65** and **64** were treated with  $\text{COCl}_2$  in the presence of  $\text{Na}_2\text{CO}_3$  in toluene/ $\text{H}_2\text{O}$  at room temperature for 10 min, the corresponding naphthoxazin-3-ones **67** and **68** and naphthoxazin-2-ones **75** and **76** were formed, in moderate yields (40-86%) in each case (Schemes 18 and 19).

For the preparation of 3- and 2-(4-chlorophenylimino)-substituted naphthoxazines **71**, **72**, **79** and **80**, aminonaphthols **60**, **61**, **65** and **66** were reacted with 4-chlorophenyl isothiocyanate (Schemes 18 and 19). Thioureas **69**, **70**, **77** and **78** were converted to the corresponding *S*-methylisothiourea derivatives with methyl iodide, and subsequent treatment with methanolic KOH gave the corresponding 3- or 2-arylimino-substituted naphthoxazines **71**, **72**, **79** and **80**, in good yields (67-82%), via methyl mercaptan elimination (Schemes 18 and 19).

The ring closures of aminonaphthols **60**, **61**, **65** and **66** with oxo compounds (*i.e.* the insertion of an  $sp^3$  carbon) resulted in naphthoxazines.

The reactions of aminonaphthols **60**, **61** and **66** with paraformaldehyde under mild conditions (at room temperature for 6 h) gave the corresponding 3- and 2-unsubstituted naphthoxazines **73**, **74** and **81** in yields of 37-49% (Schemes 18 and 19). The corresponding reaction of **65** did not lead to the desired naphthoxazine. After a reaction time of 3 h, TLC demonstrated that no starting material remained, and the TLC plots observed suggested the rapid decomposition of the expected naphthoxazine derivative.



**Scheme 19**

The analogous reactions of **60**, **61**, **65** and **66** with 4-nitrobenzaldehyde were accomplished under mild conditions. The products **83**, **84**, **87** and **88** were separated from the reaction mixture in good yields (78-84%, Scheme 20). Compounds **83-85** and **87-89** in solution can participate in three-component ring-chain tautomeric equilibria involving the C-3 (**83-85**) or C-2 (**87-89**) epimeric naphthoxazines (**B** and **C**) and the open tautomer (**A**). The tautomeric behaviour (the

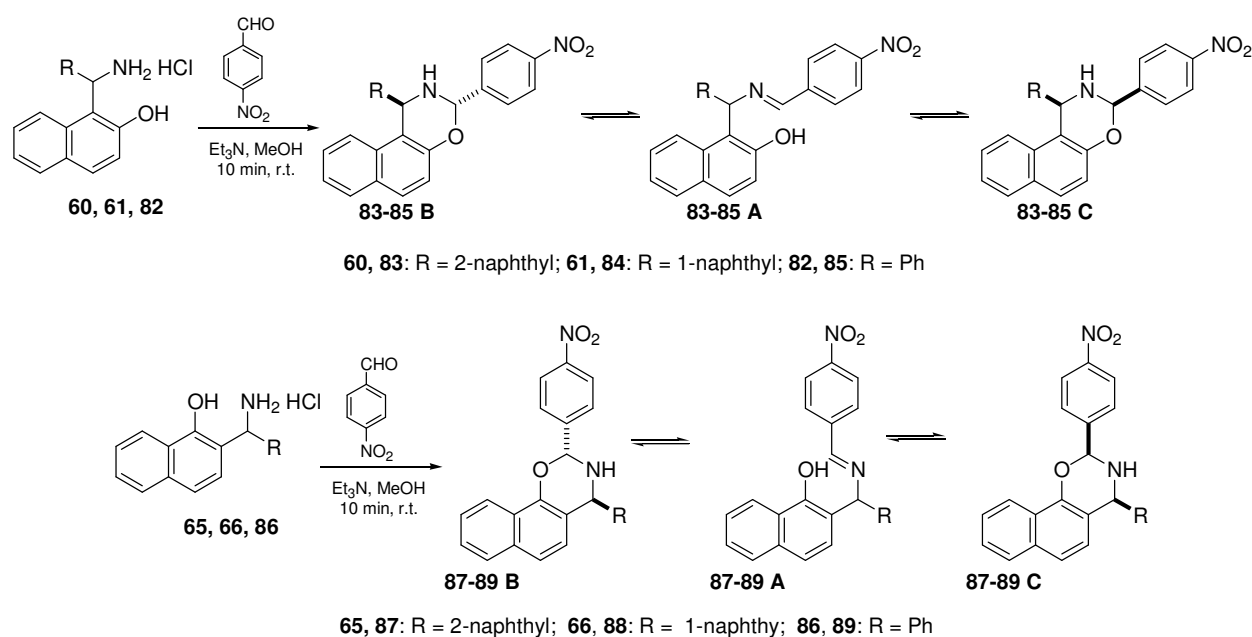


tautomeric ratios) of **83-85** and **87-89** depend on substituent R at position 1 or 4, and on the properties of the solvent in question, as revealed in Table 7.<sup>81</sup>

For **83-85**, the predominant form is the *trans* tautomer (**B**). The proportion of **B** decreases in the sequence **83** > **84** > **85**, while that of the *cis* form (**C**) displays the opposite tendency (Table 7: Entries 1-3). This can be explained in terms of steric hindrance. Relative to CDCl<sub>3</sub>, the more polar solvent DMSO causes a small increase in the proportion of the open-chain form (**A**) at the expense of form **C** for **85** (Table 7: Entry 3), but the main tendency was found to be similar with that discussed above.

For **82-89** in CDCl<sub>3</sub>, the steric hindrance of the aryl substituents at position 4 must exert the most important effect as regards the composition of the tautomeric mixture and, similarly as for 1,3-disubstituted naphth[1,2-*e*][1,3]oxazines, the phenyl ring (smaller then the naphthyl ring system) resulted in more form **C** and less form **B** (Table 7: Entries 4-6).

The effect of the change of the solvent seems to be somewhat more marked for **87-89** (Table 7: Entries 4-6) than for **83-85** (Table 7: Entries 1-3).



**Scheme 20**

**Table 7.** Proportions of tautomers (%) in **83-85** and **87-89**

Entry	Comp.	CDCl <sub>3</sub>			DMSO		
		A	B	C	A	B	C
1	<b>83</b>	-	100.0 <sup>a</sup>	-	-	100.0	-
2	<b>84</b>	-	95.4	4.6	-	94.8	5.2
3	<b>85<sup>b</sup></b>	3.1	86.1	10.8	15.0	84.8	0.2
4	<b>87</b>	13.8	68.9	17.3	34.3	46.1	19.6
5	<b>88</b>	4.5	77.6	17.9	-	82.8	17.2
6	<b>89<sup>c</sup></b>	14.9	50.1	35.0	36.9	42.6	20.5

<sup>a</sup>Either the population of tautomers **A** and **C** is too low to be detected by NMR, or the equilibration is fast on the NMR time-scale (see text below); <sup>b</sup>Data from ref. <sup>9</sup>; <sup>c</sup>Data from ref. <sup>11</sup>

### 3.2.2. Conformational analysis

Theoretical calculations were performed on the compounds studied and their global minimum-energy structures were determined. These structures were compared with the relevant NMR spectroscopic data (NOEs and *vicinal* H,H-coupling constants) to check particularly on the conformation of the (unsaturated) oxazine ring moiety. The same procedure was applied in the event of additional substitution at C-3 in the 2-naphthoxazines and at C-2 in the 1-naphthoxazines, of the  $sp^2$  hybridization of C-2 or C-4. The complete agreement of the computed structures (the preferred conformers) and the NMR parameters is strong evidence of the correctness of the calculated geometries of the compounds studied.

Both the 1- and 2-naphthyl substituents at C-1 in the 2-naphthoxazines and at C-4 in the 1-naphthoxazines were found to have only a marginal influence on the conformational equilibria, whereas in the *trans* isomers of the disubstituted 1- and 2-naphthoxazines **83**, **84**, **87** and **88** they do influence the preference for the corresponding *S/R* and *R/S* diastereomers (*vide infra*).

#### 3.2.2.1. Compounds with $sp^3$ C-2 or C-3 atoms

Compounds which are only monosubstituted with 1- and 2-naphthyl substituents at C-1 and C-4, respectively (**73**, **74** and **81**), prefer *twisted-chair* conformers (*cf.* the global minimum-energy structure of **73**, for instance, in Fig. 3). The analogue of **73** could not be obtained experimentally, but was computed at the DFT level of theory; the same *twisted-chair* conformer as in **73**, **74** and **81** was found to be preferred.

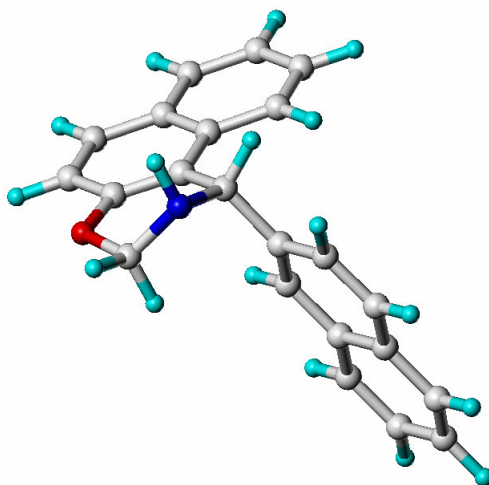


**Figure 3.**  
Minimum-energy structure of (*1S*)-**73**

This preferred conformation (*cf.* **73** in Figure 4) proves to be in excellent agreement with the experimental NMR data: NOEs were observed between H-1 and NH (the corresponding distance was computed to be only 2.243 Å) and between NH and H-3<sub>eq</sub> (computed distance 2.360 Å). Moreover, the corresponding scalar vicinal coupling constants  $^3J_{\text{H,H}}$  were 5.0 Hz (computed  $^3J_{\text{H1,NH}}$  4.7 Hz, dihedral angle 43.3°), 3.9 Hz (computed  $^3J_{\text{H-3eq,NH}}$  3.2 Hz, dihedral angle -57.3°), and 13.6 Hz (computed  $^3J_{\text{H-3ax,NH}}$  13.1 Hz, dihedral angle -178.2°). The corresponding NMR data on **74** are given in Table 8 and are likewise seen to be in excellent agreement with the computed values.

A *twisted-chair* conformer was also found for **81** (*cf.* Figure 4). As for **73** and **74**, a similar  $^3J_{\text{H,H}}$  value in the coupling fragment O(2)CH<sub>2</sub>-NH-C(4)H and similar NOEs between NH and H-2<sub>eq</sub> and H-4, respectively, were observed (*cf.* Table 8).

**Table 8.** Experimental and computed coupling constants and some calculated dihedral angles (D.a.) and distances for compounds **74** and **81**

Com- pound	$^3J_{\text{NCH-H}}$ (exp) (Hz)	$^3J_{\text{NCH-NH}}$ (calc) (Hz)	D.a. NCH- NH	$^3J_{\text{NH-OCHeq}}$ (exp) (Hz)	$^3J_{\text{NH-OCHeq}}$ (calc) (Hz)	D.a. NH- OCH <sub>eq</sub>	$^3J_{\text{NH-OCHax}}$ (exp) (Hz)	$^3J_{\text{NH-OCHax}}$ (calc) (Hz)	D.a. NH- OCH <sub>ax</sub>	Distance NCH- NH (Å)	Distance NH- OCH <sub>eq</sub> (Å)
<b>80</b>	4.9	4.8	42.8°	3.7	3.1	-57.7°	13.9	13.1	-178.6°	2.241	2.358
<b>87</b>	6.2	4.7	41.6°	5.4	2.0	-58.0°	12.2	13.2	-179.0°	2.242	2.359

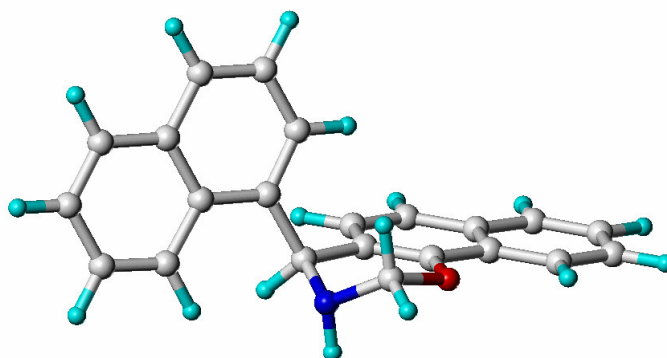


**Figure 4.**  
Minimum-energy structure of (4*S*)-**81**

If the compounds are additionally substituted at C-3 (β-naphthoxazines) or C-2 (α-naphthoxazines), tautomeric equilibria result (*cf.* Scheme 22). The major ring form **B** was isolated and studied by NMR spectroscopy. In contrast with the simple *R/S* chirality in **73**, **74** and **81**, which does not influence the NMR spectra in achiral media, in **84**, **85**, **87** and **88** *R/S* and *S/R* diastereomers have to be considered.

The global minimum-energy structure of the major ring form **B** is characterized by the *trans* arrangement of H-3 and N-H (as depicted in Figure 5 for **83B**) and prefers the *twisted-chair* conformation. The experimentally determined vicinal H,H-coupling constants  $^3J_{\text{H-2,H-3}}$  [14.0 Hz in **83B** and 13.6 Hz in **84B**] and  $^3J_{\text{H-1,H-2}}$  [5.2 Hz in **83B** and 4.9 Hz in **84B**] agree well with the computed values [*e.g.* **83B**: 12.5 Hz ( $^3J_{\text{H-2,H-3}}$ ) and 4.8 Hz ( $^3J_{\text{H-1,H-2}}$ )]. Surprisingly, a strong NOE was found between H-3 and N-H, which are in the *trans* position. This dipolar coupling, however, should be near to zero in **83B**, but some **83C** may be present in marginal concentration or in rapid equilibrium with **B** on the NMR time-scale; obviously, the reaction rate allows NOE transfer between the tautomeric species (*cf.* Table 7).

The main tautomers **87B** and **88B** also occur in a *twisted-chair* conformation, as illustrated for **88B** in Figure 6. This calculated minimum-energy structure is corroborated by the experimentally determined coupling constants  $^3J_{\text{H-3,H-4}} = 5.7$  Hz (computed dihedral angle  $40.4^\circ$ ) and  $^3J_{\text{H-2,H-3}} = 13.5$  Hz (computed dihedral angle  $177.6^\circ$ ) and the corresponding NOEs, which were found to be strong. Surprisingly, in **83**, **84** and **88** the *S/R* diastereomer proved to be more stable than the *R/S* analogue; the reverse situation was the case for **87**.

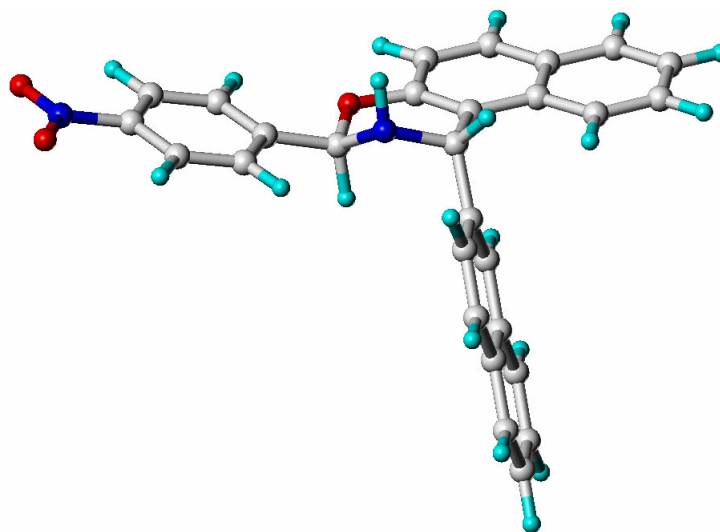


**Figure 5.**  
Minimum-energy structure of (1*S*,3*R*)-**83B**

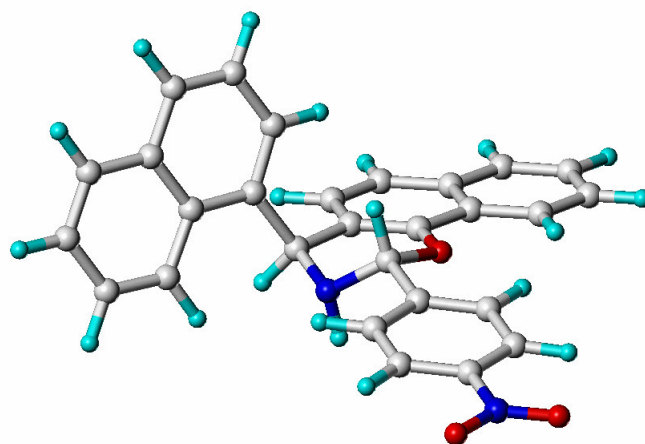


**Figure 6.**  
Minimum-energy structure of (2*R*,4*S*)-**88B**

#### 3.2.2.2. Compounds with $sp^2$ C-2 or C-3 atoms

Introduction of an  $sp^2$  carbon at position 3 (**67** and **68**) or 2 (**75** and **76**) obviously leads to very similar conformational behaviour; in accordance with this, very similar minimum-energy conformations of all of these compounds were calculated: the oxazine ring is nearly flat with a slight boat conformation (*cf.* Figure 7). Only in one case (**69**) could the coupling constant  $^3J_{\text{NH,CH}}$  be detected; it was 2.9 Hz. The corresponding signals of the other compounds were more or less broadened and the corresponding vicinal coupling constants could not be extracted. The magnitude of  $^3J_{\text{NH,CH}}$  was in good agreement with the calculated values. These were in the range 0–1.8 Hz, with calculated dihedral angles of  $59.6^\circ$ – $71.1^\circ$ , both characteristic of the *synclinal* conformation of the NH-CH moiety. The distance between these two hydrogens was computed to be in the range 2.43–2.56 Å, which corresponds to the mean NOEs determined in these compounds.

For compounds **71**, **72**, **79** and **80**, the endocyclic/exocyclic tautomerism of the C=N double bond is possible. The energy levels indicated the presence of the exocyclic form (Schemes 20 and 21). This was supported by the NMR data: NOE interactions were found between N-H and the corresponding C-H at position 1 (**71** and **72**) or 4 (**79** and **80**). *Ab initio* calculations on the title compounds pointed to the presence of the *E* isomers.

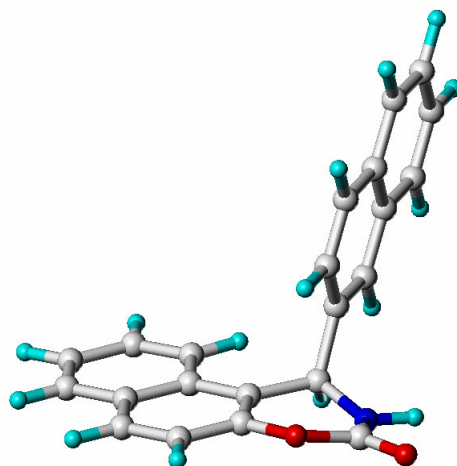


**Figure 7.**  
Minimum-energy structure of (4*R*)-**67**

The oxazine ring in **71**, **72**, **79** and **80** turned out to be nearly planar; the minimum-energy structure of **79** is shown in Figure 8.

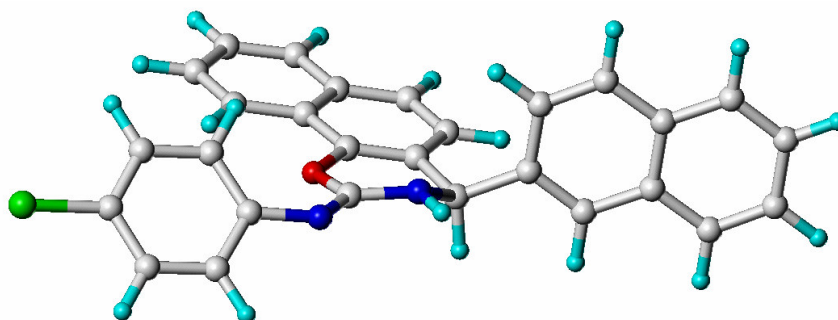


**Figure 8.**  
Minimum-energy structure of (4*R*)-**79**

### 3.3. Methods

Melting points were determined on a Kofler micro melting apparatus and are uncorrected. Merck Kieselgel 60F<sub>254</sub> plates were used for TLC. Elemental analyses were performed with a Perkin-Elmer 2400 CHNS elemental analyser.

#### *NMR measurements:*

**For compounds 46-50, 51-55 and 57:** The <sup>1</sup>H and <sup>13</sup>C NMR spectra were recorded in CDCl<sub>3</sub> or in DMSO-*d*<sub>6</sub> solution at 300 K on a Bruker Avance DRX400 spectrometer at 400.13 MHz (<sup>1</sup>H) and 100.61 MHz (<sup>13</sup>C). Chemical shifts are given in  $\delta$  (ppm) relative to TMS as internal standard. For the equilibria of tautomeric compounds to be established, the samples were dissolved in CDCl<sub>3</sub> and the solutions were allowed to stand at ambient temperature for 1 day before the <sup>1</sup>H NMR spectra was run. The number of scans was usually 64.

**For compounds 60, 61, 65-81, 83, 84, 87 and 88:** The NMR spectra were recorded in DMSO-*d*<sub>6</sub> (unless specified as CDCl<sub>3</sub>) solution in 5 mm tubes, at room temperature, on a Bruker Avance 500 spectrometer at 500.17 (<sup>1</sup>H) and 125.78 (<sup>13</sup>C) MHz, with the deuterium signal of the solvent as the lock and TMS as the internal standard for <sup>1</sup>H, or the solvent as the internal standard for <sup>13</sup>C. All spectra (<sup>1</sup>H, <sup>13</sup>C, *gs*-H,H-COSY, *gs*-HMQC *gs*-HMBC, and NOESY) were acquired and processed with the standard Bruker software.

#### *Quantum chemical calculations:*

Geometry optimizations were performed without restrictions, using the Gaussian 03 version C.02<sup>19</sup> program package. Different conformations and configurations of all studied compounds were preoptimized by using the PM3 Hamiltonian.<sup>83,84</sup> Density functional theory calculations were carried out at the B3LYP/6-31G\*\*<sup>85,86</sup> level of theory. Stationary points on the potential hypersurface were characterized by force constants. Coupling constants were computed at the same theory level, B3LYP/6-31G\*\*.<sup>87,88</sup> Different starting conformations were created and the results were analysed and displayed by using the molecular modelling program SYBYL 7.3<sup>89</sup> and the program GaussView 2.0.<sup>90</sup> Different local minimum-energy conformations were selected to analyse the relative stability and the geometrical parameter.

## 4. SUMMARY

1. 1-(1-Aminoalkyl)-2-naphthols **47-50** were synthesized by the condensation of 2-naphthol with aliphatic aldehydes in the presence of ammonia, followed by acidic hydrolysis. The overall yield was improved considerably when the solvent was evaporated off after the formation of the intermediate naphthoxazines **41-45** and the residue was directly hydrolysed with hydrochloric acid (*e.g.* for compound **46** the overall yield could be increased from 15% to 95%).
2. The condensation of **46-50** with substituted benzaldehydes after microwave irradiation led to 1-alkyl-3-aryl-2,3-dihydro-1*H*-naphth[1,2-*e*][1,3]oxazines, which proved to be three-component (*rt-o-rc*) tautomeric mixtures in CDCl<sub>3</sub> at 300 K, involving C-3 epimeric naphthoxazines (**B** and **C**) and the open tautomer (**A**).
3. The influence of the alkyl substituent at position 1 on the ring-chain tautomeric equilibria could be described by the Meyer parameter, and that of the aryl substituent at position 3 by the Hammett-Brown parameter ( $\sigma^+$ ). Linear equations were found that describe the double substituent dependence of the equilibrium constants for both the *trans*-chain and *cis*-chain equilibria. The slopes of the Meyer parameter  $V^a$  for the *trans* and *cis* forms displayed a significant difference, which was explained in terms of an alkylsubstituent-controlled stereoelectronic effect in the *trans* ring form.
4. This analysis of the disubstitution effects of R (alkyl) and X in 1-alkyl-3-(X-phenyl)-2,3-dihydro-1*H*-naphth[1,2-*e*][1,3]oxazines on the ring-chain tautomerism, the delocalization of the nitrogen and oxygen lone pairs of electrons (anomeric effect) and the calculated <sup>13</sup>C NMR chemical shifts permitted an explanation for the experimentally observed stabilization difference between the *trans* (**B**) and *cis* (**C**) ring forms.
5. Multiple linear regression analysis of the calculated overlapping energies for the lone pairs of electrons on the nitrogen and oxygen atoms showed that the relative stability difference between the two ring forms is a result of an alkyl substituent-induced quantitative conformational change in the naphthoxazine ring system. Analysis of the <sup>13</sup>C NMR



chemical shift changes induced by the substituents (SCS) for C-1 and C-3 revealed that, as a consequence of the alkyl substituent-dependent small conformational changes, the substituent-dependent anomeric effect predominates in the preponderance of the *trans* over the *cis* isomer.

6. Four new aminomethylnaphthols **60**, **61**, **65** and **66** were synthesized in good yields by the condensation of 1- or 2-naphthol with 1- or 2-naphthaldehydes in the presence of ammonia, followed by acidic hydrolysis.
7. The condensations of **60**, **61**, **65** and **66** with paraformaldehyde, 4-nitrobenzaldehyde, phosgene or 4-chlorophenyl isothiocyanate led to 1-naphthyl-naphth[1,2-*e*][1,3]oxazine and 4-naphthyl-naphth[2,1-*e*][1,3]oxazine derivatives. In the first stage of the transformations of **60**, **61**, **65** and **66** to heterocyclic derivatives, an  $sp^2$  carbon (C-3 or C-2) was inserted between the hydroxy and amino groups (condensation with phosgene resulting in yields of 40-86%, and that with 4-chlorophenyl isothiocyanate in good yields of 67-82%). The ring closures of aminonaphthols **60**, **61**, **65** and **66** with oxo compounds (*i.e.* the insertion of an  $sp^3$  carbon) resulted in naphthoxazines (condensation with paraformaldehyde or 4-nitrobenzaldehyde) in really good yields 78-84%.
8. Compounds **83-85** and **87-89** in solution proved to be three-component tautomeric mixtures. The tautomeric ratio was influenced by the steric hindrance of the aromatic rings at position 1 or 4 and by the connecting position of the naphthyl rings at the same positions. The conformational analysis revealed that the conformation of the oxazine ring moiety depends on the hybridization of the carbon at position 3 or 2. The compounds containing an  $sp^3$  carbon preferred a twisted-chair conformation, whereas the insertion of an  $sp^2$  carbon led to a nearly flat naphthoxazine ring moiety.

## 5. ACKNOWLEDGEMENTS

This work was carried out in the Institute of Pharmaceutical Chemistry, University of Szeged, during the years 2004-2008.

I would like to express my warmest thanks to my supervisor, Professor Ferenc Fülöp, head of the Institute, for his guidance of my work, his inspiring ideas, his useful advice and his constructive criticism.

My warmest thanks are due to Dr. István Szatmári, for his continuous support and interest in my activities. His advice and help have been invaluable during all stages of my work.

I am greatly indebted to Professor Erich Kleinpeter, Department of Chemistry, University of Potsdam, for providing me with the opportunity to work for 4 months in his research group.

I am grateful to Dr. David Durham for revising the English language of my thesis.

I owe very much to my family, my colleagues and my friends for creating all the circumstances enabling me to carry out this work. Without their help, this thesis could not have been prepared.

## 6. REFERENCES

1. Pagett, L. O., Ed. *Encyclopedia of Reagents for Organic Synthesis*: Wiley, UK, 1995; Vol. 4, p. 2582.
2. Tramontini, M.; Angiolini, L. *Tetrahedron*, **1990**, *46*, 1791.
3. Szatmári, I.; Fülöp, F. *Curr. Org. Synth.*, **2004**, *1*, 155.
4. Betti, M. *Gazz. Chim. Ital.*, **1901**, *31 II*, 170.
5. Betti, M. *Gazz. Chim. Ital.*, **1901**, *31 II*, 191.
6. Betti, M. *Org. Synth. Coll. Vol.*, **1941**, *1*, 381.
7. Lázár, L.; Fülöp, F. *Eur. J. Org. Chem.*, **2003**, *16*, 3025.
8. Valters, R. E.; Fülöp, F.; Korbonits, D. *Adv. Heterocyclic Chem.*, **1996**, *66*, 1.
9. Szatmári, I.; Martinek, T. A.; Lázár, L.; Fülöp, F. *Tetrahedron*, **2003**, *59*, 2877.
10. Szatmári, I.; Martinek, T. A.; Lázár, L.; Koch, A.; Kleinpeter, E.; Neuvonen, K.; Fülöp, F. *J. Org. Chem.*, **2004**, *69*, 3645.
11. Szatmári, I.; Martinek, T. A.; Lázár, L.; Fülöp, F. *Eur. J. Org. Chem.* **2004**, *10*, 2231.
12. Szatmári I.; Hetényi A.; Lázár L.; Fülöp F. *J. Heterocyclic Chem.*, **2004**, *41*, 367.
13. Heydenreich, M.; Koch, A.; Klod, S.; Szatmári, I.; Fülöp, F.; Kleinpeter, E. *Tetrahedron*, **2006**, *62*, 11081.
14. Larsen R. D.; Corley E. G.; King A. O.; Carrol J.D.; Davis P.; Verhoeven T. R.; Reider P. J.; Labelle M.; Gauthier J. Y.; Xiang Y. B.; Zamboni R. J. *J. Org. Chem.* **1996**, *61*, 3398.
15. Chen Y. L.; Fang K. C.; Shen J. Y.; Hsu S. L.; Tzeng C. C. *J. Med. Chem.* **2001**, *44*, 2374.
16. Kalluraya B.; Sreenivasa S. *Il Farmaco* **1998**, *53*, 399.
17. Doube D.; Blouin M.; Brideau C.; Chan C.; Desmarais S.; Eithier D.; Falguyret J. P.; Friesen R. W.; Girard M.; Girard Y.; Guay J.; Tagari P.; Young R. N. *Bioorg. Med. Chem. Lett.* **1998**, *8*, 1255.
18. Maguire M. P.; Sheets K. R.; McVety K.; Spada A. P.; Zilberstein A. *J. Med. Chem.* **1994**, *38*, 2129.
19. Palmieri, G. *Eur. J. Org. Chem.* **1999**, *4*, 805.
20. Phillips, J. P.; Keown, R. W.; Fernando, Q. *J. Org. Chem.*, **1954**, *19*, 907.
21. Nath, J. P.; Dash, M.; Satrusallya, S. C.; Mahapatra, G. N. *Ind. J. Chem.*, **1981**, *7*, 606.
22. Shimizu, S.; Shimada, N.; Sasaki, Y. *Green Chem.* **2006**, *8*, 608.

- 
23. Lu, Y.; Nikolovska-Colevska, Z.; Fang X.; Gao, W.; Shangary, S.; Qiu, S.; Quin, D.; Wang, S. *J. Med. Chem.* **2006**, *49*, 3759.
24. Patel M.; McHugh R. J.; Beverly J. *Bioorg. Med. Chem. Lett.* **1999**, *9*, 3221.
25. El-Shafei H. A.; Badr-Eldin S. M. *Egypt J. Microbiol.* **1994**, *27*, 353.
26. Waxman L.; Darke P. L. *Antiviral Chem. Chemother.* **2000**, *11*, 1.
27. Girgis A. S. *Pharmazie* **2000**, 466.
28. Latif N.; Mishriky N.; Assad F. M. *Aust. J. Chem.* **1982**, *35*, 1037.
29. Patel M.; Ko S. S.; McHugh R. J. Jr.; Markwalder J. A.; Srivastave A. S.; Cordova B. C.; Klabe R. M; Ericson-Viitanen S.; Trainor G. L.; Seitz S. P. *Bioorg. Med. Chem. Lett.* **1999**, *9*, 2805.
30. Toyama, M.; Otomasu, H. *Chem. Pharm. Bull.* **1985**, *33*, 5543.
31. Möhrle, H.; Miller, C. *Monatsh. Chem.* **1974**, *105*, 1151.
32. Pirrone, P. *Gazzetta*, **1940**, *70*, 520.
33. Pirrone, P. *Gazzetta*, **1941**, *71*, 320.
34. Phillips, J. P.; Keown, R.; Frenando Q. *J. Am. Chem. Soc.*, **1953**, *75*, 4306.
35. Sen, A. B.; Saxena, M. S. *J. Ind. Chem. Soc.*, **1956**, *33*, 62.
36. Wagner, H.; Woerhammer, R.; Wolff, P. *Biochem. Z.*, **1961**, *334*, 175.
37. Chaturvedi, K. K.; Goyal, M. *J. Ind. Chem. Soc.*, **1984**, *61*, 175.
38. Möhrle, H.; Miller, C.; Wendisch D. *Chem. Ber.* **1974**, *107*, 2675.
39. Szatmári, I.; Fülöp, F. *Synthesis*, **2009**, *5*, 775.
40. Cimorelli, C.; Mazzanti, A.; Palmieri, G.; Volpini, E. *J. Org. Chem.* **2001**, *66*, 4759.
41. Saidi, M. R.; Hydari A.; Ipaktschi J. *Chem. Ber.* **1994**, *127*, 1761.
42. Saidi, M. R.; Khalaji, H. R.; Ipaktschi, J. *J. Chem. Soc., Perkin Trans. 1* **1997**, *13*, 1983.
43. Saidi, M- R.; Khalaji, H. R. *J. Chem. Res. (S)* **1997**, 340.
44. Mojtahedi, M., M., Sharifi, A.; Mohsenzadeh, F.; Saidi, M. R. *Synth. Commun.* **2000**, *30*, 69.
45. Arend, M.; Westermann, B.; Risch, N. *Angew. Chem., Int. Ed.* **1998**, *37*, 1044.
46. Naimi-Jamal, M. R.; Mojtahedi, M. M.; Ipaktschi, J.; Saidi, M. R. *J. Chem. Soc., Perkin Trans. 1* **1999**, *24*, 3709.
47. Naimi-Jamal, M. R.; Ipaktschi, J.; Saidi, M. R. *Eur. J. Org. Chem.*, **2000**, *9*, 1735.
48. Saidi M. R.; Azizi N.; Zali-Boinee, H. *Tetrahedron*, **2001**, *57*, 6829.
49. Saidi; M. R.; Azizi, N.; Naimi-Jamal, M. R. *Tetrahedron Lett.*, **2001**, *42*, 8111.
50. Phillips, J. P.; Duckwall, A. L. *J. Am. Chem. Soc.*, **1955**, *77*, 5504.
51. Phillips, J. P.; Barrall, E. M. *J. Org. Chem.*, **1956**, *21*, 692.
52. Sen, A. B.; Saxena, M. S.; Mehrotra, S. *J. Ind. Chem. Soc.*, **1960**, *37*, 640.

- 
53. Miyano, S.; Abe, N.; Abe, A.; Hamachi, K. *Chem. Pharm. Bull.*, **1971**, *19*, 1131.
54. S. D. Rubbo, *Rept. Proc. 4th Intern. Congr. Microiol.*, **1949**, 1947, 149; *Chem. Abs.*, **1949**, *43*, 9163 i.
55. Zentmyer, G. A. *Science*, **1944**, *100*, 294
56. Morel, A.; Rochaix, A.; Delaborde, H. *Compt. rend. Soc. Biol.*, **1935**, *119*, 612.
57. Acharya, J. N.; Thaker K. A. *J. Ind. Chem. Soc.*, **1976**, *53*, 172.
58. Shaabani, A.; Rahmati, A.; Farhangi, E. *Tetrahedron Lett.*, **2007**, *48*, 7291.
59. Mosslemin, M. H.; Nateghi, M. R.; Mohebat, R. *Monatsh. Chem.*, **2008**, *139*, 1247.
60. Shakibaei, G. I.; Khavasi, H. R.; Mirzaei, P.; Bazgir, A. *J. Heterocyclic Chem.*, **2008**, *45*, 1481.
61. Kappe, C. O. *Angew. Chem., Int. Ed.* **2004**, *43*, 6250.
62. De Tarr, D. F.; Delahunty C. *J. Am. Chem. Soc.* **1983**, *105*, 2734.
63. Charton, M. *J. Am. Chem. Soc.* **1975**, *97*, 1552.
64. Charton, M. *J. Org. Chem.* **1976**, *41*, 2217.
65. Meyer, A. Y. *J. Chem. Soc., Perkin Trans. 2* **1986**, *10*, 1567.
66. SPSS Advanced Models 11.0, SPSS Inc., Chicago, IL.
67. Foresman, J. B.; Keith, T. A.; Wiberg, K. B.; Snoonian, J.; Frisch, M. J., *J. Phys. Chem.* **1996**, *100*, 16098.
68. Meyer, A. Y., *J. Chem. Soc., Perkin Trans. 2* **1986**, *2*, 1567.
69. SPSS Advanced Models 13.0, SPSS Inc., Chicago, IL.
70. Neuvonen, K.; Fülöp, F.; Neuvonen, H.; Koch, A.; Kleinpeter, E.; Pihlaja, K. *J. Org. Chem.* **2001**, *66*, 4132.
71. Neuvonen, K.; Fülöp, F.; Neuvonen, H.; Pihlaja, K. *J. Org. Chem.* **1994**, *59*, 5895.
72. Neuvonen, K.; Fülöp, F.; Neuvonen, H.; Simeonov, M.; Pihlaja, K. *J. Phys. Org. Chem.* **1997**, *10*, 55.
73. Ehrenson, S.; Brownlee, R. T. C.; Taft, R. W. *Prog. Phys. Org. Chem.* **1973**, *10*, 1.
74. Craik, D. J.; Brownlee, R. T. C. *Prog. Phys. Org. Chem.* **1983**, *14*, 1.
75. Reynolds, W. F. *Prog. Phys. Org. Chem.* **1983**, *14*, 165.
76. Kawasaki, A. *J. Chem. Soc., Perkin Trans. 2* **1990**, *2*, 223-228.
77. Shen, A. Y.; Tsai, C. T.; Chen, C. L. *Eur. J. Med. Chem.*, **1999**, *34*, 877.
78. Shaterian, H. R.; Yarahmadi, H. *Tetrahedron Lett.*, **2008**, *49*, 1297.
79. Shaterian, H. R.; Yarahmadi, H.; Ghashang, M. *Tetrahedron*, **2008**, *64*, 1263.
80. Shaterian, H. R.; Yarahmadi, H.; Ghashang, M. *Bioorg. Med. Chem. Lett.*, **2008**, *18*, 788.
81. Duff, C.; Bills E. J. *J. Chem. Soc.* **1934**, 1305.

- 
82. Turgut, Z.; Pelit, E.; Köycü, A. *Molecules*, **2007**, *12*, 345.
83. Stewart, J. J. P. *Comp. Chem.*, **1989**, *10*, 209.
84. Stewart, J. J. P. *Comp. Chem.*, **1989**, *10*, 221.
85. Hehre, W. J.; Radom, L.; Schleyer P. v. R.; Pople, J. A., Pople, *Ab Initio Molecular Orbital Theory* Wiley, New York, **1986**.
86. Becke, A. D. *J. Chem. Phys.* **1993**, *98*, 1372.
87. Helgaker, T.; Watson, M.; Handy, N. C. *J. Chem. Phys.* **2000**, *113*, 9402.
88. Barone V.; Peralta, J. E.; Contreras, R. H.; Snyder, J. P. *J. Phys. Chem.* **2002**, *106*, 5607.
89. SYBYL 7.3, Tripos Inc., 1699 South Hanley Rd. St. Louis, MO 63144, USA **2006**.
90. GaussView 2.0, Gaussian Inc. Carnegie Office Park, Building 6, Pittsburgh, PA 15106, USA.

## **ANNEX**

**I.**



## FULL PAPER

DOI: 10.1002/ejoc.200600447

Substituent Effects in the Ring–Chain Tautomerism of 1-Alkyl-3-arylnaphth-[1,2-*e*][1,3]oxazinesDiana Tóth,<sup>[a]</sup> István Szatmári,<sup>[a]</sup> and Ferenc Fülöp<sup>\*[a]</sup>*Dedicated to Professor Erich Kleinpeter on the occasion of his 60th birthday***Keywords:** Aminonaphthols / Naphthoxazines / Betti bases / Substituent effects / Ring-chain tautomerism

New 1-(1-aminoalkyl)-2-naphthols **8–11** have been synthesised by the condensation of 2-naphthol with aliphatic aldehydes in the presence of ammonia, followed by acidic hydrolysis. The condensation of **7–11** with substituted benzaldehydes after microwave irradiation led to 1-alkyl-3-aryl-2,3-dihydro-1*H*-naphth[1,2-*e*][1,3]oxazines, which proved to be three-component (*r*<sup>4</sup>-*o*-*r*<sup>3</sup>) tautomeric mixtures in CDCl<sub>3</sub> at 300 K. The electronic effects of the 1-alkyl and 3-aryl groups on the tautomeric ratios could be determined for both the ring<sup>*trans*</sup>-chain and the ring<sup>*cis*</sup>-chain equi-

libria with the aid of two-variant linear equations. A significant difference was found between the coefficients of the Meyer parameter *V*<sup>a</sup>, which characterises the volume of the portion of the alkyl substituent within 0.3 nm of the reaction centre, for ring<sup>*trans*</sup>-chain and ring<sup>*cis*</sup>-chain equilibria, and this is explained in terms of the stereoelectronic effect caused by the alkyl substituent at position 1.

(© Wiley-VCH Verlag GmbH & Co. KGaA, 69451 Weinheim, Germany, 2006)

## Introduction

The structures and reactivities of numerous five- and six-membered, saturated, 1,3-X,N-heterocycles (X = O, S, NR) can be characterised by the ring–chain tautomeric equilibria of these heterocycles and the corresponding Schiff bases. Oxazolidines and tetrahydro-1,3-oxazines are the saturated 1,3-X,N-heterocycles whose ring–chain tautomerism has been studied most thoroughly. From quantitative studies on their tautomeric equilibria, it has been concluded that the tautomeric ratios for oxazolidines and tetrahydro-1,3-oxazines bearing a substituted phenyl group at position 2 can be characterised by an aromatic substituent dependence [Equation (1)]

$$\log K_X = \rho\sigma^+ + \log K_{X=H} \quad (1)$$

where  $K_X$  is the [ring]/[chain] ratio and  $\sigma^+$  is the Hammett–Brown parameter (electronic character) of substituent X on the 2-phenyl group.<sup>[1,2]</sup>

The scope and limitations of Equation (1) have been thoroughly studied from the point of view of the applicability of this equation in the case of complex tautomeric mixtures containing several types of open and/or cyclic forms, and the influence of the steric and/or electronic ef-

fects of the substituents at positions other than 2 on the parameters in this equation.<sup>[3–8]</sup>

Our quantitative investigations on the ring–chain tautomeric equilibria of 1,3-diaryl-2,3-dihydro-1*H*-naphth[1,2-*e*][1,3]oxazines have led to the first precise mathematical formulae with which to characterise the effects of substituents situated elsewhere than between the heteroatoms. For example, we have demonstrated that the tautomeric ratio is influenced not only by the aryl substituent at position 3, but also by that at position 1. This additional stabilisation effect was explained as an anomeric effect in the *trans* ring form.<sup>[9]</sup> When the tautomeric equilibria of 3-alkyl-1-aryl-2,3-dihydro-1*H*-naphth[1,2-*e*][1,3]oxazines were analysed, the results of multiple linear regression analysis of the  $\log K_R$  values revealed a significant dependence on the inductive effect of substituent Y ( $\sigma_F$ ), which was further evidence of the anomeric effect in the *trans* ring form.<sup>[9]</sup> Systematic quantitative investigations on the ring–chain tautomeric equilibria of 2,4-diarylnaphth[2,1-*e*][1,3]oxazines have demonstrated an analogous inductive influence on the ring<sup>*trans*</sup>-chain tautomeric equilibria.<sup>[10]</sup>

The stereoelectronic effect relating to the relative configurations of C-1 and C-3 in these naphthoxazines could originate from the aryl substituent at position 1. There appears to be no published examples of the study of such effects of an alkyl group at the same position. We therefore set out to synthesise and investigate the substituent effects in a new 1,3-disubstituted naphthoxazine model system bearing an

[a] Institute of Pharmaceutical Chemistry, University of Szeged, P. O. Box 427, 6701 Szeged, Hungary  
Fax: +36-62-545705  
E-mail: fulop@pharm.u-szeged.hu

alkyl substituent at position 1 and an aryl substituent at position 3.

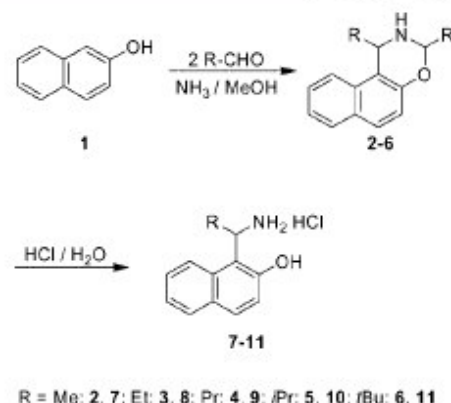
## Results and Discussion

One hundred years ago, Betti reported a straightforward synthesis of 1-( $\alpha$ -aminobenzyl)-2-naphthol (the Betti base) from 2-naphthol, benzaldehyde and ammonia.<sup>[11]</sup> The Betti procedure can be interpreted as an extension of the Mannich condensation, with formaldehyde replaced by an aromatic aldehyde, the secondary amine by ammonia and the C–H acid by an electron-rich aromatic compound, such as 2-naphthol.<sup>[11,12]</sup> As a consequence of the potential utility of Mannich-type phenolic bases, the aminoalkylation of naphthol derivatives is a subject of current chemical interest.<sup>[12]</sup>

The classical Betti procedure has generally been confined to the use of aromatic aldehydes (e.g. benzaldehyde) as the aldehyde component,<sup>[12]</sup> and only a few examples are known where benzaldehyde has been replaced by some other aldehyde. For the synthesis of the desired model compounds, our interest focused on the application of aliphatic aldehydes in the Betti reaction. Formaldehyde was the first aliphatic aldehyde to be used in this three-component reaction.<sup>[13,14]</sup> For the preparation of 1-(1-aminoethyl)-2-naphthol, the classical Betti procedure was altered: the intermediate naphthoxazine was formed by refluxing 2-naphthol, acetaldehyde and ammonia in benzene to give 1,3-dimethyl-2,3-dihydro-1*H*-naphth[1,2-*e*][1,3]oxazine. Acidic hydrolysis of this led to 1-(1-aminoethyl)-2-naphthol hydrochloride in an overall yield of 70%.<sup>[15]</sup> A different synthetic pathway was applied to produce 1-(1-amino-2,2,2-trifluoroethyl)-2-naphthol, namely the preparation of 1-[2,2,2-trifluoro-1-(1-naphth-1-yl-ethylamino)ethyl]-2-naphthol, followed by catalytic hydrogenation.<sup>[16,17]</sup>

In our experiments, naphthoxazines 2–6 were formed by the condensation of 2-naphthol (1) and the corresponding aliphatic aldehyde in the presence of methanolic ammonia solution in absolute methanol at 60 °C for 6–72 h (Scheme 1). The acidic hydrolysis of 2–6 led to the desired aminonaphthol hydrochlorides 7–11 in low yields in a two-step process. The overall yield was improved considerably when the solvent was evaporated off after the formation of the intermediate naphthoxazines (2–6) and the residue was directly hydrolysed with hydrochloric acid (e.g. for compound 7 the overall yield could be increased from 15% to 95%).

Because of the instability of the Betti base derivatives, compounds 7–11 were isolated as hydrochlorides, which in subsequent transformations were basified *in situ* with triethylamine. The condensation of aminonaphthols 7–11 with one equivalent of aromatic aldehyde in absolute methanol in the presence of triethylamine at ambient temperature did not lead to the formation of the desired naphthoxazines. This failure was followed by a more modern attempt to synthesise our target compounds: microwave irradiation treatment<sup>[18]</sup> was tried, and in this way the preparation of 12–



Scheme 1.

16 was successful. After the controlled microwave agitation (CEM microwave reactor, 10 min at 80 °C), the mixture was left to stand at room temperature to crystallise.

The <sup>1</sup>H NMR spectra of 12–15 reveal that, in CDCl<sub>3</sub> solution at 300 K, the members a–g of each set of compounds 12–15 exist in three-component ring–chain tautomeric mixtures containing the C-3 epimeric naphthoxazines (B and C) and also the open tautomer (A). The proportion of the ring forms decreases as the alkyl substituent at position 1 becomes more bulky. Accordingly, for some 1-isopropyl-3-arylnaphthoxazine derivatives (15) the proportions of the ring forms (B and C) were close to the limiting error and in the case of 16 only the derivatives 16a, 16e and 16f were synthesised. As expected, ring forms B and C of compounds 16 (Scheme 2) were not found at all in the tautomeric mixture. In order to acquire reliable results, more sample data were needed and the series of compounds was therefore expanded to include naphthoxazines 18. The tautomeric behaviour of analogues 18 (18a, 18d–g) is known from the literature, but compounds 18b and 18c were absent and were therefore synthesised according to Scheme 3.<sup>[14]</sup>

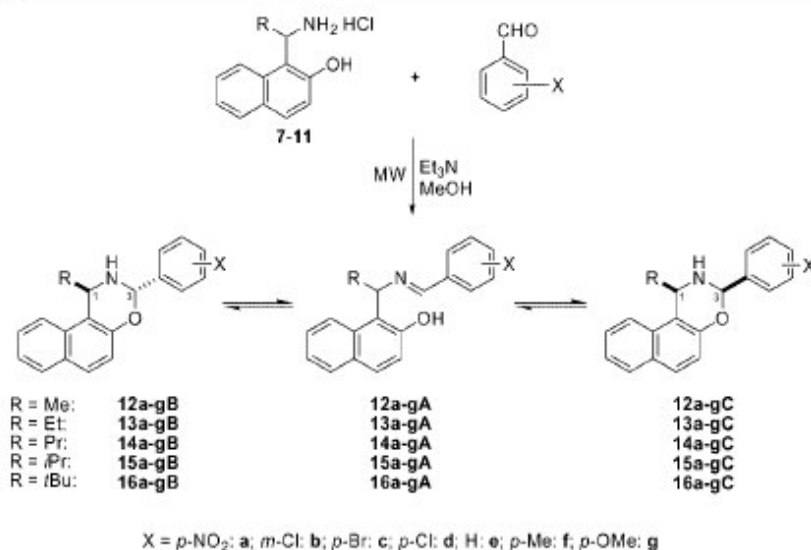
Table 1 shows the proportions of the diastereomeric ring forms (B and C) from the tautomeric equilibria of 12–16 and 18, as determined by integration of the well-separated O–CHAr–N (ring) and N=CHAr (chain) proton signals in the <sup>1</sup>H NMR spectra. As a consequence of the very similar NMR spectroscopic characteristics of 1-alkyl-3-aryl-2,3-dihydro-1*H*-naphth[1,2-*e*][1,3]oxazines 12–16, only the data for 12a were chosen to illustrate the <sup>1</sup>H NMR spectra of the prepared tautomeric compounds (see Exp. Sect.).

To study the double substituent dependence of log *K<sub>B</sub>* and log *K<sub>C</sub>*, the following Hansch-type quantitative structure-properties relationship model equation [Equation (2)] was set up

$$\log K_{B/C} = k + \rho^R P^R + \rho^X \sigma^{+X} \quad (2)$$

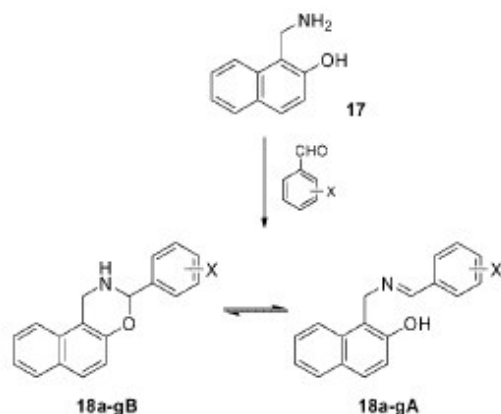
where *K<sub>B</sub>* = [B]/[A], *K<sub>C</sub>* = [C]/[A], *P<sup>R</sup>* is an alkyl substituent parameter and  $\sigma^{+X}$  is the Hammett–Brown parameter of the aryl substituent at position 3. In order to find the accurate dependence of log *K<sub>B/C</sub>*, three different alkyl substituent parameters were studied: *E<sub>s</sub>* (calculated from the hydrolysis





Scheme 2.

or aminolysis of esters)<sup>[19]</sup> and two other steric parameters that are independent of any kinetic data, namely  $v$ , derived from the van der Waals radii,<sup>[20,21]</sup> and  $V^a$ , the volume of the portion of the substituent that is within 0.3 nm of the reaction centre.<sup>[22]</sup>



Scheme 3.

Multiple linear regression analysis of Equation (2) was performed with the SPSS statistical software, and a value of 0.05 was chosen as the significance level.<sup>[23]</sup> Good correlations were found for all three alkyl substituent parameters. The linear regression analysis data for the series 12–15 and 18 are given in Table 2. The best correlations were observed for the Meyer parameter ( $V^a$ ) of the alkyl substituents, and this was used for the further examinations.

Table 2. Multiple linear regression analysis of  $\log K_B$  and  $\log K_C$  values for 12–15 and 18.

		$k$	$\rho^R$	$\rho^X$	$r$
$\rho^R =$	12–15,18B=12–15,18A	0.605	–0.320	0.848	0.965
	12–15,18C=12–15,18A	0.413	–0.464	0.978	0.994
$\rho^R = E_s$	12–15,18B=12–15,18A	0.609	0.948	0.809	0.938
	12–15,18C=12–15,18A	0.524	1.442	0.881	0.992
$\rho^R = v$	12–15,18B=12–15,18A	0.624	–2.250	0.822	0.946
	12–15,18C=12–15,18A	0.516	–3.356	0.886	0.994

The parameters given in Table 2 indicate that the tautomeric interconversion (e.g.  $\log K_B$  and  $\log K_C$  values) can be described by using two substituent parameters ( $V^a$  and  $\sigma^+$ ),

Table 1. Proportions [%] of the ring-closed tautomeric forms (B and C) in tautomeric equilibria for compounds 12–16 and 18 (CDCl<sub>3</sub>, 300 K).

Compound	X	R $V^a$ $\sigma^+$	18	12	C	13	C	14	C	15	C	16	C
			H 0 B	Me 2.84 B		Et 4.31 B		Pr 4.78 B		<i>i</i> Pr 5.74 B		<i>t</i> Bu 7.16 B	
a	<i>p</i> -NO <sub>2</sub>	0.79	95.2	70.3	10.0	59.4	4.8	60.3	4.4	8.9	~0	~0	~0
b	<i>m</i> -Cl	0.40	86.5	52.8	7.7	21.3	6.8	25.3	2.6	3.5	2.5	–	–
c	<i>p</i> -Br	0.15	81.1	39.5	6.0	26.5	2.7	23.4	1.5	1.2	0.7	–	–
d	<i>p</i> -Cl	0.11	79.4	39.4	6.3	25.2	2.2	24.8	1.5	1.8	1.1	–	–
e	H	0	72.3	30.4	5.2	18.4	1.9	12.8	~0	~0	~0	~0	~0
f	<i>p</i> -Me	–0.31	58.3	18.0	2.5	11.6	~0	9.1	~0	~0	~0	~0	~0
g	<i>p</i> -OMe	–0.78	45.4	10.9	1.7	3.5	~0	3.9	~0	~0	~0	–	–

which means that, when  $\log K_B$  or  $\log K_C$  is plotted against the Meyer parameter ( $\rho^A$ ) and the Hammett–Brown parameter ( $\sigma^+$ ), a plane can be fitted to the data points (Figure 1, a and b).

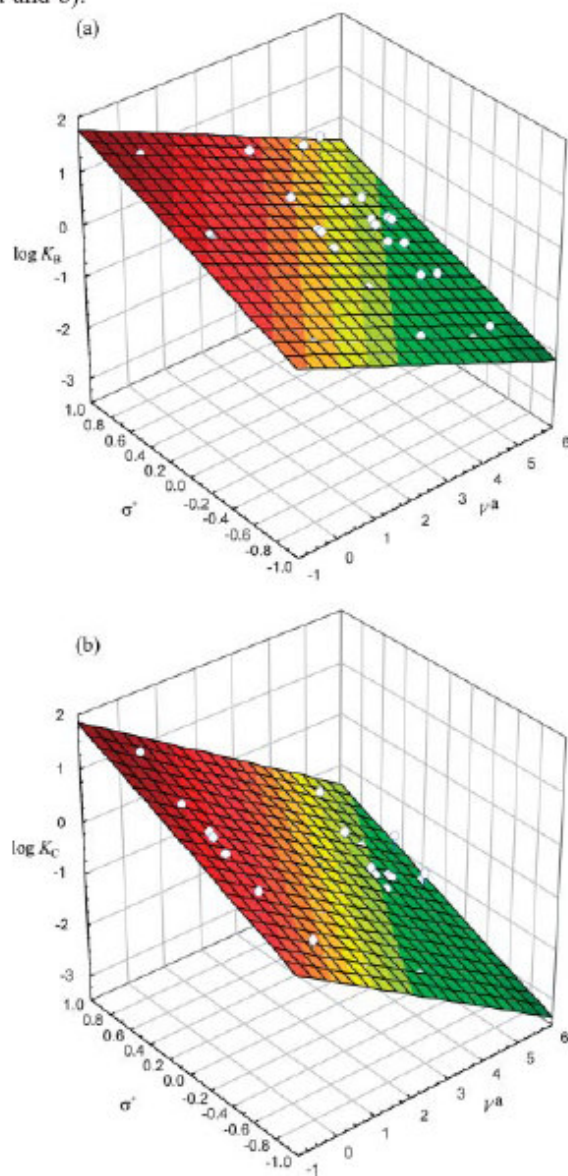


Figure 1. (a) Plots of  $\log K_B$  for 12–15B and 18B vs. Meyer ( $\rho^A$ ) and Hammett–Brown parameters ( $\sigma^+$ ). (b) Plots of  $\log K_C$  for 12–15C and 18C vs. Meyer ( $\rho^A$ ) and Hammett–Brown parameters ( $\sigma^+$ ).

The slopes of the alkyl substituent parameters ( $\rho^R$ ) for the equilibria  $B \rightleftharpoons A$  and  $C \rightleftharpoons A$  exhibit a significant difference (–0.320 vs. –0.464). This difference can be explained by an additional stabilisation effect caused by the alkyl substituents.

## Conclusions

New alkyl-substituted Betti base analogue aminonaphthols have been synthesised from aliphatic aldehydes. The

reactions of these aminoalkynaphthol derivatives with substituted benzaldehydes lead to 1-alkyl-3-aryl-2,3-dihydro-1H-naphth[1,2-e][1,3]oxazines, which have proved to be three-component tautomeric mixtures in  $CDCl_3$  at 300 K, involving C-3 epimeric naphthoxazines (B and C) and the open tautomer (A). The influence of the alkyl substituent at position 1 on the ring-chain tautomeric equilibria can be described by the Meyer parameter, and that of the aryl substituent at position 3 by the Hammett–Brown parameter ( $\sigma^+$ ). Linear equations have been found that describe the double substituent dependence of the equilibrium constants for both the *trans*-chain and *cis*-chain equilibria. The slopes of the Meyer parameter  $\rho^A$  for the *trans* and *cis* forms display a significant difference, which is explained in terms of an alkyl-substituent-controlled stereoelectronic effect in the *trans* ring form. Theoretical examinations of this alkyl substituent effect and its connection with the preferred geometry (relating to the relative configurations of C-1 and C-3) are still in progress.

## Experimental Section

Melting points were determined with a Kofler micro melting apparatus and are uncorrected. Elemental analyses were performed with a Perkin–Elmer 2400 CHNS elemental analyser. Merck Kiesegel 60  $F_{254}$  plates were used for TLC. The  $^1H$  and  $^{13}C$  NMR spectra were recorded in  $CDCl_3$  or in  $[D_6]DMSO$  solution at 300 K with a Bruker Avance DRX400 spectrometer at 400.13 ( $^1H$ ) and 100.61 MHz ( $^{13}C$ ). Chemical shifts are given in  $\delta$  (ppm) relative to TMS as internal standard. For the equilibria of tautomeric compounds to be established, the samples were dissolved in  $CDCl_3$  and the solutions were allowed to stand at ambient temperature for 1 d before the  $^1H$  NMR spectra was run. The number of scans was usually 64.

**General Method for the Synthesis of 1-Aminoalkyl-2-naphthols 7–11:** The appropriate aliphatic aldehyde (62.5 mmol) and 25% methanolic ammonia solution (20 mL) were added to a solution of 2-naphthol (1; 3.6 g, 25 mmol) in absolute MeOH (30 mL). The mixture was then stirred at 60 °C for 4–72 h. The MeOH was removed under reduced pressure and intermediates 2–6 were suspended in 10% HCl (210 mL). The mixture was stirred and heated for 3 h at 60 °C, and the solvent was evaporated off. The crystalline hydrochloride of 7–11 that separated out from EtOAc (50 mL) was filtered off, washed with  $CHCl_3$  and  $Et_2O$ , and recrystallised from  $Et_2O/MeOH$  (4:1).

**1-(1-Aminoethyl)-2-naphthol Hydrochloride (7):** Condensation time: 4 h. White crystals, 5.02 g (95%), m.p. 210–212 °C.  $^1H$  NMR ( $[D_6]DMSO$ ):  $\delta$  = 1.62 (d,  $J$  = 6.55 Hz, 3 H,  $CH_3$ ), 5.07–5.17 (m, 1 H,  $CH_3CH$ ), 7.28–7.36 (m, 2 H, naphthyl), 7.52 (t,  $J$  = 7.55 Hz, 1 H, naphthyl), 7.80–7.87 (m, 2 H, naphthyl), 7.98 (d,  $J$  = 8.56 Hz, 1 H, naphthyl), 8.28 (s, 3 H,  $NH_3$ ), 10.84 (s, 1 H, OH) ppm.  $^{13}C$  NMR ( $[D_6]DMSO$ ):  $\delta$  = 18.4, 44.4, 115.1, 118.6, 121.4, 122.8, 127.0, 128.0, 128.7, 129.9, 131.4, 153.6 ppm.  $C_{12}H_{14}ClNO$  (223.70): calcd. C 64.43, H 6.31, N 6.26; found C 64.59, H 6.33, N 6.27.

**1-(1-Aminopropyl)-2-naphthol Hydrochloride (8):** Condensation time: 3 h. White crystals, 2.37 g (42%), m.p. 191–193 °C.  $^1H$  NMR ( $[D_6]DMSO$ ):  $\delta$  = 0.79 (t,  $J$  = 7.55 Hz, 3 H,  $CH_3$ ), 2.07–2.19 (m, 2 H,  $CH_2$ ), 4.94 (m, 4.83–4.94, 1 H,  $CH$ ), 7.33 (t,  $J$  = 7.55 Hz, 1 H, naphthyl), 7.39 (d,  $J$  = 8.56 Hz, 1 H, naphthyl), 7.50 (t,  $J$  = 7.55 Hz, 1 H, naphthyl), 7.83 (t,  $J$  = 8.06 Hz, 2 H, naphthyl), 8.02 (d,  $J$  =



## FULL PAPER

D. Tóth, I. Szatmári, F. Fülöp

8.56 Hz, 1 H, naphthyl), 8.32 (s, 3 H,  $\text{NH}_3$ ), 10.87 (s, 1 H, OH) ppm.  $^{13}\text{C}$  NMR ( $[\text{D}_6]\text{DMSO}$ ):  $\delta$  = 10.5, 25.2, 113.6, 118.4, 121.7, 122.6, 126.8, 127.9, 128.7, 130.0, 132.6, 153.8 ppm.  $\text{C}_{13}\text{H}_{16}\text{ClNO}$  (237.73): calcd. C 65.68, H 6.78, N 5.89; found C 65.45, H 6.77, N 5.89.

**1-(1-Aminobutyl)-2-naphthol Hydrochloride (9):** Condensation time: 72 h. White crystals, 1.71 g (27%), m.p. 202–204 °C.  $^1\text{H}$  NMR ( $[\text{D}_6]\text{DMSO}$ ):  $\delta$  = 0.82 (t,  $J$  = 7.55 Hz, 3 H,  $\text{CH}_3$ ), 0.98–1.13 (m, 1 H,  $\text{CH}_2\text{CH}_2$ ), 1.25–1.40 (m, 1 H,  $\text{CH}_2\text{CH}_2$ ), 1.98–2.18 (m, 2 H,  $\text{CH}_2\text{CH}$ ), 4.99 (s, 1 H,  $\text{CH}_2\text{CH}$ ), 7.19–7.52 (m, 3 H, naphthyl), 7.82 (t,  $J$  = 9.06 Hz, 2 H, naphthyl), 7.99 (d,  $J$  = 8.56 Hz, 1 H, naphthyl), 8.29 (s, 3 H,  $\text{NH}_3$ ), 10.82 (s, 1 H, OH) ppm.  $^{13}\text{C}$  NMR ( $[\text{D}_6]\text{DMSO}$ ):  $\delta$  = 13.8, 18.9, 34.2, 113.9, 118.5, 121.9, 122.6, 126.9, 127.9, 128.7, 129.9, 133.0, 153.9 ppm.  $\text{C}_{14}\text{H}_{18}\text{ClNO}$  (251.75): calcd. C 66.79, H 7.21, N 5.56; found C 66.81, H 7.22, N 5.57.

**1-(1-Amino-2-methylpropyl)-2-naphthol Hydrochloride (10):** Condensation time: 72 h. White crystals, 5.03 g (80%), m.p. 229–232 °C.  $^1\text{H}$  NMR ( $[\text{D}_6]\text{DMSO}$ ):  $\delta$  = 0.65 (d,  $J$  = 6.04 Hz, 3 H,  $\text{CH}_3$ ), 1.18 (d,  $J$  = 6.56 Hz, 3 H,  $\text{CH}_3$ ), 2.26 (s, 1 H,  $\text{CH}_2\text{CH}$ ), 4.63 (s, 1 H,  $\text{CH}_2\text{CHCH}$ ), 7.31 (t,  $J$  = 7.05 Hz, 2 H, naphthyl), 7.41 (s, 1 H, naphthyl), 7.82 (t,  $J$  = 9.06 Hz, 2 H, naphthyl), 8.01 (d,  $J$  = 8.05 Hz, 1 H, naphthyl) ppm.  $^{13}\text{C}$  NMR ( $[\text{D}_6]\text{DMSO}$ ):  $\delta$  = 19.8, 30.4, 54.1, 114.2, 118.5, 121.8, 122.6, 126.8, 127.8, 128.7, 129.9, 132.9, 153.8 ppm.  $\text{C}_{14}\text{H}_{18}\text{ClNO}$  (251.75): calcd. C 66.79, H 7.21, N 5.56; found C 66.31, H 7.19, N 5.55.

**1-(1-Amino-2,2-dimethylpropyl)-2-naphthol Hydrochloride (11):** 2-Naphthol: 0.56 g (3.88 mmol); condensation time: 72 h. White crystals, 0.39 g (38%), m.p. 236–239 °C.  $^1\text{H}$  NMR ( $[\text{D}_6]\text{DMSO}$ ):  $\delta$  = 1.04 [s, 9 H,  $(\text{CH}_3)_3\text{C}$ ], 4.86 (d,  $J$  = 4.03 Hz, 1 H, CCHN), 7.318 (t,  $J$  = 7.55 Hz, 1 H, naphthyl), 7.39 (d,  $J$  = 9.07 Hz, 1 H, naphthyl), 7.49 (t,  $J$  = 7.55 Hz, 1 H, naphthyl), 7.82 (d,  $J$  = 9.06 Hz, 2 H, naphthyl), 8.04 (d,  $J$  = 8.56 Hz, 1 H, naphthyl), 8.21 (s, 3 H,  $\text{NH}_3$ ), 10.80 (s, 1 H, OH) ppm.  $^{13}\text{C}$  NMR ( $[\text{D}_6]\text{DMSO}$ ):  $\delta$  = 28.3, 37.9, 57.7, 113.2, 119.8, 123.4, 123.7, 127.5, 128.8, 129.5, 130.9, 134.3, 154.9 ppm.  $\text{C}_{15}\text{H}_{20}\text{ClNO}$  (265.2): calcd. C 67.72, H 7.54, N 5.27; found C 67.49, H 7.53, N 5.28.

**General Method for the Synthesis of 1-Alkyl-3-aryl-2,3-dihydro-1H-naphth[1,2-e][1,3]oxazines (12–16 and 18):** The aminonaphthol (0.39 mmol), one equivalent of X-substituted benzaldehyde, 1.1 equiv. of  $\text{Et}_3\text{N}$  and absolute MeOH (7 mL) were mixed in a 10-mL pressurized reaction vial, which was heated for 10 min at 80 °C in a CEM microwave reactor. The crystalline product was filtered off, and washed with MeOH. All of the new compounds 12–16 and 18 gave satisfactory elemental analysis data (C, H, N  $\pm 0.3\%$ ). The compounds were recrystallised from  $\text{dPr}_2\text{O}$ . The physical and analytical data for compounds 12–16 and 18 are listed in Table 3.

As regards the similarities in the  $^1\text{H}$  NMR spectroscopic data, a full characterisation is reported only for compound 12a. The  $^1\text{H}$  NMR chemical shifts of the characteristic O-CHAr-N protons of

Table 3. Physical, analytical and NMR spectroscopic data for naphth[1,2-e][1,3]oxazines 12–16 and 18.

Compd.	M.p. [°C]	Yield [%]	Formula	MW	Elemental analysis			$\delta$ [ppm]	N-CH-O	N-CH-O
					C found (calcd.)	H found (calcd.)	N found (calcd.)	(A)	(B)	(C)
12a	155–158	64	$\text{C}_{19}\text{H}_{16}\text{N}_2\text{O}_3$	320.35	71.04 (71.24)	5.04 (5.03)	8.75 (8.74)	8.62	6.15	5.73
12b	135–138	59	$\text{C}_{19}\text{H}_{16}\text{ClNO}$	309.80	73.02 (73.66)	5.21 (5.21)	4.52 (4.52)	8.44	6.03	5.60
12c	176–178	51	$\text{C}_{19}\text{H}_{16}\text{BrNO}$	354.25	64.65 (64.42)	4.53 (4.55)	3.94 (3.95)	8.42	6.01	5.58
12d	178–180	60	$\text{C}_{19}\text{H}_{16}\text{ClNO}$	309.80	73.46 (73.66)	5.22 (5.21)	4.51 (4.52)	8.44	6.03	5.60
12e	119–121	56	$\text{C}_{19}\text{H}_{17}\text{NO}$	275.35	83.05 (82.88)	6.23 (6.22)	5.11 (5.09)	8.46	6.06	5.53
12f	145–148	54	$\text{C}_{20}\text{H}_{19}\text{NO}$	289.38	83.55 (83.01)	6.63 (6.62)	4.85 (4.84)	8.42	6.04	5.59
12g	131–132	67	$\text{C}_{20}\text{H}_{19}\text{NO}_2$	305.38	78.56 (78.66)	6.28 (6.27)	4.58 (4.59)	8.41	6.06	5.62
13a	121–124	71	$\text{C}_{20}\text{H}_{18}\text{N}_2\text{O}_3$	334.38	72.01 (71.84)	5.42 (5.43)	8.39 (8.38)	8.56	6.09	5.72
13b	145–149	33	$\text{C}_{20}\text{H}_{18}\text{ClNO}$	323.83	73.90 (74.18)	5.62 (5.60)	4.34 (4.33)	8.38	5.97	5.79
13c	97–100	55	$\text{C}_{20}\text{H}_{18}\text{BrNO}$	368.28	65.32 (65.23)	4.91 (4.93)	3.80 (3.80)	8.37	5.95	5.57
13d	170–172	32	$\text{C}_{20}\text{H}_{18}\text{ClNO}$	323.83	74.42 (74.18)	5.62 (5.60)	4.34 (4.33)	8.37	5.99	5.60
13e	158–160	56	$\text{C}_{20}\text{H}_{19}\text{NO}$	289.38	83.19 (83.01)	6.62 (6.62)	4.83 (4.84)	8.42	6.02	5.62
13f	181–185	15	$\text{C}_{21}\text{H}_{21}\text{NO}$	303.41	82.89 (83.13)	6.88 (6.89)	4.63 (4.62)	8.37	5.98	–
13g	160–163	42	$\text{C}_{21}\text{H}_{21}\text{NO}_2$	319.41	79.13 (78.97)	6.64 (6.63)	4.41 (4.39)	8.32	5.96	–
14a	133–136	76	$\text{C}_{21}\text{H}_{20}\text{N}_2\text{O}_3$	348.40	72.16 (72.40)	5.80 (5.79)	8.04 (8.04)	8.52	6.08	5.68
14b	114–116	33	$\text{C}_{21}\text{H}_{20}\text{ClNO}$	337.84	74.82 (74.66)	5.98 (5.97)	4.14 (4.15)	8.38	5.99	5.61
14c	148–150	47	$\text{C}_{21}\text{H}_{20}\text{BrNO}$	382.29	65.98 (66.14)	5.27 (5.28)	3.65 (3.66)	8.36	5.98	5.58
14d	122–125	43	$\text{C}_{21}\text{H}_{20}\text{ClNO}$	337.40	74.80 (74.66)	5.97 (5.97)	4.14 (4.15)	8.38	5.99	5.60
14e	101–103	20	$\text{C}_{21}\text{H}_{21}\text{NO}$	303.40	83.53 (83.13)	6.99 (6.98)	4.62 (4.62)	8.41	6.03	–
14f	129–130	21	$\text{C}_{22}\text{H}_{23}\text{NO}$	317.42	83.74 (83.24)	7.29 (7.30)	4.40 (4.41)	8.35	6.00	–
14g	128–131	38	$\text{C}_{22}\text{H}_{23}\text{NO}_2$	333.42	78.96 (79.25)	6.96 (6.95)	4.21 (4.20)	8.32	5.99	–
15a	139–140	52	$\text{C}_{21}\text{H}_{20}\text{N}_2\text{O}_3$	348.41	72.68 (72.40)	5.93 (5.79)	8.01 (8.04)	8.51	6.19	–
15b	153–155	48	$\text{C}_{21}\text{H}_{20}\text{ClNO}$	337.85	74.39 (74.66)	6.09 (5.97)	4.21 (4.15)	8.34	6.10	5.51
15c	121–125	36	$\text{C}_{21}\text{H}_{20}\text{BrNO}$	382.30	65.76 (65.98)	5.07 (5.27)	3.50 (3.66)	8.34	6.08	5.51
15d	139–141	45	$\text{C}_{21}\text{H}_{20}\text{ClNO}$	337.85	74.93 (74.66)	5.83 (5.97)	4.10 (4.15)	8.35	6.10	5.52
15e	125–129	34	$\text{C}_{21}\text{H}_{21}\text{NO}$	303.41	83.11 (83.24)	7.38 (7.30)	4.59 (4.41)	8.36	–	–
15f	120–123	16	$\text{C}_{22}\text{H}_{23}\text{NO}$	289.38	83.41 (83.01)	6.42 (6.62)	4.71 (4.84)	8.33	–	–
15g	106–108	26	$\text{C}_{22}\text{H}_{23}\text{NO}_2$	333.43	79.17 (79.25)	6.79 (6.95)	4.32 (4.20)	8.29	–	–
16a	138–140	61	$\text{C}_{22}\text{H}_{22}\text{N}_2\text{O}_3$	362.42	73.16 (72.91)	6.12 (6.11)	7.73 (7.72)	8.51	–	–
16e	164–166	81	$\text{C}_{22}\text{H}_{23}\text{NO}$	317.42	83.41 (83.24)	7.31 (7.30)	4.42 (4.41)	8.39	–	–
16f	145–147	73	$\text{C}_{22}\text{H}_{25}\text{NO}$	331.45	83.19 (83.34)	7.61 (7.60)	4.22 (4.23)	8.29	–	–
18b	109–110	64	$\text{C}_{18}\text{H}_{14}\text{ClNO}$	295.76	72.95 (73.10)	4.76 (4.76)	4.75 (4.74)	8.43	5.84	–
18c	171–172	93	$\text{C}_{18}\text{H}_{14}\text{BrNO}$	340.21	63.66 (63.55)	4.14 (4.15)	4.12 (4.11)	8.46	5.85	–

each tautomeric form for compounds **12–16** and **18** are given in Table 3.

**1-Methyl-3-*p*-nitrophenyl-2,3-dihydro-1*H*-naphth[1,2-*c*][1,3]oxazine (12a):** A tautomeric mixture of Schiff base **12aA** (19.7%), *cis*-ring form **12aC** (10%) and *trans*-ring form **12aB** (70.3%). Selected signals:  $^1\text{H}$  NMR ( $\text{CDCl}_3$ , 300 K):  $\delta$  = 4.72 (q,  $J$  = 7.05 Hz, 1 H,  $\text{CH}_3\text{CHN}$ , Schiff base), 5.06 (q,  $J$  = 5.04 Hz, 1 H,  $\text{CH}_3\text{CHN}$ , *cis*), 5.58 (q,  $J$  = 7.05 Hz, 1 H,  $\text{CH}_3\text{CHNH}$ , Schiff base), 5.73 (s, 1 H, NCHO, *cis*), 6.15 (s, 1 H, NCHO, *trans*), 8.62 (s, 1 H, NCHO, Schiff base) ppm.  $^{13}\text{C}$  NMR ( $\text{CDCl}_3$ , 300 K):  $\delta$  = 22.5 (*trans*), 22.8 (*cis*), 23.1 (Schiff base), 45.8 (*trans*), 47.9 (*cis*), 66.8 (Schiff base), 80.7 (*trans*), 85.5 (*cis*), and 158.8 (Schiff base) ppm. Assignments of the aromatic region could not be made because of the low concentrations of **B** and **C** and the overlapping nature of the signals.

## Acknowledgments

The authors thanks are due to the Hungarian Research Foundation (OTKA grant D48669) for financial support.

- [1] R. E. Valters, F. Fülöp, D. Korbonits, *Adv. Heterocycl. Chem.* **1996**, *66*, 1–71.
- [2] L. Lázár, F. Fülöp, *Eur. J. Org. Chem.* **2003**, 3025–3042.
- [3] B. L. Milman, A. A. Potekhin, *Khim. Geterotsikl Soedin.* **1973**, 902–907.
- [4] F. Fülöp, K. Pihlaja, J. Mattinen, G. Bernáth, *J. Org. Chem.* **1987**, *52*, 3821–3825.
- [5] F. Fülöp, L. Lázár, G. Bernáth, R. Sillanpää, K. Pihlaja, *Tetrahedron* **1993**, *49*, 2115–2122.
- [6] A. Göblyös, L. Lázár, F. Evanics, F. Fülöp, *Heterocycles* **1999**, *51*, 2431–2438.
- [7] A. Star, B. Fuchs, *J. Org. Chem.* **1999**, *64*, 1166–1172.
- [8] A. Hetényi, Z. Szakonyi, K. D. Klika, F. Fülöp, K. Pihlaja, *J. Org. Chem.* **2003**, *68*, 2175–2182.
- [9] I. Szatmári, T. A. Martinek, L. Lázár, A. Koch, E. Kleinpeter, K. Neuvonen, F. Fülöp, *J. Org. Chem.* **2004**, *69*, 3645–3653.
- [10] I. Szatmári, T. A. Martinek, L. Lázár, F. Fülöp, *Eur. J. Org. Chem.* **2004**, 2231–2238.
- [11] M. Betti, *Org. Synth. Coll. Vol. 1* **1941**, 381–383.
- [12] I. Szatmári, F. Fülöp, *Curr. Org. Synth.* **2004**, *1*, 155–165.
- [13] C. Duff, E. J. Bills, *J. Chem. Soc.* **1934**, 1305–1308.
- [14] I. Szatmári, T. A. Martinek, L. Lázár, F. Fülöp, *Tetrahedron* **2003**, *59*, 2877–2884.
- [15] W. J. Bruke, R. J. Reynolds, *J. Am. Chem. Soc.* **1954**, *76*, 1291–1293.
- [16] Y. Gong, K. Kato, *Tetrahedron: Asymmetry* **2001**, *12*, 2121–2127.
- [17] Y. Gong, K. Kato, H. Kimoto, *Bull. Chem. Soc. Jpn.* **2002**, *75*, 2637–2646.
- [18] C. O. Kappe, *Angew. Chem. Int. Ed.* **2004**, *43*, 6250–6284.
- [19] D. F. De Tarr, C. Delahunty, *J. Am. Chem. Soc.* **1983**, *105*, 2734–2739.
- [20] M. Charton, *J. Am. Chem. Soc.* **1975**, *97*, 1552–1556.
- [21] M. Charton, *J. Org. Chem.* **1976**, *41*, 2217–2220.
- [22] A. Y. Meyer, *J. Chem. Soc., Perkin Trans. 2* **1986**, 1567–1572.
- [23] SPSS Advanced Models 11.0, SPSS Inc., Chicago, IL.

Received: May 23, 2006

Published Online: August 11, 2006

**II.**



## FULL PAPER

DOI: 10.1002/ejoc.200600563

Study of the Substituent-Influenced Anomeric Effect in the Ring-Chain Tautomerism of 1-Alkyl-3-aryl-naphth[1,2-*e*][1,3]oxazinesIstván Szatmári,<sup>[a]</sup> Diána Tóth,<sup>[a]</sup> Andreas Koch,<sup>[b]</sup> Matthias Heydenreich,<sup>[b]</sup> Erich Kleinpeter,<sup>[b]</sup> and Ferenc Fülöp<sup>\*,[a]</sup>**Keywords:** Naphthoxazines / Conformational analysis / Ab initio calculations / NBO analysis / Anomeric effect / Ring-chain tautomerism.

The stabilities of the *trans* (B) and *cis* (C) tautomeric ring forms that are experimentally observed in the ring-chain tautomeric interconversion of 1-alkyl-3-aryl-2,3-dihydro-1H-naphth[1,2-*e*][1,3]oxazines has been investigated. Stability differences are explained by the analysis of the natural bond

orbital results for the lone pairs of electrons that are on the heteroatoms in the oxazine ring system and by regression analysis of the calculated <sup>13</sup>C NMR chemical shift values. (© Wiley-VCH Verlag GmbH & Co. KGaA, 69451 Weinheim, Germany, 2006)

## Introduction

The general rules relating to the interactions of electronic orbitals in space (stereoelectronic effects) are important for the comprehension of molecular properties and general chemical reactivity.<sup>[1]</sup> In many cases, hyperconjugation influences conformational equilibria,<sup>[2–5]</sup> modifies reactivity,<sup>[6–8]</sup> determines the selectivity of reactions,<sup>[9]</sup> and is enhanced dramatically in excited, radical, and ionic species.<sup>[10]</sup>

Lone pairs of electrons on oxygen, nitrogen, sulfur, and other heteroatoms are particularly well-suited for the role of donor in hyperconjugative interactions and stereoelectronic effects, and their participation is well-documented in the scientific literature. Arguably, among these interactions, the most intensively studied effect is the anomeric effect.<sup>[2,11]</sup>

Recent studies indicate that the substituent-dependent anomeric effect plays an important role in the observed stabilities of two specific geometries of the same molecule. In particular, the anomeric effect is instrumental in two-electron, two-orbital hyperconjugative interactions that results in an excess of stabilization energy.<sup>[12,13]</sup>

The hyperconjugative interactions of the nitrogen lone pair of electrons with the C2-associated antibonding orbital have been experimentally observed to be substituent-

dependent.<sup>[14]</sup> The epimerization reactions of conformationally inflexible 2-aryl-1,3-*N,N*-heterocycles could be used as model systems for the determination of the role of the nitrogen lone pair of electrons in relation to the anomeric effect.

We pointed out earlier that in the ring-chain tautomeric interconversion of 1-(Y-phenyl)-3-(X-phenyl)-2,3-dihydro-1H-naphth[1,2-*e*][1,3]oxazines and 1-(Y-phenyl)-3-alkyl-1-aryl-2,3-dihydro-1H-naphth[1,2-*e*][1,3]oxazines, the experimentally observed differences between the stabilities of the two ring forms could be explained by the substituent-dependent anomeric effect caused by the aryl substituent in the 1-position.<sup>[15]</sup>

In the present work, we set out to extend the application of the concept of the anomeric effect by the exploitation of the tautomeric equilibrium that exists for 1-alkyl-3-aryl-2,3-dihydro-1H-naphth[1,2-*e*][1,3]oxazines (1–5, Scheme 1). We also hoped to demonstrate from the regression analysis of the log *K* values, with *V*<sup>a</sup> (the Meyer parameter, which characterizes the volume of the alkyl substituent at the 1-position)<sup>[16]</sup> and  $\sigma^+$  (the Hammett-Brown parameter, which characterizes the electronic behavior of the aryl substituent at the 3-position) as independent variables, that the significant difference between the slopes of the *V*<sup>a</sup> values for the ring-*trans*-chain [Equation (1)] and ring-*cis*-chain [Equation (2)] equilibria (–0.32 versus –0.46) can be explained by substituent-dependent stereoelectronic stabilization effects.<sup>[17]</sup> The synthesis of model compounds 1-alkyl-3-aryl-naphth[1,2-*e*][1,3]oxazines 1–5 (Scheme 1) was previously described.<sup>[17]</sup>

$$\log K_B = 0.61 - 0.32V^a + 0.85\sigma^+ \quad (1)$$

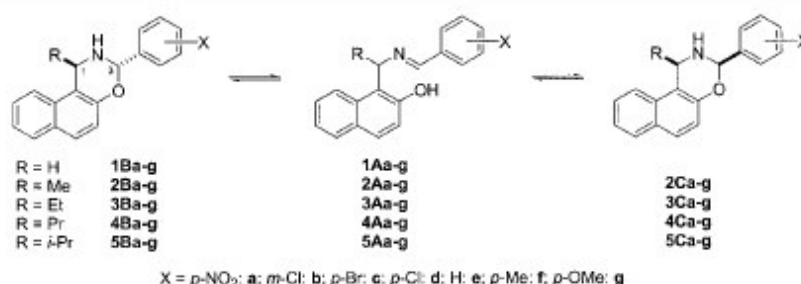
$$\log K_C = 0.41 - 0.46V^a + 0.98\sigma^+ \quad (2)$$

[a] Institute of Pharmaceutical Chemistry, University of Szeged and Research Group for Heterocyclic Chemistry, Hungarian Academy of Sciences, University of Szeged, P.O. Box 427, 6701 Szeged, Hungary  
Fax: +36-62-545705  
E-mail: fulop@pharm.u-szeged.hu

[b] Department of Chemistry, University of Potsdam, P.O. Box 691553, 14415 Potsdam, Germany

Supporting information for this article is available on the WWW under <http://www.eurjoc.org> or from the author.





Scheme 1.

## Results and Discussion

### Computational Methods

The conformational search protocol involved PM3 geometry minimization, followed by geometry optimization without restrictions. All calculations were carried out with the Gaussian 03 program package.<sup>[18]</sup> The density functional theory (DFT) calculations include electron correlation effects. This is important for the analysis of electron delocalizations. The B3LYP<sup>[19]</sup> DFT hybrid method and the 6-31G\*<sup>[20]</sup> double zeta split valence basis set were used for all calculations.

The natural bond orbital population analysis and all of the properties – the coupling constants and the chemical shifts – were calculated at this level of theory.

Calculated  $^1\text{H}$ - and  $^{13}\text{C}$  NMR chemical shift values were measured as the difference in the magnetic shielding of tetramethylsilane relative to the studied compounds.

The molecular modeling software package SYBYL 7.1 was used to display results and geometries [SYBYL 7.1, Tripos Inc. 1699 South Hanley Rd. St. Louis, MO 2005].

### Conformational Analysis

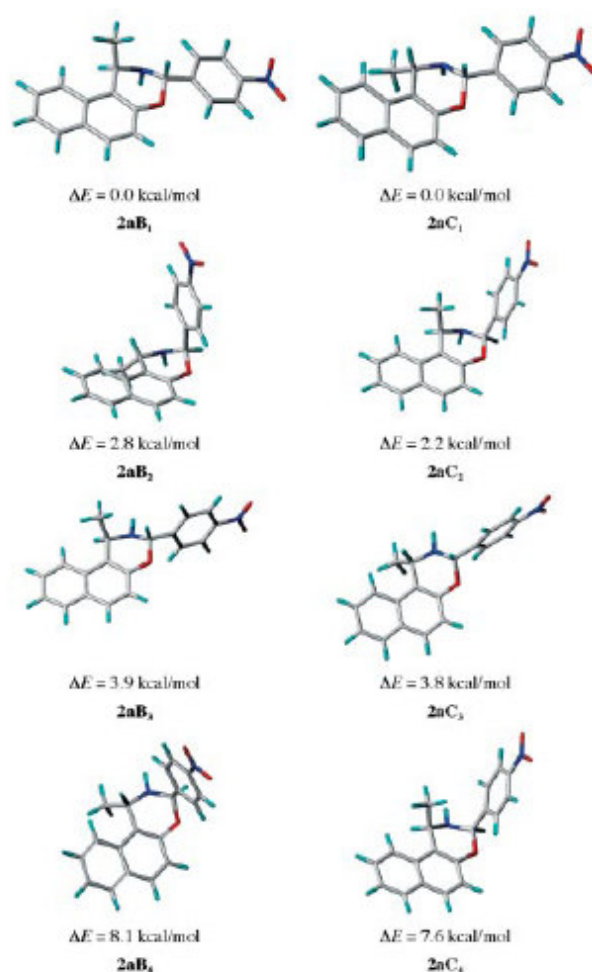
Because stereoelectronic interactions are highly dependent on the geometry of the studied molecules, a thorough conformational analysis was performed. Our goal was to determine the predominant geometry for all of the models.

The relevant calculated conformations that can be attributed to nitrogen–ring inversions of **2aB** and **2aC**, as examples, are shown in Figure 1. Chemical shift values and coupling constants were calculated at the same level of theory; selected bond lengths (for comparison with NOE measurements) and NMR parameters are given in Table 1.

In the analysis of **2a**, the strong NOE interaction between the C1-*Me* protons and C3-*H* (for B) or between C1-*H* and C3-*H* (for C) predicted the presence of **B**<sub>1</sub> and **B**<sub>3</sub>, or **C**<sub>1</sub> and **C**<sub>3</sub> geometries, respectively (Table 1, Entries 1 and 2). The only difference between **B**<sub>1</sub> and **B**<sub>3</sub>, or **C**<sub>1</sub> and **C**<sub>3</sub> is a nitrogen inversion. To decide between the **B**<sub>1</sub> and **C**<sub>1</sub> or the **B**<sub>3</sub> and **C**<sub>3</sub> geometries, the  $^3J$  coupling constants between N-*H* and C1-3-*H* of **2a** that are observed with low temperature  $^1\text{H}$  NMR techniques ( $\text{CD}_2\text{Cl}_2$ , 173 K) should be taken into account. These values (Table 1, Entries 3 and 4) were in very good agreement with the coupling constants

calculated for conformers **B**<sub>1</sub> and **C**<sub>1</sub>. This finding, together with the comparison of the energy values (the data were calculated for the full set of compounds, but are only shown for **2a**; Figure 1) allows for the conclusion that, for all of our model compounds, **B**<sub>1</sub> and **C**<sub>1</sub> are the global minimum conformers.

The NMR calculations were performed at the B3LYP/6-31G\* level, with geometries optimized at the same level. Table 1 (Entries 5–8) summarizes the measured and calcu-

Figure 1. Calculated global energy minimum conformations for **2a**.

## FULL PAPER

I. Szatmári, D. Tóth, A. Koch, M. Heydenreich, E. Kleinpeter, F. Fülöp

Table 1. Some measured and calculated NMR parameters for 2a.

Entry	Parameter	2aB[a]	2aB <sub>1</sub> [b]	2aB <sub>2</sub> [b]	2aB <sub>3</sub> [b]	2aB <sub>4</sub> [b]	2aC[a]	2aC <sub>1</sub> [b]	2aC <sub>2</sub> [b]	2aC <sub>3</sub> [b]	2aC <sub>4</sub> [b]
1	d <sub>C1-Me-C3-H</sub> [c]	yes	2.78	4.39	2.83	4.43	—	—	—	—	—
2	d <sub>C1-H-C3-H</sub> [c]	—	—	—	—	—	yes	2.77	4.04	2.81	4.07
3	J <sub>C1-H-N-H</sub>	4.6[d]	4.80	7.77	1.01	3.42	8.8[d]	7.37	4.98	5.13	1.22
4	J <sub>C3-H-N-H</sub>	14.2[d]	12.84	4.84	0.58	2.53	14.0[d]	12.85	6.53	0.83	1.24
5	δ <sub>C1-H</sub>	4.65	4.51	4.53	4.71	4.66	5.01	5.02	4.33	4.98	4.58
6	δ <sub>C3-H</sub>	6.06	6.15	5.85	5.93	5.81	5.66	5.60	6.04	5.43	6.09
7	δ <sub>C1</sub>	45.8	48.3	44.0	48.9	44.7	47.9	48.9	46.8	50.8	46.6
8	δ <sub>C3</sub>	80.7	78.5	83.7	81.6	82.2	85.5	84.1	82.9	85.7	81.8

[a] Measured NMR parameters. [b] Calculated NMR parameters. [c] Observed NOE interaction/calculated distances. [d] The coupling constants were measured in CD<sub>2</sub>Cl<sub>2</sub> at 173 K.

lated <sup>1</sup>H NMR (C1-H and C3-H) and <sup>13</sup>C NMR (C1 and C3) chemical shift values for 2a.

## Natural Bond Orbital (NBO) Analysis

The extra stabilization of the conformers that is observed with alkyl substituents in the 1-position of the *trans* ring form, indicated by the slope values (−0.32 versus −0.46),<sup>[17]</sup> may originate from a substituent-dependent stereoelectronic effect. Analysis of the delocalization energy contributions to this effect is a complex problem that can be tackled through a second-order perturbative analysis of the elements of the Fock matrix elements in the frame of the DFT hybrid method in the NBO basis.

The NBO<sup>[21]</sup> calculations were performed at the B3LYP/6-31G\* level, with geometries optimized at the same level. The solvent effect can be taken into account with a self-consistent reaction field method. The self-consistent isodensity polarized continuum model (SCIPCM)<sup>[22]</sup> used the isodensity surface of the electron density, which was influenced consistently by a dielectric continuum outside the molecule. The solvent effect was checked for series of compounds 12 (data not included). A dielectric constant ε = 4.81 (chloroform) and a value of 0.0004 a.u. for the isodensity surface were used in the calculations. The difference between the epimerization energy without a solvent effect (ΔE<sub>B-C</sub> = 1.12 kcal/mol) and that including a solvent effect

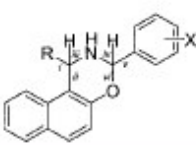
(ΔE<sub>B-C</sub> = 1.21 kcal/mol) was found to be 0.09 kcal/mol for the most polar compound 12a; in further calculations, the effect of the solvent was neglected.

We were interested in the substituent dependence of the calculated NBO parameters. The calculated occupancy values (Table S1) and the energies for the overlap (Tables S2–S4) of the lone pairs of electrons on the nitrogen and oxygen atoms are given in the Supporting Information. Accordingly, multiple linear regression analysis of these values as dependent variables (DV), with *V*<sup>a</sup> and σ<sup>+</sup> as independent variables, was performed with SPSS statistical software according to Equation (3). A value of 0.05 was chosen to denote the level of significance.<sup>[23]</sup>

$$DV = k + \rho^1 V^a + \rho^2 \sigma^+ \quad (3)$$

The calculated occupancy values indicate the level of overlap (%) with different antibonding orbitals. Comparison of the results of the regression analysis for the level of overlap of the lone pair of electrons (*n*) on the nitrogen atom (Table 2, Entry 1) for the *trans* (B) and *cis* (C) ring forms revealed a somewhat higher slope for the B form (0.12 versus 0.04) compared to that of C. This was in accordance with our experimental findings.<sup>[17]</sup> It was also concluded that the extra stabilization energy could result from a complex stereoelectronic interaction between *n*<sub>N</sub> and the vicinal antibonding orbitals. Hence, regression analysis of the overlapping energies (kcal/mol) was performed for the

Table 2. Multiple linear regression analysis of the occupancy and overlapping energy values for the lone pair of electrons on the nitrogen atom as dependent variables according to Equation (3) for 1–5.



Entry	Dependent variable (DV)	B				C			
		k	ρ <sup>1</sup>	ρ <sup>2</sup>	r	k	ρ <sup>1</sup>	ρ <sup>2</sup>	r
1	Occupancy[a]	10.47	0.12	−0.12	0.906	10.51	0.04	−0.11	0.774
2	<i>n</i> <sub>N</sub> →σ* <sub>l</sub>	2.57	−0.13	−[b]	0.702	—	—	—	—
3	<i>n</i> <sub>N</sub> →σ* <sub>ll</sub>	6.92	−0.13	−0.11	0.949	6.75	−0.20	−[b]	0.953
4	<i>n</i> <sub>N</sub> →σ* <sub>lll</sub>	—	—	—	—	2.60	0.15	−[b]	0.905
5	<i>n</i> <sub>N</sub> →σ* <sub>tr</sub>	0.79	0.09	−[b]	0.746	0.79	−0.01	0.05	0.751
6	<i>n</i> <sub>N</sub> →σ* <sub>tr</sub>	0.78	−0.03	0.05	0.946	0.87	0.03	−[b]	0.764
7	<i>n</i> <sub>N</sub> →σ* <sub>tr</sub>	15.93	0.10	−0.18	0.781	16.00	0.07	−0.19	0.795

[a] For regression analysis, the ratios of the occupancy values in % were used. [b] Insignificant (significance value > 0.05).



six possible vicinal antibonding orbitals (three around C1 and three around C3). The results showed that the overlap of  $n_N$  with the antibonding orbital of the C1–R bond ( $\sigma^*_{C1-R}$ ) in **B** or the C1–H bond ( $\sigma^*_{C1-H}$ ) in **C** had relatively similar intensities (around 2.6 kcal/mol; Table 2, Entry 2). The opposite slope can be explained by the change in the relative configuration of C1 and is in accordance with the experimental findings.<sup>[17]</sup> The overlap of  $n_N$  with  $\sigma^*_{C1-H}$  in **B** and the corresponding overlap in **C** (Table 2, Entry 3) showed similar intensities and similar tendencies.

The low intercept values of **C** (0.79 and 0.87, respectively; Table 2, Entries 5 and 6) and the slope (around 0) indicate that, around C3, the most important and the strongest overlap occurs in the direction of the most polar C–O ( $\nu_i$ ) bond (Table 2, Entry 7). No comparable difference was observed between ring forms **B** and **C** either in the slope of  $V^a$  or in the slope of  $\sigma^+$ . The value of 0.1 for  $V^a$  can be explained by the small inductive influence of the alkyl substituents. The slope of  $\sigma^+$ , which is double the expected value, can be the result of the polarization of bond  $\nu_i$ , induced by substituent X.

From the analysis of the overlapping behavior of  $n_N$ , the additional stabilization of the conformers that is observed when alkyl substituents are in the 1-position can be nicely explained, but in order to map the summed influence of the alkyl and aryl substituents, an analysis of the overlapping behaviour of the oxygen lone pairs of electrons ( $n_{O1}$  and  $n_{O2}$ ) was also necessary.

A comparison of the overlapping levels of  $n_{O1}$  and  $n_{O2}$  (Table 3, Entries 1 and 7, respectively) leads to the conclusion that  $n_{O2}$  ( $\pi$ -like lone pair) participates in overlapping interactions to a greater extent than  $n_{O1}$  does (see intercepts, Table 3, Entries 1 and 7), and because of the low slope values (Table 3, Entry 1) the substituent dependence on the overlapping level of  $n_{O1}$  can be neglected. The occupancy level of  $n_{O2}$  is strongly influenced by the aryl substituent in the 3-position (–0.38 and –0.34, respectively, Table 3, Entry

7). The comparison of the slopes of  $V^a$  for the ring forms yielded low values, but the different tendencies (0.08 versus –0.07, Table 3, Entry 7) indicates that there is some influence of the alkyl substituent in the 1-position. Because of the large difference between the interaction of the alkyl substituent with  $n_{O2}$  and the pure electronic character of an alkyl substituent alone, this dependence can be explained only in terms of an alkyl substituent-controlled quantitative change in the torsion angle between  $n_{O2}$  and the corresponding antibonding orbital (e.g. by an alkyl substituent-dependent conformational change).

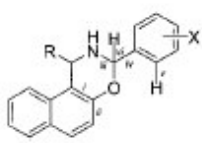
The NBO analyses demonstrated that negative hyperconjugation ( $n \rightarrow \sigma^*$ ) and conjugation ( $n \rightarrow \pi^*$ ) play important roles in the ring-chain tautomeric interconversions of **1**–**5**. The results also indicate that these conjugative interactions, which result from substituent-dependent conformational changes, explain the relative stability differences between ring forms **B** and **C**.

### Shifted Carbon Chemical Shift (SCS) Analysis

The changes in the  $^{13}\text{C}$  NMR chemical shift values that are induced by phenyl substituents (SCS) on C2 have been analyzed by various dual substituent parameter approaches.<sup>[24–26]</sup> The best correlation was obtained with the equation  $\text{SCS} = \rho_F \sigma_F + \rho_R \sigma_R$ , where  $\sigma_F$  characterizes the inductive effect, and  $\sigma_R$  the resonance effect, of the aryl substituent. In a previous study on the ring-chain tautomerism of 1,3-diaryl-2,3-dihydro-1*H*-naphth[1,2-*e*][1,3]oxazines, by means of a dual substituent parameter treatment of SCS, the difference in the stabilities of ring forms **B** and **C** was explained by the changes in the  $sp^2$  and  $sp^3$  hybridized character of the carbon atom, which is influenced by the aryl substituents on C1 and C3.<sup>[15]</sup>

The low concentrations of the minor forms of **B** and **C** in the tautomeric mixtures did not allow for the measure-

Table 3. Multiple linear regression analysis of the occupancy and overlapping energy values for the lone pairs of electrons on the oxygen atom as dependent variables according to Equation (3) for **1**–**5**.



Entry	Dependent variable (DV)	<b>B</b>				<b>C</b>			
		k	$\rho^1$	$\rho^2$	r	k	$\rho^1$	$\rho^2$	r
1	Occupancy ( $n_{O1}$ ) <sup>[a]</sup>	4.05	0.03	–[b]	0.897	4.04	–0.01	0.02	0.834
2	$n_{O1} \rightarrow \sigma^*_{C1-R}$	6.58	0.07	–0.16	0.880	6.55	–0.05	–0.15	0.937
3	$n_{O1} \rightarrow \sigma^*_{C1-H}$	0.50	0.02	–[b]	0.857	–	–	–	–
4	$n_{O1} \rightarrow \sigma^*_{C3-H}$	2.62	0.21	–[b]	0.785	2.66	–0.12	–[b]	0.914
5	$n_{O1} \rightarrow \sigma^*_{C3-R}$	1.09	–0.03	–[b]	0.645	1.05	–0.01	0.06	0.940
6	$n_{O1} \rightarrow \sigma^*_{C3-N}$	0.58	0.01	0.01	0.799	0.57	–0.01	0.03	0.681
7	Occupancy ( $n_{O2}$ ) <sup>[a]</sup>	15.21	0.08	–0.38	0.907	15.15	–0.07	–0.34	0.928
8	$n_{O2} \rightarrow \pi^*_{C1-R}$	28.17	0.28	–0.93	0.896	27.79	–0.46	–0.82	0.935
9	$n_{O2} \rightarrow \sigma^*_{C1-H}$	5.13	–0.41	–[b]	0.720	4.93	0.15	0.20	0.904
10	$n_{O2} \rightarrow \sigma^*_{C3-H}$	5.51	–0.08	0.21	0.599	5.34	–0.06	0.20	0.945

[a] For regression analysis, the ratios of the occupancy values in % were used. [b] Insignificant (significance value > 0.05).



## FULL PAPER

ment of the  $^{13}\text{C}$  NMR chemical shift values of C1 and C3. They were therefore calculated for all compounds at the B3LYP/6-31G\* level with geometries optimized at the same level, and they are listed in Table S5. The chemical shift changes induced by the alkyl substituent in the 1-position and by the aryl substituent in the 3-position (SCS) for a given compound were calculated as the differences in the calculated  $^{13}\text{C}$  NMR chemical shift values for the substituted relative to the unsubstituted ( $\text{R} = \text{H}$ ,  $\text{X} = \text{H}$ ) compound. The multiple regression analysis<sup>[23]</sup> data obtained from Equation (4) for C1 and C3 are presented in Table 4.

$$DV = \rho^1 I^A + \rho^2 \sigma_F + \rho^3 \sigma_R \quad (4)$$

Table 4. Multiple linear regression analysis of the calculated SCS values for C1 and C3 according to Equation (4) for 1–5.

Dependent variable (DV)	B				C			
	$\rho^1$	$\rho^2$	$\rho^3$	r	$\rho^1$	$\rho^2$	$\rho^3$	r
SCS <sub>C1</sub>	2.22	–[a]	–[a]	0.996	2.34	–[a]	–[a]	0.997
SCS <sub>C3</sub>	–	–	–[a]	0.967	0.09	–	–[a]	0.931
	0.98	1.79				1.02		

[a] Insignificant (significance value > 0.05).

Table 4 shows that the calculated  $^{13}\text{C}$  NMR chemical shift values for C1 are influenced only by the alkyl substituents in the 1-position. The small difference in slope between ring forms B and C indicates that the behavior of the alkyl substituent in the 1-position in relation to the conformational changes around C1 is similar in the two ring forms.

The calculated  $^{13}\text{C}$  NMR chemical shift values for C3 seem to depend much more on the changes in the relative configurations. In comparison, the influence of an alkyl substituent in the 1-position (–0.98 versus 0.09; Table 4) on the SCS values for C3 was found to be strongly dependent on the relative configurations of C1 and C3. This provides further evidence for the theory that alkyl substituents stabilize the *trans* (B) ring form, which can be explained in terms of an alkyl substituent-induced stereoelectronic effect. This results in small alkyl substituent-induced conformational changes in B.

The reverse trend in the inductive substituent effect ( $\sigma_F$ ) for unsaturated carbon is well-documented.<sup>[25–30]</sup> The negative slope of  $\sigma_F$  for saturated carbon centers such as those situated between the two heteroatoms in 1,3-*O,N*-heterocycles was explained by Neuvonen et al. to be due to the substituent-sensitive polarization of the N–C–O system.<sup>[24]</sup> The *trans* and *cis* series in the present work offered an interesting opportunity for the study of this type of reverse trend in the substituent effect ( $\sigma_F$ ) on the calculated SCS values. Table 4 shows that negative slopes of  $\sigma_F$  (–1.79 versus –1.02) were obtained for both series B and C, which is in accordance with the concept found for similar carbon centers.<sup>[15,24]</sup> The difference between the slopes is a further consequence of the stronger substituent-induced stereoelectronic effect in the *trans* (B) ring form.

## Conclusions

This analysis of the disubstitution effects of R (alkyl) and X in 1-alkyl-3-(X-phenyl)-2,3-dihydro-1*H*-naphth[1,2-*e*]-[1,3]oxazines on ring-chain tautomerism, the delocalization of the nitrogen and oxygen lone pairs of electrons (anomeric effect), and the calculated  $^{13}\text{C}$  NMR chemical shifts permitted an explanation for the experimentally observed stabilization difference between the *trans* (B) and *cis* (C) ring forms.

The multiple linear regression analysis of the calculated overlapping energies for the lone pairs of electrons on the nitrogen and oxygen atoms showed that the relative stability difference between the two ring forms is the result of an alkyl substituent-induced quantitative conformational change in the naphthoxazine ring system. The analysis of the  $^{13}\text{C}$  NMR chemical shift changes induced by the substituents (SCS) for C1 and C3 revealed that, by the alkyl substituent-dependent small conformational changes, the substituent-dependent anomeric effect predominates in the preponderance of the *trans* over the *cis* isomer.

**Supporting Information** (see footnote on the first page of this article): Calculated occupancy values (Table S1), calculated overlapping energies (kcal/mol) of *lpN* (Table S2), calculated overlapping energies (kcal/mol) of *lpO1* (Table S3), calculated overlapping energies (kcal/mol) of *lpO2* (Table S4) and calculated  $^{13}\text{C}$  NMR chemical shifts (Table S5) of naphthoxazines 1–5.

## Acknowledgments

The author's thanks are due to the Deutsche Forschungsgemeinschaft (DFG 436 UNG 113/161) and the Hungarian Research Foundation (OTKA No. D48669) for financial support.

- [1] I. V. Alabugin, M. Manoharan, T. A. Zeidan, *J. Am. Chem. Soc.* **2003**, *125*, 14014–14031.
- [2] P. P. Graczyk, M. Mikolajczyk, *Top. Stereochem.* **1994**, *21*, 159–349.
- [3] P. R. Schreiner, *Angew. Chem. Int. Ed.* **2002**, *41*, 3579–3583.
- [4] V. Pophristic, L. Goodman, N. Guchhait, *J. Phys. Chem. A* **1997**, *101*, 4290–4297.
- [5] K. T. Lu, F. Weinhold, J. C. Weishaar, *J. Chem. Phys.* **1995**, *102*, 6787–6805.
- [6] I. H. Um, E. K. Chung, S. M. Lee, *Can. J. Chem.* **1998**, *76*, 729–737.
- [7] B. P. Roberts, A. J. Steel, *Tetrahedron Lett.* **1993**, *34*, 5167–5170.
- [8] M. E. Maier, *Angew. Chem. Int. Ed.* **2000**, *39*, 2073–2077.
- [9] A. L. J. Beckwith, P. J. Duggan, *Tetrahedron* **1998**, *54*, 6919–6928.
- [10] B. Ganguly, B. Fuchs, *J. Org. Chem.* **1997**, *62*, 8892–8901.
- [11] C. Romers, C. Altona, H. R. Buys, E. Havinga, *Top. Stereochem.* **1969**, *4*, 39–97.
- [12] P. v. R. Schleyer, A. Kos, *Tetrahedron* **1983**, *39*, 1141–1150.
- [13] I. V. Alabugin, *J. Org. Chem.* **2000**, *65*, 3910–3919.
- [14] A. Hetényi, T. A. Martinek, L. Lázár, Z. Zalán, F. Fülöp, *J. Org. Chem.* **2003**, *68*, 5705–5712.
- [15] I. Szatmári, T. A. Martinek, L. Lázár, A. Koch, E. Kleinpeter, K. Neuvonen, F. Fülöp, *J. Org. Chem.* **2004**, *69*, 3645–3653.
- [16] A. Y. Meyer, *J. Chem. Soc. Perkin Trans. 2* **1986**, *2*, 1567–1572.
- [17] D. Tóth, I. Szatmári, F. Fülöp, *Eur. J. Org. Chem.*, DOI: 10.1002/ejoc.200600447.
- [18] Gaussian 03, Revision C.02, M. J. Frisch, G. W. Trucks, H. B. Schlegel, G. E. Scuseria, M. A. Robb, J. R. Cheeseman, J. A.

- Montgomery Jr, T. Vreven; K. N. Kudin, J. C. Burant, J. M. Millam, S. S. Iyengar, J. Tomasi, V. Barone, B. Mennucci, M. Cossi, G. Scalmani, N. Rega, G. A. Petersson, H. Nakatsuji, M. Hada, M. Ehara, K. Toyota, R. Fukuda, J. Hasegawa, M. Ishida, T. Nakajima, Y. Honda, O. Kitao, H. Nakai, M. Klene, X. Li, J. E. Knox, H. P. Hratchian, J. B. Cross, C. Adamo, J. Jaramillo, R. Gomperts, R. E. Stratmann, O. Yazyev, A. J. Austin, R. Cammi, C. Pomelli, J. W. Ochterski, P. Y. Ayala, K. Morokuma, G. A. Voth, P. Salvador, J. J. Dannenberg, V. G. Zakrzewski, S. Dapprich, A. D. Daniels, M. C. Strain, O. Farkas, D. K. Malick, A. D. Rabuck, K. Raghavachari, J. B. Foresman, J. V. Ortiz, Q. Cui, A. G. Baboul, S. Clifford, J. Cioslowski, B. B. Stefanov, G. Liu, A. Liashenko, P. Piskorz, I. Komaromi, R. L. Martin, D. J. Fox, T. Keith, M. A. Al-Laham, C. Y. Peng, A. Nanayakkara, M. Challacombe, P. M. W. Gill, B. Johnson, W. Chen, M. W. Wong, C. Gonzalez, J. A. Pople, Gaussian, Inc., Wallingford CT, 2004.
- [19] A. D. Becke, *J. Chem. Phys.* **1993**, *98*, 1372–1377.
- [20] W. J. Hehre, L. Radom, P. v. R. Schleyer, J. A. Pople, *Ab initio Molecular Orbital Theory*, Wiley, New York, 1986.
- [21] E. D. Glendening, J. K. Badenhoop, A. E. Reed, J. E. Carpenter, J. A. Bohmann, C. M. Morales, F. Weinhold, Theoretical Chemistry Institute, University of Wisconsin, Madison, 2001.
- [22] J. B. Foresman, T. A. Keith, K. B. Wiberg, J. Snoonian, M. J. Frisch, *J. Phys. Chem.* **1996**, *100*, 16098–16104.
- [23] SPSS Advanced Models 13.0, SPSS Inc., Chicago, IL.
- [24] K. Neuvonen, F. Fülöp, H. Neuvonen, A. Koch, E. Kleinpeter, K. Pihlaja, *J. Org. Chem.* **2001**, *66*, 4132–4140.
- [25] K. Neuvonen, F. Fülöp, H. Neuvonen, K. Pihlaja, *J. Org. Chem.* **1994**, *59*, 5895–5900.
- [26] K. Neuvonen, F. Fülöp, H. Neuvonen, M. Simeonov, K. Pihlaja, *J. Phys. Org. Chem.* **1997**, *10*, 55–66.
- [27] S. Ehrenson, R. T. C. Brownlee, R. W. Taft, *Prog. Phys. Org. Chem.* **1973**, *10*, 1–80.
- [28] D. J. Craik, R. T. C. Brownlee, *Prog. Phys. Org. Chem.* **1983**, *14*, 1–73.
- [29] W. F. Reynolds, *Prog. Phys. Org. Chem.* **1983**, *14*, 165–203.
- [30] A. Kawasaki, *J. Chem. Soc. Perkin Trans. 2* **1990**, 223–228.

Received: June 30, 2006

Published Online: September 4, 2006

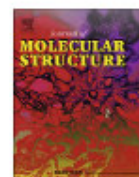
### **III.**





Contents lists available at ScienceDirect

Journal of Molecular Structure

journal homepage: [www.elsevier.com/locate/molstruc](http://www.elsevier.com/locate/molstruc)

# Synthesis and conformational analysis of naphthyl-naphthoxazine derivatives

Diána Tóth<sup>a,b</sup>, István Szatmári<sup>a,b</sup>, Matthias Heydenreich<sup>c</sup>, Andreas Koch<sup>c</sup>,  
Erich Kleinpeter<sup>c</sup>, Ferenc Fülöp<sup>a,b,\*</sup>

<sup>a</sup> Institute of Pharmaceutical Chemistry, University of Szeged, H-6720 Szeged, Eötvös u. 6, Hungary

<sup>b</sup> Research Group for Stereochemistry Hungarian Academy of Sciences, University of Szeged, H-6720 Szeged, Eötvös u. 6, Hungary

<sup>c</sup> Department of Chemistry, University of Potsdam, P.O. Box 601553, D-14415 Potsdam, Germany

## ARTICLE INFO

### Article history:

Received 26 March 2009

Received in revised form 6 April 2009

Accepted 7 April 2009

Available online 18 April 2009

### Keywords:

Aminonaphthols

Naphthoxazines

Conformational analysis

DFT calculations

NBO analysis

## ABSTRACT

Four new primary aminonaphthols (**4**, **5**, **9** and **10**) were synthesized from 1- or 2-naphthol and 1- or 2-naphthaldehyde via naphthoxazines in modified Mannich condensations. Simple ring-closure reactions of these aminonaphthols with paraformaldehyde, 4-nitrobenzaldehyde, phosgene or 4-chlorophenyl isothiocyanate led to new heterocyclic derivatives. In these transformations, either an  $sp^2$  or an  $sp^3$  carbon was inserted between the hydroxy and amino groups. The effects of substituents and the naphthyl ring on the conformation were investigated by means of NMR measurements, employing both dipolar and scalar couplings. The structures were confirmed by DFT quantum chemical calculations involving computed coupling constants, intramolecular distances between nuclei and the relative energies of the preferred conformers.

© 2009 Elsevier B.V. All rights reserved.

## 1. Introduction

The chemistry of the Betti bases dates from the beginning of the 20th century, when Betti reported the synthesis of 1-( $\alpha$ -aminobenzyl)-2-naphthol [1,2]. The three-component modified Mannich reaction involving 2-naphthol, benzaldehyde and ammonia resulted in 1,3-diphenylnaphthoxazine, which was subsequently hydrolysed to 1-( $\alpha$ -aminobenzyl)-2-naphthol.

The reaction can be extended by using chiral amines instead of ammonia, which furnishes non-racemic *N*-substituted aminonaphthol derivatives; this opened up a new area of application of these enantiopure compounds as chiral ligands in asymmetric transformations [3–7]. As a result of an integrated, virtual database screening, 7-[anilin( $\alpha$ -phenyl)methyl]-2-methyl-8-quinolinol was found to represent a promising new class of non-peptide inhibitors of the MDM2–p53 interaction [8].

Interest in the synthesis of primary aminonaphthols has greatly increased during the past few years following an evaluation of the hypotensive and bradycardiac effects of 1-aminomethyl-2-naphthol derivatives [9], and the synthesis of a wide variety of such compounds were recently achieved through the hydrolysis of 1-

amidomethyl-2-naphthols [10–12]. Through the use of aliphatic aldehydes, e.g. formaldehyde [13], acetaldehyde, propionaldehyde, butyraldehyde, isobutyraldehyde and pivalaldehyde, 1-(1-aminomethyl)-2-naphthols have been synthesized [14,15], while from heteroaromatic aldehydes primary aminonaphthols have been prepared and their ring-chain tautomeric behaviour has been studied [16].

Our present aim was to prepare new primary aminonaphthols from 1- or 2-naphthol and 1- or 2-naphthaldehyde and to extend the applicability of these compounds for the preparation of new heterocyclic derivatives by simple ring-closure reactions with paraformaldehyde, 4-nitrobenzaldehyde, phosgene or 4-chlorophenyl isothiocyanate. We additionally investigated the influence of the substituents at position 3 or 2 and the connecting position of the naphthalene ring on the conformation.

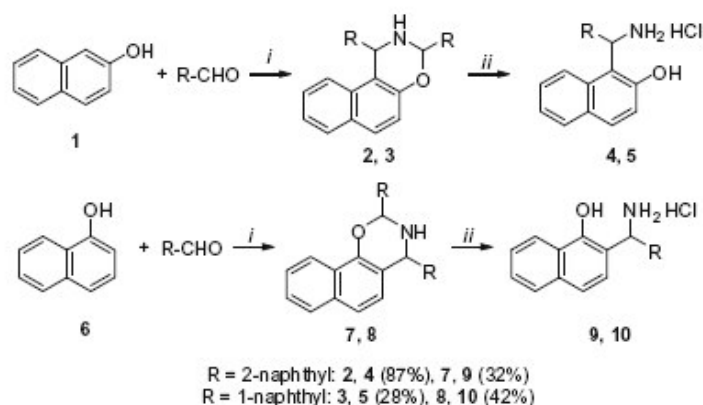
## 2. Results and discussion

### 2.1. Syntheses

The aminonaphthols **4**, **5**, **9** and **10** were prepared via the reactions of the corresponding 1- or 2-naphthol with 1- or 2-naphthaldehyde in the presence of methanolic ammonia solution in absolute methanol at room temperature for 24 h. This led to the naphthoxazines **2**, **3**, **7** and **8** (Scheme 1: i), acidic hydrolysis of which gave the desired aminonaphthol hydrochlorides **4**, **5**, **9** and **10** (Scheme 1: ii). Because of the instability of the aminonaphthyl

\* Corresponding author. Address: Institute of Pharmaceutical Chemistry, University of Szeged, and Research Group for Stereochemistry Hungarian Academy of Sciences, Eötvös u. 6, H-6720 Szeged, Hungary. Tel.: +36 62 545564; fax: +36 62 545705

E-mail address: [fulop@pharm.u-szeged.hu](mailto:fulop@pharm.u-szeged.hu) (F. Fülöp).

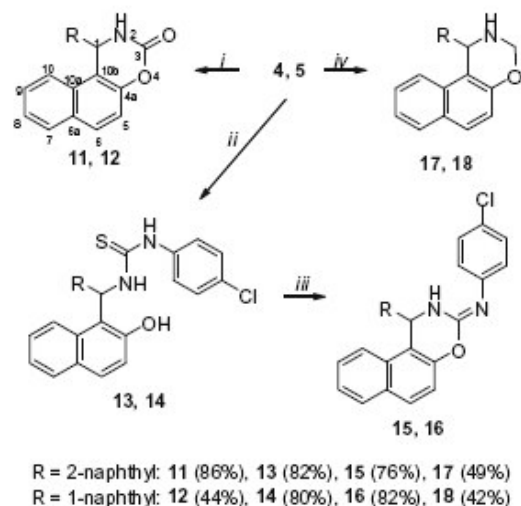
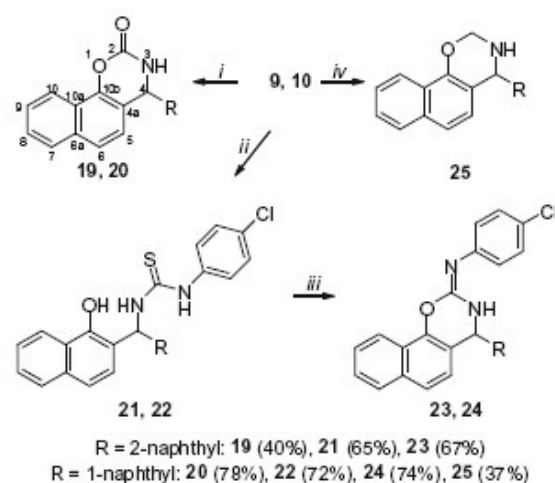
Scheme 1. Reagents and conditions: (i)  $\text{NH}_3/\text{MeOH}$ , r.t.; (ii)  $60\text{ }^\circ\text{C}$  for 2–3 h,  $\text{HCl}/\text{H}_2\text{O}$ .

naphthol derivatives, compounds **4**, **5**, **9** and **10** were isolated as their hydrochlorides, in moderate to good yields (28–87%).

In the first stage of the transformations of **4**, **5**, **9** and **10** to heterocyclic derivatives, an  $\text{sp}^2$  carbon (C-3 or C-2) was inserted between the hydroxy and amino groups (Schemes 2 and 3).

When aminonaphthols **4**, **5**, **9** and **10** were treated with  $\text{COCl}_2$  in the presence of  $\text{Na}_2\text{CO}_3$  in toluene/ $\text{H}_2\text{O}$  solution at room temperature for 10 min., the corresponding naphthoxazin-3-ones **11** and **12** and naphthoxazin-2-ones **19** and **20** were formed, in moderate yields (40–86%) in each case (Schemes 2 and 3: i).

For the preparation of 3- and 2-(4-chlorophenylimino)-substituted naphthoxazines **15**, **16**, **23** and **24**, aminonaphthols **4**, **5**, **9** and **10** were reacted with 4-chlorophenyl isothiocyanate (Schemes 2 and 3: ii). Thioureas **13**, **14**, **21** and **22** were converted to the corresponding *S*-methylisothiourea derivatives with methyl iodide, and subsequent treatment with methanolic KOH gave the corresponding 3- or 2-arylimino-substituted naphthoxazines **15**, **16**, **23** and **24**, in good yields (67–82%), via methyl mercaptan elimination (Schemes 2 and 3: iii).

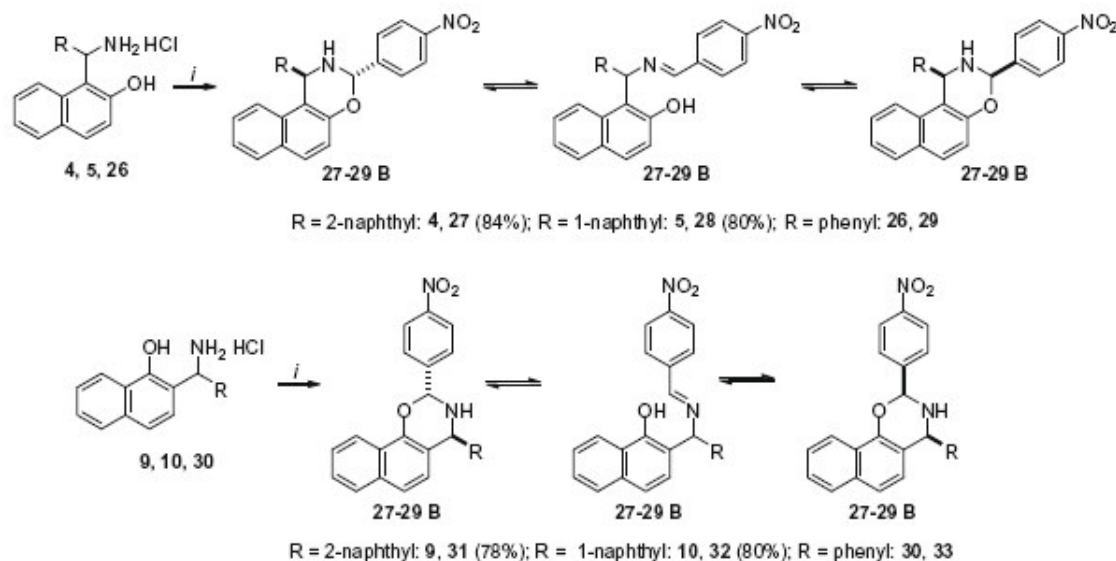
Scheme 2. Reagents and conditions: (i)  $\text{COCl}_2$ , toluene/ $\text{H}_2\text{O}$ ,  $\text{Na}_2\text{CO}_3$ , 10 min, r.t.; (ii) 4- $\text{ClC}_6\text{H}_4\text{NCS}$ ,  $\text{Et}_3\text{N}$ , toluene, r.t.; (iii)  $\text{MeI}$ ,  $\text{KOH}$ ,  $\text{MeOH}$ , r.t.; (iv) paraformaldehyde,  $\text{Et}_3\text{N}$ ,  $\text{CHCl}_3$ , 6 h, r.t.Scheme 3. Reagents and conditions: (i)  $\text{COCl}_2$ , toluene/ $\text{H}_2\text{O}$ ,  $\text{Na}_2\text{CO}_3$ , 10 min, r.t.; (ii) 4- $\text{ClC}_6\text{H}_4\text{NCS}$ ,  $\text{Et}_3\text{N}$ , toluene, r.t.; (iii)  $\text{MeI}$ ,  $\text{KOH}$ ,  $\text{MeOH}$ , r.t.; (iv) paraformaldehyde,  $\text{Et}_3\text{N}$ ,  $\text{CHCl}_3$ , 6 h, r.t.

The ring closures of aminonaphthols **4**, **5**, **9** and **10** with oxo compounds (i.e. the insertion of an  $\text{sp}^3$  carbon) resulted in naphthoxazines.

The reactions of aminonaphthols **4**, **5** and **10** with paraformaldehyde under mild conditions (at room temperature for 6 h) gave the corresponding 3- and 2-unsubstituted naphthoxazines **17**, **18** and **25** in yields of 37–49% (Schemes 2 and 3: iv). The corresponding reaction of **9** did not lead to the desired naphthoxazine. After a reaction time of 3 h TLC demonstrated that no starting material remained, and the TLC plots observed suggested the rapid decomposition of the expected naphthoxazine derivative.

The analogous reactions of **4**, **5**, **9** and **10** with 4-nitrobenzaldehyde were accomplished under mild conditions. The products **27**, **28**, **31** and **32** were separated from the reaction mixture in good yields (78–84%, Scheme 4: i). Compounds **27**–**29** and **31**–**33** in solution can participate in three-component ring-chain tautomeric equilibria involving the C-3 (27–29) or C-2 (31–33) epimeric naphthoxazines (B and C) and the open tautomer (A). The tautomeric behaviour (the tautomeric ratios) of **27**–**29** and **31**–**33** depend on substituent R at position 1 or 4, and on the properties of the solvent in question, as revealed in Table 1 [13].



Scheme 4. Reagents and conditions: (i) 4-nitrobenzaldehyde, Et<sub>3</sub>N, MeOH, 10 min., r.t.

For 27–29, the predominant form is the *trans* tautomer (B). The portion of B decreases in the sequence 27 > 28 > 29, while that of the *cis* form (C) displays the opposite tendency (Table 1: entries 1–3). This can be explained in terms of steric hindrance. Relative to CDCl<sub>3</sub>, the more polar solvent DMSO causes a small increase in the proportion of the open-chain form (A) at the expense of form (C) for 29 (Table 1: entry 3), but the main tendency was found to be similar with that discussed above.

For 31–33 in CDCl<sub>3</sub>, the steric hindrance of the aryl substituents at position 4 must exert the most important effect as regards the composition of the tautomeric mixture and, similar as for 1,3-disubstituted naphth[1,2-*e*][1,3]oxazines, the phenyl ring (smaller than the naphthyl ringsystem) resulted in more form (C) and less form (B) (Table 1: entries 4–6).

The effect of the change of the solvent seems to be somewhat more marked for 31–33 (Table 1: entries 4–6) than for 27–29 (Table 1: entries 1–3).

## 2.2. Conformational analysis

Theoretical calculations were performed on the compounds studied and their global minimum-energy structures were determined. These structures were compared with the relevant NMR spectroscopic data (NOEs and *vicinal* H,H-coupling constants) to

check particularly on the conformation of the (unsaturated) oxazine ring moiety. The same procedure was applied in the event of additional substitution at C-3 in the 2-naphthoxazines and at C-2 in the 1-naphthoxazines, of the *sp*<sup>2</sup> hybridization of C-2 or C-4. The complete agreement of the computed structures (the preferred conformers) and the NMR parameters is strong evidence of the correctness of the calculated geometries of the compounds studied.

Both the 1- and 2-naphthyl substituents at C-1 in the 2-naphthoxazines and at C-4 in the 1-naphthoxazines, respectively, were found to have only marginal influence on the conformational equilibria, whereas in the *trans* isomers of the disubstituted 1- and 2-naphthoxazines 27, 28, 31 and 32 they do influence the preference for the corresponding *S/R* and *R/S* diastereomers, respectively (*vide infra*).

### 2.2.1. Compounds with *sp*<sup>3</sup> C-2 or C-3 atoms

Compounds which are only mono-substituted with 1- and 2-naphthyl substituents at C-1 and C-4, respectively (17, 18 and 25), prefer *twisted-chair* conformers (cf. the global minimum-energy structure of 17, for instance, in Fig. 1). The analogue of 17 could not be obtained experimentally, but was computed at the DFT level of theory; the same *twisted-chair* conformer as in 17, 18 and 25 was found to be preferred.

This preferred conformation (cf. 17 in Fig. 1) proves to be in excellent agreement with the experimental NMR data: NOEs were observed between H-1 and NH (the corresponding distance was computed to be only 2.243 Å) and between NH and H-3<sub>eq</sub> (computed distance –2.360 Å). Moreover, the corresponding scalar *vicinal* <sup>3</sup>*J*<sub>H,H</sub> coupling constants were 5.0 Hz (<sup>3</sup>*J*<sub>H1NH</sub> computed 4.7 Hz, dihedral angle 43.3°), 3.9 Hz (<sup>3</sup>*J*<sub>H-3eqNH</sub> computed 3.2 Hz, dihedral angle –57.3°), and 13.6 Hz (<sup>3</sup>*J*<sub>H-3axNH</sub> computed 13.1 Hz, dihedral angle –178.2°). The corresponding NMR data of 18 are given in Table 2 and are likewise seen to be in excellent agreement with the computed values.

A *twisted-chair* conformer was also found for 25 (cf. Fig. 2). As for 17 and 18, a similar <sup>3</sup>*J*<sub>H,H</sub> value in the O(2)CH<sub>2</sub>–NH–C(4)H coupling fragment and similar NOEs between NH and H-2<sub>eq</sub> and H-4, respectively, were observed (cf. Table 2).

Table 1  
Proportions of tautomers (%) in 27–29 and 31–33.

Entry	Comp.	CDCl <sub>3</sub>			DMSO		
		A	B	C	A	B	C
1	27	–	100.0 <sup>a</sup>	–	–	100.0	–
2	28	–	95.4	4.6	–	94.8	5.2
3	29 <sup>b</sup>	3.1	86.1	10.8	15.0	84.8	0.2
4	31	13.8	68.9	17.3	34.3	46.1	19.6
5	32	4.5	77.6	17.9	–	82.8	17.2
6	33 <sup>c</sup>	14.9	50.1	35.0	36.9	42.6	20.5

<sup>a</sup> Either the population of tautomers A and C is too low to be detected by NMR, or the equilibration is fast on the NMR time scale (see text below).

<sup>b</sup> Data from Ref. [17].

<sup>c</sup> Data from Ref. [18].

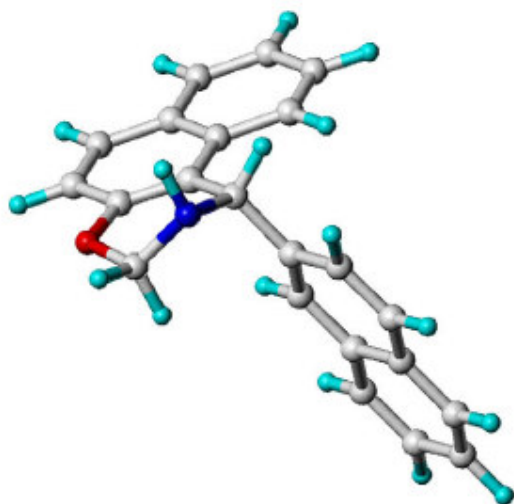


Fig. 1. Energy-minimum structure of (1S)-17.

If the compounds are additionally substituted at C-3 ( $\beta$ -naphthoxazines) or C-2 ( $\alpha$ -naphthoxazines), tautomeric equilibria result (cf. Scheme 4). The major ring form B was isolated and studied by NMR spectroscopy. In contrast with the simple *R/S* chirality in 17, 18 and 25, which does not influence the NMR spectra in achiral media, in 28, 29, 31 and 32 *R/S* and *S/R* diastereomers have to be considered.

The global minimum-energy structure of the major ring form B is characterized by the *trans* arrangement of H-3 and N–H (as depicted in Fig. 3 for 27B) and prefers the *twisted-chair* conformation. The experimentally determined vicinal H,H-coupling constants  $^3J_{H-2,H-3}$  [14.0 Hz in 27B and 13.6 Hz in 28B] and  $^3J_{H-1,H-2}$  [5.2 Hz in 27B

and 4.9 Hz in 28B] agree well with the computed values [e.g. 27B: 12.5 Hz ( $^3J_{H-2,H-3}$ ) and 4.8 Hz ( $^3J_{H-1,H-2}$ )]. Surprisingly, a strong NOE was found between H-3 and N–H, which are in *trans* position. This dipolar coupling, however, should be near to zero in 27B, but some 27C may be present in marginal concentration or in rapid equilibrium with B on the NMR time-scale; obviously, the reaction rate allows NOE transfer between the tautomeric species (cf. Table 1).

The main tautomers 31B and 32B also occur in a *twisted-chair* conformation, as illustrated for 32B in Fig. 4. This calculated minimum-energy structure is corroborated by the experimentally determined coupling constants  $^3J_{H-3,H-4} = 5.7$  Hz (computed dihedral angle 40.4°) and  $^3J_{H-2,H-3} = 13.5$  Hz (computed dihedral angle 177.6°) and the corresponding NOEs, which were found to be strong between N–H and H-4 (computed distance 2.243 Å) and weak between H-2 and N–H (2.902 Å).

Surprisingly, in 27, 28 and 32 the *S/R* diastereomer proved to be more stable than the *R/S* analogue; the reverse situation was the case for 31.

## 2.2.2. Compounds with $sp^2$ C-2 or C-3 atoms

Introduction of an  $sp^2$  carbon at position 3 (11 and 12) or 2 (19 and 20) obviously leads to very similar conformational behaviour; in accordance with this, very similar minimum-energy conformations of all of these compounds were calculated: the oxazine ring is nearly flat with a slight boat conformation (cf. Fig. 5). Only in one case (11) could the  $^3J_{NH,CH}$  coupling constant be detected; it was 2.9 Hz. The corresponding signals of the other compounds were more or less broadened and the corresponding vicinal coupling constants could not be extracted. The magnitude of  $^3J_{NH,CH}$  was in good agreement with the calculated values. These were in the range 0–1.8 Hz, with calculated dihedral angles of 59.6–71.1°, both characteristic of the *syn-clinal* conformation of the NH–CH moiety. The distance between these two hydrogens was computed to be in the range 2.43–2.56 Å, which corresponds to the mean NOEs determined in these compounds.

Table 2

Experimental and computed coupling constants and some calculated dihedral angles and distances for compounds 18 and 25.

Compound	$^3J_{NCH-NH}$ (exp) (Hz)	$^3J_{NCH-NH}$ (calc) (Hz)	Dihedral angle NCH–NH	$^3J_{NH-OCH_{eq}}$ (exp) (Hz)	$^3J_{NH-OCH_{eq}}$ (calc) (Hz)	Dihedral angle NH– OCH <sub>eq</sub>	$^3J_{NH-OCH_{ax}}$ (exp) (Hz)	$^3J_{NH-OCH_{ax}}$ (calc) (Hz)	Dihedral angle NH–OCH <sub>ax</sub>	Distance NCH–NH (Å)	Distance NH–OCH <sub>eq</sub> (Å)
18	4.9	4.8	42.8°	3.7	3.1	–57.7°	13.9	13.1	–178.6°	2.241	2.358
25	6.2	4.7	41.6°	5.4	2.0	–58.0°	12.2	13.2	–179.0°	2.242	2.359

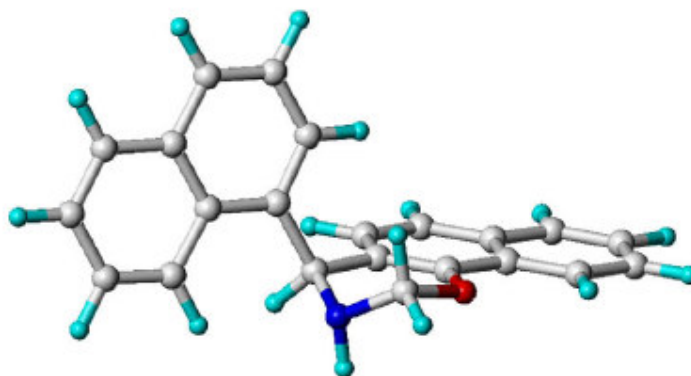


Fig. 2. Minimum-energy structure of (4S)-25.

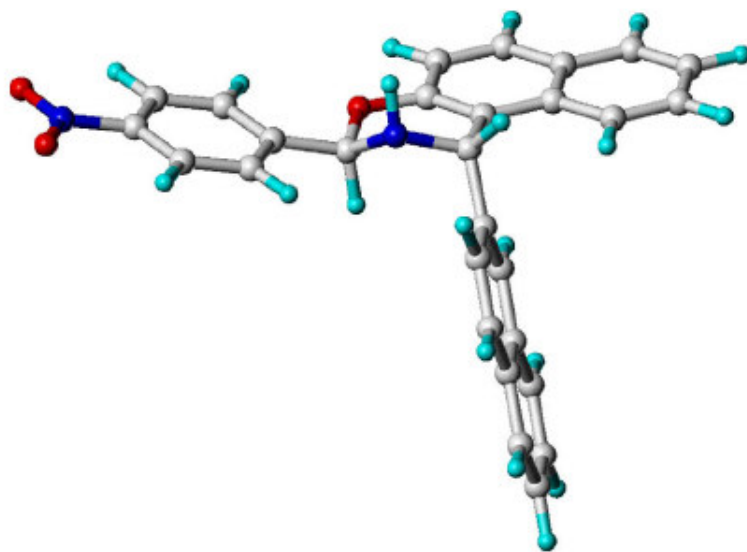


Fig. 3. Minimum-energy structure of (1S,3R)-27B.

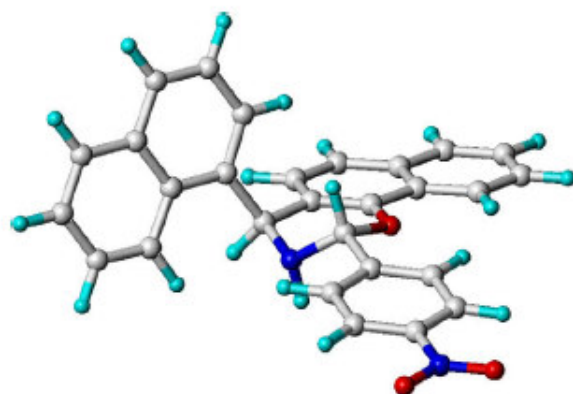


Fig. 4. Minimum-energy structure of (2R,4S)-32B.

For compounds 15, 16, 23 and 24 the endocyclic/exocyclic tautomerism of the C=N double bond is possible. The energy levels indicated the presence of the exocyclic form (Schemes 2 and 3). This was supported by the NMR data: NOE interactions were found between N–H and the corresponding C–H at position 1 (15 and

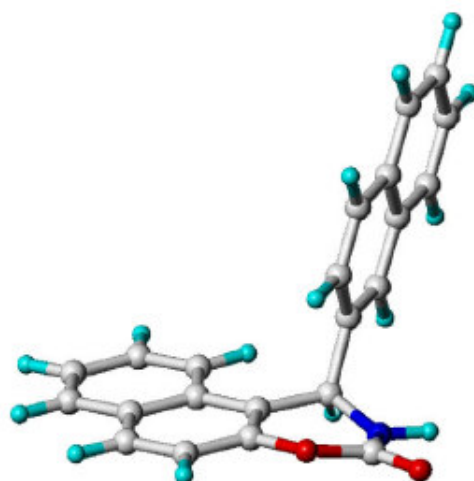


Fig. 5. Minimum-energy structure of (4R)-11.

16) or 4 (23 and 24). *Ab initio* calculations on the title compounds pointed to the presence of the *E* isomers.

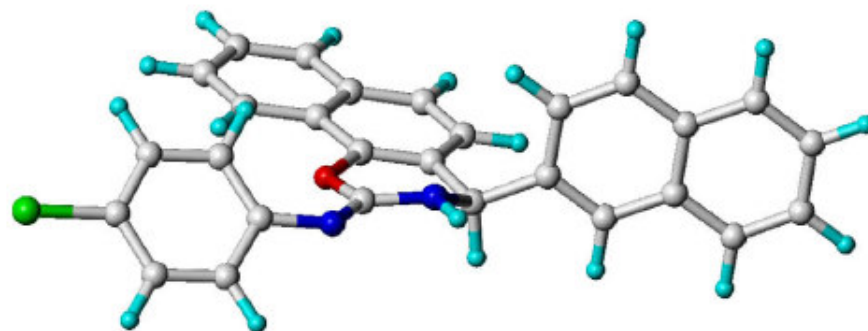


Fig. 6. Minimum-energy structure of (4R)-23.



The oxazine ring in **15**, **16**, **23** and **24** turned out to be nearly planar; the minimum-energy structure of **23** is shown in Fig. 6.

### 3. Conclusions

Four new aminomethylnaphthols (**4**, **5**, **9** and **10**) were synthesized by the condensation of 1- or 2-naphthol with 1- or 2-naphthaldehydes in the presence of ammonia, followed by acidic hydrolysis. The condensation of **4**, **5**, **9** and **10** with paraformaldehyde, 4-nitrobenzaldehyde, phosgene or 4-chlorophenyl isothiocyanate led to naphthoxazine derivatives. Compounds **27–29** and **31–33** in solution proved to be three-component tautomeric mixtures. The tautomeric ratio influenced by the steric hindrance of the aromatic rings at position 1 or 4 and by the connecting position of the naphthyl rings at the same positions. The conformational analysis revealed that the conformation of the oxazine ring moiety depends on the hybridization of the carbon at position 3 or 2. The compounds containing an  $sp^3$  carbon preferred a twisted-chair conformation, whereas the insertion of an  $sp^2$  carbon led to a nearly flat naphthoxazine ring moiety.

### 4. Experimental

Melting points were determined on a Kofler micro melting apparatus and are uncorrected. Merck Kieselgel 60F<sub>254</sub> plates were used for TLC.

The NMR spectra were recorded in DMSO- $d_6$  (unless specified as CDCl<sub>3</sub>) solution in 5 mm tubes, at room temperature, on a BRUKER AVANCE 500 spectrometer at 500.17 (<sup>1</sup>H) and 125.78 (<sup>13</sup>C) MHz, with the deuterium signal of the solvent as the lock and TMS as the internal standard for <sup>1</sup>H or the solvent as the internal standard for <sup>13</sup>C. All spectra (<sup>1</sup>H, <sup>13</sup>C, gs-H, H-COSY, gs-HMQC, gs-HMBC, and NOESY) were acquired and processed with the standard BRUKER software.

Geometry optimizations were performed without restrictions, using the Gaussian 03 version C.02[19] program package. Different conformation and configurations of all studied compounds were preoptimized by using the PM3 Hamiltonian [20,21]. Density functional theory calculations were carried out at the B3LYP/6-31G\*\* [22,23] level of theory. Stationary points on the potential hypersurface were characterized by force constants. Coupling constants were computed at the same theory level, B3LYP/6-31G\*\* [24,25].

Different starting conformations were created and the results were analysed and displayed by using the molecular modelling program SYBYL 7.3 [26] and the program GaussView 2.0. [27] Different local minimum-energy conformations were selected to analyse the relative stability and the geometrical parameter.

Results were calculated on a SGI and on a Linux cluster.

#### 4.1. General method for the synthesis of aminomethylnaphthyl naphthols (**4**, **5**, **9** and **10**)

To a solution of 1- or 2-naphthol (3.6 g, 25 mmol) in absolute MeOH (30 mL), the appropriate 1- or 2-naphthaldehyde (9.75 g, 62.5 mmol) and 25% methanolic ammonia solution (20 mL) were added. The mixture was allowed to stand at room temperature for 48 h. The solvent was removed under reduced pressure and 10% aq. HCl (210 mL) was added to the residue. The mixture was stirred and heated for 3 h at 60 °C, and the solvent was evaporated off. The crystalline hydrochloride of **4**, **5**, **9** or **10** that separated out from EtOAc (50 mL) was filtered off, washed with CHCl<sub>3</sub> and Et<sub>2</sub>O, and recrystallized from Et<sub>2</sub>O–MeOH (4:1).

##### 4.1.1. 1-[Aminomethyl-(2-naphthyl)]-2-naphthol hydrochloride (**4**)

White crystals, yield 7.29 g (87%), m.p. 193–195 °C. <sup>1</sup>H NMR (DMSO- $d_6$ ):  $\delta$  6.45 (H: CH, 1H, s), 7.35 (H: 8, 1H, t,  $J$  = 7.5 Hz), 7.46 (H: 3, 1H, d,  $J$  = 8.9 Hz), 7.48–7.55 (H: 7', 1', 2H, m), 7.59 (H: 6', 1H, d,  $J$  = 7.5 Hz), 7.85–7.91 (H: 4, 4', 8', 3', 5', 5', 6H, m), 8.07 (H: 7, 1H, s), 8.10 (H: 6, 1H, d,  $J$  = 8.6 Hz), 9.05 (H: NH<sub>3</sub>, 3H, s), 11.06 (H: OH, 1H, s) ppm. <sup>13</sup>C NMR (DMSO- $d_6$ ):  $\delta$  51.0 (C: CH), 113.7 (C: 1), 118.7 (C: 3), 121.9 (C: 6), 123.0 (C: 8), 125.2 (C: 6'), 125.9 (C: 7), 126.5 (C: 7'), 126.7 (C: 1'), 127.3 (C: 4'), 127.6 (C: 8'), 127.9 (C: 5'), 128.2 (C: 4a, 3'), 128.9 (C: 5), 130.8 (C: 4), 131.9 (C: 4a'), 132.4 (C: 8a), 132.5 (C: 8a'), 135.1 (C: 2'), 153.9 (C: 2) ppm. C<sub>21</sub>H<sub>18</sub>ClNO (335.83): calcd. C 75.11, H 5.40, N 4.17; found C 75.05, H 5.41, N 4.18.

##### 4.1.2. 1-[Aminomethyl-(1-naphthyl)]-2-naphthol hydrochloride (**5**)

White crystals, yield 2.34 g (28%), m.p. 202–204 °C. <sup>1</sup>H NMR (DMSO- $d_6$ ):  $\delta$  6.96 (H: CH, 1H, s), 7.25 (H: 2', 1H, t,  $J$  = 7.1 Hz), 7.33 (H: 4', 1H, t,  $J$  = 7.4 Hz), 7.4 (H: 3, 1H, d,  $J$  = 16.0 Hz), 7.51–7.55 (H: 3', 6', 2H, m), 7.79–7.88 (H: 6, 7', 8', 7, 5', 5H, m), 7.92–7.97 (H: 4, 5, 2H, m), 8.31–8.32 (H: 8, 1H, m), 8.96 (H: NH<sub>3</sub>, 3H, s), 11.92 (H: OH, 1H, s) ppm. <sup>13</sup>C NMR (DMSO- $d_6$ ):  $\delta$  48.3 (C: CH), 113.8 (C: 1), 118.8 (C: 3), 121.8 (C: 6), 122.9 (C: 8), 123.2 (C: 2'), 125.2 (C: 6'), 126.1 (C: 7'), 126.2 (C: 8'), 126.9 (C: 3'), 127.1 (C: 4'), 128.3 (C: 4a), 128.9 (C: 4), 128.9 (C: 5), 129.1 (C: 7), 130.1 (C: 8a'), 130.9 (C: 5'), 131.9 (C: 8a), 133.1 (C: 4a'), 133.5 (C: 1'), 154.2 (C: 2) ppm. C<sub>21</sub>H<sub>18</sub>ClNO (335.83): calcd. C 75.11, H 5.40, N 4.17; found C 75.15, H 5.42, N 4.19.

##### 4.1.3. 2-[Aminomethyl-(2-naphthyl)]-1-naphthol hydrochloride (**9**)

White crystals, yield 2.69 g (32%), m.p. 168–171 °C. <sup>1</sup>H NMR (DMSO- $d_6$ ):  $\delta$  6.32 (H: HC–NH<sub>3</sub>, 1H, s), 7.51–7.57 (H: 7, 6, 3', 8', 6', 5H, m), 7.63–7.56 (H: 5, 4a', 2H, m), 7.86–7.88 (H: 7', 1H, m), 7.89–7.95 (H: 4, 5', 4', 3H, m), 8.09 (H: 1', 1H, s), 8.35 (H: 8, 1H, dd,  $J$  = 6.20 Hz), 9.27 (H: NH<sub>3</sub>, 3H, s), 10.17 (H: OH, 1H, s) ppm. <sup>13</sup>C NMR (DMSO- $d_6$ ):  $\delta$  52.1 (C: HC–NH<sub>3</sub>), 119.5 (C: 2), 120.1 (C: 5'), 122.6 (C: 8), 124.9 (C: 3), 125.3 (C: 8'), 125.3 (C: 8a'), 125.6 (C: 7'), 125.6 (C: 1'), 126.6 (C: 2'), 126.8 (C: 6, 4'), 127.6 (C: 4), 127.8 (C: 6), 127.9 (C: 6'), 128.4 (C: 3'), 132.4 (C: 4a'), 132.5 (C: 8a), 134.0 (C: 4a), 135.7 (C: 2), 150.0 (C: 1) ppm. C<sub>21</sub>H<sub>18</sub>ClNO (335.83): calcd. C 75.11, H 5.40, N 4.17; found C 75.12, H 5.39, N 4.16.

##### 4.1.4. 2-[Aminomethyl-(1-naphthyl)]-1-naphthol hydrochloride (**10**)

White crystals, yield 3.52 g (42%), m.p. 161–164 °C. <sup>1</sup>H NMR (DMSO- $d_6$ ):  $\delta$  6.87 (H: HC, 1H, s), 7.25 (H: 3, 1H, d,  $J$  = 8.7 Hz), 7.34 (H: 4, 1H, d,  $J$  = 8.7 Hz), 7.47–7.56 (H: 8', 6', 5', 7, 4H, m), 7.68 (H: 3', 1H, t,  $J$  = 7.7 Hz), 7.78 (H: 6, 1H, d,  $J$  = 7.5 Hz), 7.94–7.98 (H: 4', 7', 2H, m), 8.03–8.06 (H: 5, 2', 2H, m), 8.45 (H: 8, 1H, d,  $J$  = 8.2 Hz), 9.23 (H: NH<sub>3</sub>, 3H, s), 10.54 (H: OH, 1H, s) ppm. <sup>13</sup>C NMR (DMSO- $d_6$ ):  $\delta$  48.3 (C: CH), 119.0 (C: 2), 120.0 (C: 4), 122.9 (C: 5, 8), 123.6 (C: 2'), 125.2 (C: 3'), 125.4 (C: 3), 125.4 (C: 8a), 125.6 (C: 8'), 126.2 (C: 5'), 126.9 (C: 6'), 126.9 (C: 7), 127.7 (C: 6), 128.7 (C: 4'), 128.9 (C: 7'), 129.8 (C: 4a'), 133.4 (C: 1'), 133.8 (C: 8a'), 134.2 (C: 4a), 150.0 (C: 1) ppm. C<sub>21</sub>H<sub>18</sub>ClNO (335.83): calcd. C 75.11, H 5.40, N 4.17; found C 75.11, H 5.45, N 4.16.

#### 4.2. General method for the synthesis of naphthyl naphthoxazinones (**11**, **12**, **19** and **20**)

Aminonaphthol **4**, **5**, **9** or **10** (0.50 g, 1.49 mmol) was dissolved in toluene–H<sub>2</sub>O 1:1 (50 mL), phosgene (0.32 mL; 20% in toluene, 1.64 mmol) and sodium carbonate (0.69 g, 1.64 mmol) were added. The mixture was stirred at r.t. for 10 min. and the resulting white precipitate was filtered off and recrystallized from iPr<sub>2</sub>O (30 mL).

#### 4.2.1. 1-(2-Naphthyl)-2,3-dihydro-1H-naphth[1,2-e][1,3]oxazin-3-one (**11**)

White crystals, yield 0.42 g (86%), m.p. 260–264 °C.  $^1\text{H}$  NMR (DMSO- $d_6$ ):  $\delta$  7.01 (H: 2', 1H, d,  $J$  = 7.1 Hz), 7.13 (H: 1, 1H, s), 7.31 (H: 7', 1H, s), 7.33 (H: 3', 1H, d,  $J$  = 3.8 Hz), 7.37 (H: 4', 1H, d,  $J$  = 7.2 Hz), 7.41 (H: 6', 1H, t,  $J$  = 8.1 Hz), 7.47 (H: 6, 1H, d,  $J$  = 8.9 Hz), 7.65 (H: 8, 1H, t,  $J$  = 7.3), 7.74 (H: 9, 1H, t,  $J$  = 7.2 Hz), 7.88 (H: 8', 1H, d,  $J$  = 8.1 Hz), 7.96 (H: 5', 1H, d,  $J$  = 8.1 Hz), 8.02 (H: 7, 1H, d,  $J$  = 8.1 Hz), 8.05 (H: 5, 1H, d,  $J$  = 9.0 Hz), 8.95 (H: NH, 1 H, d,  $J$  = 2.9 Hz) ppm.  $^{13}\text{C}$  NMR (DMSO- $d_6$ ):  $\delta$  49.7 (C: CH), 114.0 (C: 10b), 116.9 (C: 6), 122.8 (C: 6'), 123.5 (C: 10), 125.1 (C: 7'), 125.3 (C: 2'), 125.9 (C: 4'), 126.3 (C: 3'), 126.0 (C: 9), 127.4 (C: 3'), 128.7 (C: 7), 128.8 (C: 5'), 128.8 (C: 8'), 129.1 (C: 8a'), 130.0 (C: 1'), 130.4 (C: 10a), 130.5 (C: 4a'), 133.7 (C: 6a), 148.1 (C: 3), 149.3 (C: 4a) ppm.  $\text{C}_{22}\text{H}_{15}\text{NO}_2$  (325.36): calcd. C 81.21, H 4.65, N 4.30; found C 81.28, H 4.66, N 4.28.

#### 4.2.2. 1-(1-Naphthyl)-2,3-dihydro-1H-naphth[1,2-e][1,3]oxazin-3-one (**12**)

White crystals, yield 0.21 g (44%), m.p. 262–265 °C.  $^1\text{H}$  NMR (DMSO- $d_6$ ):  $\delta$  6.38 (H: 1, 1H, s), 7.39–7.49 (H: 3', 6', 5', 6, 4H, m), 7.49–7.53 (H: 8, 8', 2H, m), 7.85–7.89 (H: 4', 7, 9, 7, 4H, m), 7.93 (H: 1', 1H, s), 7.95 (H: 10, 1H, d,  $J$  = 7.6 Hz), 8.03 (H: 5, 1H, d,  $J$  = 9.0 Hz), 8.95 (H: 2, 1H, d,  $J$  = 2.9 Hz) ppm.  $^{13}\text{C}$  NMR (DMSO- $d_6$ ):  $\delta$  55.6 (C: 1), 115.1 (C: 10a), 118.4 (C: 6), 124.5 (C: 7'), 126.1 (C: 3'), 126.5 (C: 5'), 127.3 (C: 1'), 127.9 (C: 8), 128.1 (C: 8'), 128.8 (C: 6'), 128.9 (C: 4'), 129.4 (C: 7), 130.1 (C: 10), 130.4 (C: 9), 130.5 (C: 6a), 131.9 (C: 5), 131.9 (C: 8a'), 133.9 (C: 4a'), 134.1 (C: 2'), 141.3 (C: 10b), 148.6 (C: 4a), 150.8 (C: 3) ppm.  $\text{C}_{22}\text{H}_{15}\text{NO}_2$  (325.36): calcd. C 81.21, H 4.65, N 4.30; found C 81.23, H 4.63, N 4.29.

#### 4.2.3. 4-(2-Naphthyl)-2,3-dihydro-1H-naphth[2,1-e][1,3]oxazin-2-one (**19**)

White crystals, yield 0.19 g (40%), m.p. 227–232 °C.  $^1\text{H}$  NMR (DMSO- $d_6$ ):  $\delta$  6.04 (H: 4, 1H, s), 7.20 (H: 5, 1H, d,  $J$  = 8.4 Hz), 7.49 (H: 1', 1H, d,  $J$  = 8.4 Hz), 7.51–7.56 (H: 4', 5', 2H, m), 7.59–7.68 (H: 9, 7, 6, 3H, m), 7.89–7.96 (H: 8', 7', 6', 8, 3', 5H, m), 8.24 (H: 10, 1H, d,  $J$  = 8.3 Hz), 8.86 (H: 3, 1H, s) ppm.  $^{13}\text{C}$  NMR (DMSO- $d_6$ ):  $\delta$  56.6 (C: 4), 115.9 (C: 2'), 120.6 (C: 10), 122.5 (C: 8a'), 123.8 (C: 8), 124.1 (C: 5), 124.8 (C: 1'), 125.7 (C: 3'), 126.5 (C: 4'), 126.7 (C: 6'), 127.0 (C: 8), 128.0 (C: 9), 128.9 (C: 7'), 132.6 (C: 4a'), 132.8 (C: 10a), 133.1 (C: 6a), 140.5 (C: 4a), 143.5 (C: 10b), 149.2 (C: 2) ppm.  $\text{C}_{22}\text{H}_{15}\text{NO}_2$  (325.36): calcd. C 81.21, H 4.65, N 4.30; found C 81.20, H 4.61, N 4.29.

#### 4.2.4. 4-(1-Naphthyl)-2,3-dihydro-1H-naphth[2,1-e][1,3]oxazin-2-one (**20**)

White crystals, yield 0.38 g (78%), m.p. 234–237 °C.  $^1\text{H}$  NMR (DMSO- $d_6$ ):  $\delta$  6.70 (H: 4, 1H, s), 6.94 (H: 5, 1H, d,  $J$  = 8.5 Hz), 7.48 (H: 2', 1H, d,  $J$  = 6.8 Hz), 7.53 (H: 3', 1H, t,  $J$  = 7.8 Hz), 7.55–7.57 (H: 6, 6', 8', 3H, m), 7.61 (H: 8, 1H, t,  $J$  = 7.6 Hz), 7.68 (H: 9, 1H, t,  $J$  = 7.3 Hz), 7.89 (H: 5', 1H, d,  $J$  = 8.1 Hz), 7.95 (H: 4', 1H, d,  $J$  = 7.9 Hz), 8.00–8.02 (H: 7', 1H, m), 8.36 (H: 10, 1H, d,  $J$  = 8.3 Hz), 8.33 (H: 7, 1H, d,  $J$  = 7.1 Hz), 8.80 (H: 3, 1H, s) ppm.  $^{13}\text{C}$  NMR (DMSO- $d_6$ ):  $\delta$  53.7 (C: 4), 116.4 (C: 1'), 120.6 (H: 10), 122.5 (C: 5), 123.4 (C: 7), 123.5 (C: 4a), 123.8 (C: 6), 125.8 (C: 8'), 126.0 (C: 6'), 126.7 (C: 2'), 126.9 (C: 8), 127.1 (C: 9, 3'), 127.9 (C: 5'), 128.9 (C: 4', 7'), 130.3 (C: 8a'), 133.2 (C: 6a), 133.9 (C: 10a) ppm.  $\text{C}_{22}\text{H}_{15}\text{NO}_2$  (325.36): calcd. C 81.21, H 4.65, N 4.30; found C 81.20, H 4.64, N 4.32.

#### 4.3. General method for the synthesis of thiourea derivatives (**13**, **14**, **21** and **22**)

A mixture of aminonaphthol **4**, **5**, **9** or **10** (0.30 g, 0.89 mmol) and 4-chlorophenyl isothiocyanate (0.22 g, 1.29 mmol) in abs. tol-

uene (10 mL) was stirred at room temperature for 6 h. The crystals that separated out were filtered off and washed with toluene (2  $\times$  10 mL). The product was purified by column chromatography (silica gel, eluent: *n*-hexane–EtOAc, 3:1).

#### 4.3.1. *N*'-[ $\alpha$ -(1-hydroxynaphth-2-yl)naphth-2-yl-methyl]-*N*'-(4-chlorophenyl)thiourea (**21**)

Light-yellow crystals, yield 0.26 g (65%), m.p. 125–129 °C.  $^1\text{H}$  NMR (DMSO- $d_6$ ):  $\delta$  7.51 (H: 4, 1', 7', 8, 8', 3', 7, 2'', CH, 10H, m), 7.63 (H: 4', 6, 2H, d,  $J$  = 15.0 Hz), 7.77 (H: 3, 1H, s), 7.83–7.91 (H: 3', 5', 5, 4H, m), 8.22–8.25 (H: 6', 1H, m), 8.78 (H: CHNH, 1H, d,  $J$  = 13.9 Hz), 9.69 (H: CNH, 1H, s), 9.87 (H: OH, 1H, s) ppm.  $^{13}\text{C}$  NMR (DMSO- $d_6$ ):  $\delta$  56.4 (C: HC–NH), 119.8 (C: 4), 122.1 (C: 6'), 123.4 (C: 2, 8a), 124.2 (C: 4'), 124.7 (C: 3), 125.1 (C: 6), 125.4 (C: 4a), 125.7 (C: 1'), 125.8 (C: 7'), 126.0 (C: 8), 126.2 (C: 8', 3'), 126.4 (C: 7), 127.5 (C: 5), 127.7 (C: 3''), 127.9 (C: 5'), 128.4 (C: 2'), 132.0 (C: 4a', 2'), 132.8 (C: 4''), 133.7 (C: 8a'), 138.7 (C: 4a'), 140.0 (C: 1'), 149.6 (C: 1), 180.2 (C: CS) ppm.  $\text{C}_{28}\text{H}_{21}\text{ClN}_2\text{OS}$  (469.00): calcd. C 71.71, H 4.51, N 5.97; found C 71.78, H 4.50, N 5.98.

#### 4.3.2. *N*'-[ $\alpha$ -(1-hydroxynaphth-2-yl)naphth-1-yl-methyl]-*N*'-(4-chlorophenyl)thiourea (**22**)

Light-yellow crystals: yield 0.29 g (72%), m. p. 158–160 °C.  $^1\text{H}$  NMR (DMSO- $d_6$ ):  $\delta$  7.30–7.34 (C: 2'', 2, 5, 4H, m), 7.43–7.56 (C: 6, 7', 8', 3', 4', 8, 6H, m), 7.63 (C: H: 3'', 2H, d,  $J$  = 8.5 Hz), 7.82–7.89 (C: CH, 3, 6', 3H, m), 7.95 (H: 2, 1H, d,  $J$  = 7.9 Hz), 8.23–8.26 (H: 2, 7, 2H, m), 8.67 (H: HC–NH, 1H, d,  $J$  = 7.7 Hz), 9.63 (H: OH, 1H, s), 9.75 (H: HN–SC, 1H, s) ppm.  $^{13}\text{C}$  NMR (DMSO- $d_6$ ):  $\delta$  52.7 (C: CH), 119.6 (C: 4), 122.1 (C: 7), 123.0 (C: 2), 123.8 (C: 3''), 124.3 (C: 2'), 125.1 (C: 6), 125.2 (C: 4a), 125.3 (C: 5), 125.8 (C: 7', 8'), 125.9 (C: 3'), 126.3 (C: 4'), 127.4 (C: 8a), 127.7 (C: 3, 6'), 128.2 (C: 2''), 128.6 (C: 8), 131.0 (C: 4a'), 133.5 (C: 8a'), 133.7 (C: 1'), 138.2 (C: 4''), 138.8 (C: 1''), 149.4 (C: 1), 179.8 (C: CS) ppm.  $\text{C}_{28}\text{H}_{21}\text{ClN}_2\text{OS}$  (469.00): calcd. C 71.71, H 4.51, N 5.97; found C 71.74, H 4.51, N 5.97.

#### 4.3.3. *N*'-[ $\alpha$ -(2-hydroxynaphth-1-yl)naphth-2-yl-methyl]-*N*'-(4-chlorophenyl)thiourea (**13**)

Light-yellow crystals: yield 0.342 g (82%), m.p. 193–197 °C.  $^1\text{H}$  NMR (DMSO- $d_6$ ):  $\delta$  7.26–7.44 (H: 1', 8', 7, 6', 7', 3, 6H, m), 7.50–7.61 (H: 3', 3'', 4, 4H, m), 7.81–7.87 (H: 5', 5, 2', 4H, m), 7.94–8.03 (H: 8, 6, 2H, m), 8.30 (H: CH, 1H, d,  $J$  = 8.6 Hz), 8.36–8.39 (H: 4', 1H, m), 8.65 (H: HC–NH, 1H, d,  $J$  = 5.7 Hz), 9.96 (H: OH, 1H, s), 10.21 (H: HNC, 1H, s) ppm.  $^{13}\text{C}$  NMR (DMSO- $d_6$ ):  $\delta$  52.32 (C: HC–NH), 117.7 (C: 1), 118.8 (C: 3), 122.6 (C: 8) 123.8 (C: 3', 3'), 125.2 (C: 6), 125.7 (C: 6', 7'), 126.4 (C: 7), 126.7 (C: 8'), 127.9 (C: 1'), 128.3 (C: 2'), 128.4 (C: 4'), 128.6 (C: 4), 128.8 (C: 5), 129.5 (C: 8a, 5'), 131.2 (C: 4a'), 132.6 (C: 4a'), 132.6 (C: 8a'), 133.6 (C: 4''), 136.1 (C: 1''), 138.6 (C: 2'), 153.8 (C: 2), 179.2 (C: CS) ppm.  $\text{C}_{28}\text{H}_{21}\text{ClN}_2\text{OS}$  (469.00): calcd. C 71.71, H 4.51, N 5.97; found C 71.69, H 4.49, N 5.93.

#### 4.3.4. *N*'-[ $\alpha$ -(2-hydroxynaphth-1-yl)naphth-1-yl-methyl]-*N*'-(4-chlorophenyl)thiourea (**14**)

Light-yellow crystals: yield 0.33 g (80%), m.p. 88–92 °C.  $^1\text{H}$  NMR (DMSO- $d_6$ ):  $\delta$  12.01–12.27 (H: 3, 4, 5, 8', 6', 7, 7', 4', 2'', CH, 11H, m), 12.39 (H: 2', d,  $J$  = 8.8 Hz), 12.53 (H: 6, 1H, s), 12.60–12.64 (H: 3', 3'', 5', 4H, m), 12.98–13.01 (H: 8, 1H, m), 13.55 (H: NHCH, 1H, d,  $J$  = 8.4 Hz), 14.45 (H: SCNH, 1H, s), 14.63 (H: OH, 1H, s) ppm.  $^{13}\text{C}$  NMR (DMSO- $d_6$ ):  $\delta$  56.4 (C: CH), 119.8 (C: 3), 122.1 (C: 8), 123.4 (C: 1), 124.2 (C: 2'), 124.7 (C: 6), 125.2 (C: 8'), 125.4 (C: 8a'), 125.7 (C: 4, 5), 125.8 (C: 6'), 126.0 (C: 7), 126.2 (C: 7'), 126.4 (C: 4'), 127.5 (C: 3'), 127.7 (C: 3''), 127.9 (C: 5'), 128.3 (C: 2''), 132.0 (C: 4a), 132.8 (C: 8a), 133.7 (C: 4a'), 138.7 (C: 1'), 140.0 (C: 1'), 149.6 (C: 4'', 2), 180.3 (C: CS) ppm.  $\text{C}_{28}\text{H}_{21}\text{ClN}_2\text{OS}$  (469.00): calcd. C 71.71, H 4.51, N 5.97; found C 71.68, H 4.49, N 6.00.



#### 4.4. General method for the synthesis of naphthyl-(4-chlorophenylimino)naphthoxazine (**15**, **16**, **23** and **24**)

To a solution of thiourea **13**, **14**, **21** or **22** (0.10 g, 0.23 mmol) in MeOH (6 mL), MeI (0.10 mL, 6.43 mmol) was added and the solution was stirred for 4 h. After evaporation of the solvent, the residue was stirred in 3 M methanolic KOH (10 mL) for 4 h, after which the resultant white precipitate was filtered off and recrystallized from *n*-hexane–iPr<sub>2</sub>O (5:1, 36 mL).

##### 4.4.1. 1-(2-Naphthyl)-3-(4-chlorophenylimino)-2,3-dihydro-1H-naphth[1,2-*e*]1,3-oxazine (**15**)

Yellow crystals, yield 0.07 g (76%), m.p. 102–105 °C. <sup>1</sup>H NMR (DMSO-*d*<sub>6</sub>): δ 6.61 (H: 6', 1H, d, *J* = 7.0 Hz), 7.13 (H: 1, 1H, s), 7.15–7.23 (H: 3'', 7'', 3H, m), 7.32–7.45 (H: 5, 1', 5', 3', 4H, m), 7.56–7.64 (H: 8, 2'', 2H, m), 7.75–7.82 (H: 10, 8', 2H, m), 7.96–7.99 (H: 7, 1H, m), 8.06–8.07 (H: 6, 1H, d, *J* = 9.0 Hz), 7.88–8.89 (H: 9, 1H, d, *J* = 8.5 Hz), 9.43 (H: 2, 1H, s) ppm. <sup>13</sup>C NMR (DMSO-*d*<sub>6</sub>): δ 51.3 (C: 1), 114.8 (C: 10a), 116.2 (C: 5), 119.3 (C: 1'), 122.9 (C: 3'), 123.9 (H: 6'), 124.7 (C: 9), 124.8 (C: 4'), 124.9 (C: 8a'), 125.5 (C: 7'), 126.0 (C: 8), 126.4 (C: 4a'), 127.2 (C: 8''), 127.8 (C: 7), 128.2 (C: 3''), 128.4 (C: 10a), 128.5 (C: 6a), 128.7 (C: 2''), 129.7 (C: 6), 129.8 (C: 10), 130.7 (C: 10b), 130.9 (C: 2'), 133.8 (C: 1''), 139.6 (C: 4''), 144.6 (C: 3), 147.7 (C: 4a) ppm. C<sub>28</sub>H<sub>19</sub>ClN<sub>2</sub>O (434.92): calcd. C 77.33, H 4.40, N 6.44; found: C 77.30, H 4.42, N 6.48.

##### 4.4.2. 1-(1-Naphthyl)-3-(4-chlorophenylimino)-2,3-dihydro-1H-naphth[1,2-*e*]1,3-oxazine (**16**)

Yellow crystals, yield 0.075 g (82%), m.p. 115–119 °C. <sup>1</sup>H NMR (DMSO-*d*<sub>6</sub>): δ 7.20 (H: 5, 1H, d, *J* = 7.6 Hz), 7.32–7.51 (H: 10, 9, 6', 4', 7, 7', 7'', 1', 8, 9H, m), 7.61 (H: 2'', 2H, d, *J* = 7.4), 7.70 (H: 2', 1H, s), 7.79–7.84 (H: 3'', 5', 6, 3, 4, 6H, m), 8.09 (H: CH, 1H, s), 8.19 (H: NH, 1H, s), <sup>13</sup>C NMR (DMSO-*d*<sub>6</sub>): δ 53.7 (C: 1), 119.7 (C: 10b), 120.3 (C: 5), 123.9 (C: 10), 125.2 (C: 8), 125.9 (C: 2''), 126.4 (C: 9), 127.0 (C: 4'), 127.6 (C: 6'), 128.4 (C: 2'), 128.8 (C: 3''), 129.1 (C: 6, 7), 129.4 (C: 6a), 130.1 (C: 7'), 130.2 (C: 3'), 133.3 (C: 8a', 4'), 134.0 (C: 1'), 134.1 (C: 10a, 4a'), 139.8 (C: 1''), 141.5 (C: 4a), 181.7 (C: 3) ppm. C<sub>28</sub>H<sub>19</sub>ClN<sub>2</sub>O (434.92): calcd. C 77.33, H 4.40, N 6.44; found: C 77.31, H 4.38, N 6.48.

##### 4.4.3. 4-(2-Naphthyl)-2-(4-chlorophenylimino)-2,3-dihydro-1H-naphth[2,1-*e*]1,3-oxazine (**23**)

Yellow crystals, yield 0.062 g (67%), m.p. 185–188 °C. <sup>1</sup>H NMR (DMSO-*d*<sub>6</sub>): δ 6.06 (H: NH–CH, 1H, s), 7.19 (H: 4', 1H, d, *J* = 8.4 Hz), 7.31 (H: 2'', 2H, d, *J* = 8.8 Hz), 7.43–7.52 (H: 3', 8, 5, 3 H, m), 7.56–7.63 (H: 10, 7', 2H, m), 7.67 (H: 9, 1H, t, *J* = 7.3 Hz), 7.74 (7, 6, 2H, d, *J* = 8.3 Hz), 7.86–7.93 (H: 3'', 5', 8', 1', 5H, m), 8.30 (H: 6', 1H, d, *J* = 8.3 Hz) ppm. <sup>13</sup>C NMR (DMSO-*d*<sub>6</sub>): δ 57.7 (C: 4), 118.2 (C: 4a), 119.8 (C: 6), 120.6 (C: 6'), 122.4 (C: 10a), 123.6 (C: 7'), 124.5 (C: 4'), 124.9 (C: 1'), 125.4 (C: 5), 125.7 (C: 8), 126.0 (C: 3'), 126.4 (C: 9), 126.6 (C: 7), 126.8 (C: 10), 127.6 (C: 5'), 127.9 (C: 2'), 128.5 (C: 3'), 128.6 (C: 4a', 8'), 132.3 (C: 6a), 132.9 (C: 8a', 4'') ppm. C<sub>28</sub>H<sub>19</sub>ClN<sub>2</sub>O (434.92): calcd. C 77.33, H 4.40, N 6.44; found: C 77.35, H 4.43, N 6.45.

##### 4.4.4. 4-(1-Naphthyl)-2-(4-chlorophenylimino)-2,3-dihydro-1H-naphth[2,1-*e*]1,3-oxazine (**24**)

Yellow crystals, yield 0.068 g (74%), m.p. 195–196 °C. <sup>1</sup>H NMR (DMSO-*d*<sub>6</sub>): δ 6.68 (H: 4, 1H, s), 7.03 (H: 8', 1H, d, *J* = 8.3 Hz), 7.09 (H: 7', 1H, d, *J* = 15.0 Hz), 7.23 (H: 2'', 2H, d, *J* = 8.4 Hz), 7.41 (H: 6', 1H, t, *J* = 7.6 Hz), 7.57–7.72 (H: 4', 9, 3'', 6, 5, 8, 7H, m), 7.86 (H: 5'', 1H, d, *J* = 8.0 Hz), 7.95 (H: 2', 7, 2H, dd, *J* = 8.0, 19.8 Hz), 8.33 (H: 3', 1H, d, *J* = 8.2 Hz), 8.55 (H: 10, 1H, d, *J* = 8.1 Hz), 9.54 (H: 3, 1H, br) ppm. <sup>13</sup>C NMR (DMSO-*d*<sub>6</sub>): δ 54.3 (C: 4), 117.9 (C: 4a, 1'), 119.5 (C: 9), 120.5 (C: 3'), 122.4 (C: 10a), 123.5 (C: 5),

124.3 (C: 8'), 124.4 (C: 6), 124.8 (C: 4'), 125.4 (C: 7'), 125.6 (C: 10), 125.8 (C: 6'), 126.2 (C: 4'), 126.6 (C: 3''), 126.7 (C: 3''), 127.8 (C: 9, 5'), 128.3 (C: 2''), 128.6 (2''), 130.9 (C: 8a'), 132.9 (C: 4a'), 133.7 (C: 6a), 140.4 (C: 10b), 143.8 (C: 1''), 144.8 (C: 2) ppm. C<sub>28</sub>H<sub>19</sub>ClN<sub>2</sub>O (434.92): calcd. C 77.33, H 4.40, N 6.44; found: C 77.35, H 4.37, N 6.42.

#### 4.5. General method for the synthesis of naphthyl-naphth[1,3]oxazines (**17**, **18** and **25**)

Aminonaphthol **4**, **5** or **10** (0.15 g, 0.45 mmol), 3 equivalents of paraformaldehyde, 1.1 equivalent of Et<sub>3</sub>N and chloroform (8 mL) were mixed in room temperature for 6 h and the solvent was then evaporated off. The product was purified by column chromatography (silica gel, eluent: *n*-hexane–EtOAc).

##### 4.5.1. 1-(2-Naphthyl)-2,3-dihydro-1H-naphth[1,2-*e*]1,3-oxazine (**17**)

Eluent for column chromatography: hexane–EtOAc (4:1), white crystals, yield 0.067 g (49%), m.p. 157–160 °C. <sup>1</sup>H NMR (DMSO-*d*<sub>6</sub>): δ 4.35–4.39 (H: 2, 1H, m), 4.60 (H: 3, 1H, dd, *J* = 10.2, 13.65 Hz), 4.89 (H: 3, 1H, dd, *J* = 3.8, 9.8 Hz), 5.675 (H: 1, 1H, d, *J* = 5.0 Hz), 7.14 (H: 1, 1H, d, *J* = 12.9 Hz), 7.22–7.29 (H: 10, 1', 2H, m), 7.34–7.36 (H: 5, 1H, m), 7.39–7.41 (H: 9, 1', 2H, m), 7.46 (H: 6', 1H, t, *J* = 7.1 Hz), 7.61 (H: 7, 1H, d, *J* = 8.1 Hz), 7.67 (H: 8', 1H, d, *J* = 8.0 Hz), 7.83–7.94 (H: 6, 5', 7', 4', 4H, m) ppm. <sup>13</sup>C NMR (DMSO-*d*<sub>6</sub>): δ 51.9 (C: 1), 73.2 (C: 3), 114.8 (C: 10b), 119.1 (C: 5), 122.5 (C: 10), 122.9 (C: 8), 125.9 (C: 6'), 126.1 (C: 7), 126.4 (C: 9), 127.4 (C: 1'), 127.5 (C: 3'), 127.6 (C: 4'), 127.8 (C: 8'), 127.9 (C: 7'), 128.3 (C: 6a), 128.5 (C: 5'), 128.9 (C: 6), 131.4 (C: 10'), 132.2 (C: 4a'), 132.5 (C: 8a'), 140.8 (C: 10a), 152.0 (C: 4a) ppm. C<sub>22</sub>H<sub>17</sub>NO (311.38): calcd. C 84.86, H 5.50, N 4.50; found: C 84.87, H 5.49, N 4.51.

##### 4.5.2. 1-(1-Naphthyl)-2,3-dihydro-1H-naphth[1,2-*e*]1,3-oxazine (**18**)

Eluent for column chromatography: *n*-hexane–EtOAc (3:1), white crystals, yield 0.057 g (42%), m.p. 135–140 °C. <sup>1</sup>H NMR (DMSO-*d*<sub>6</sub>): δ 4.31–4.34 (H: 2, 1H, m), 4.63 (H: 3, 1H, dd, *J* = 10.4, 13.8 Hz), 4.86 (H: 3, 1H, dd, *J* = 3.6, 9.8 Hz), 6.33 (H: 1, 1H, d, *J* = 4.9 Hz), 6.81 (H: 2', 1H, d, *J* = 6.7 Hz), 7.08 (H: 10, 1H, d, *J* = 8.3 Hz), 7.16–7.25 (H: 5', 5, 3', 9, 4H, m), 7.60 (H: 6', 1H, t, *J* = 7.5 Hz), 7.67 (H: 8, 1H, t, *J* = 7.6 Hz), 7.81–7.84 (H: 4', 6, 8', 3H, m), 7.98 (H: 7', 1H, d, *J* = 8.0 Hz), 8.63 (H: 7, 1H, d, *J* = 8.3 Hz) ppm. <sup>13</sup>C NMR (DMSO-*d*<sub>6</sub>): δ 48.4 (C: 1), 73.2 (C: 3), 114.8 (C: 10b), 119.0 (C: 5), 122.3 (C: 10), 122.9 (C: 9), 124.5 (C: 7), 124.7 (C: 3'), 125.8 (C: 8), 126.2 (C: 6'), 126.4 (C: 6), 127.4 (C: 2'), 127.8 (C: 4'), 128.3 (C: 6a), 128.5 (C: 8'), 128.6 (C: 5'), 128.8 (C: 7'), 131.0 (C: 8a'), 131.3 (C: 1'), 133.9 (C: 4a'), 138.0 (C: 10a), 152.3 (C: 4a) ppm. C<sub>22</sub>H<sub>17</sub>NO (311.38): calcd. C 84.86, H 5.50, N 4.50; found: C 84.81, H 5.51, N 4.53.

##### 4.5.3. 4-(1-Naphthyl)-2,3-dihydro-1H-naphth[2,1-*e*]1,3-oxazine (**25**)

Eluent for column chromatography: hexane–EtOAc (3:1), white crystals, yield 0.052 g (37%), m.p. 141–145 °C. <sup>1</sup>H NMR (DMSO-*d*<sub>6</sub>): δ 4.34 (H: 3, 1H, ddd, *J* = 5.4; 6.2, 12.2 Hz), 4.75 (H: 2, 1H, dd, *J* = 10.3, 12.2 Hz), 5.06 (H: 2, 1H, dd, *J* = 5.4, 10.0 Hz), 6.03 (H: 4, 1H, d, *J* = 6.2 Hz), 6.93 (1H, d, *J* = 7.0 Hz), 6.96 (1H, d, *J* = 8.4 Hz), 7.36 (1H, t, *J* = 7.7 Hz), 7.38 (1H, d, *J* = 8.5 Hz), 7.59 (4H, m), 7.86 (2H, d, *J* = 8.8 Hz), 7.98 (1H, d, *J* = 8.0 Hz), 8.14 (1H, m), 6.47 (1H, d, *J* = 8.4 Hz) ppm. <sup>13</sup>C NMR (DMSO-*d*<sub>6</sub>): δ 52.9 (C: 4), 75.3 (C: 2), 117.4 (C: 7), 119.6 (C: 2'), 121.4 (C: 6'), 123.7 (C: 8'), 124.9 (C: 6), 125.3 (C: 1'), 125.6 (C: 10), 125.8 (C: 8), 126.3 (C: 7), 126.5 (C: 6'), 126.6 (C: 5), 127.6 (C: 3'), 128.2 (C: 4'), 128.6 (C: 5'), 128.9 (C: 9), 129.3 (C: 10a), 131.7 (C: 8a'), 133.6 (C: 6a), 134.2 (C: 4a'), 138.1 (C: 6a), 150.3 (C: 10b) ppm. C<sub>22</sub>H<sub>17</sub>NO (311.38): calcd. C 84.86, H 5.50, N 4.50; found: C 84.82, H 5.53, N 4.50.

#### 4.6. General method for the synthesis of naphthyl-(4-nitrophenyl)-2,3-dihydro-1H-naphth[1,3]oxazines (27, 28, 31 and 32)

Aminonaphthol 4, 5, 9 or 10 (0.15 g, 0.45 mmol), 1 equivalent amount of 4-nitrobenzaldehyde, 1.1 equivalent of Et<sub>3</sub>N and methanol (2 mL) were mixed at room temperature for 10 min, and the resulting crystals were filtered off and recrystallized from iPr<sub>2</sub>O (30 mL).

##### 4.6.1. 1-(2-Naphthyl)-3-(4-nitrophenyl)-2,3-dihydro-1H-naphth[1,2-e][1,3]oxazine (27)

Yellow crystals, yield 0.162 g (84%), m.p. 232–235 °C. <sup>1</sup>H NMR (DMSO-*d*<sub>6</sub>): δ 4.72 (H: 2, 1H, dd, *J* = 5.3, 13.9 Hz), 5.82 (H: 3, 1H, d, *J* = 13.9 Hz), 6.47 (H: 1, 1H, d, *J* = 5.2 Hz), 6.93 (H: 3', 1H, d, *J* = 7.0 Hz), 7.13 (H: 6', 1H, d, *J* = 8.3 Hz), 7.22 (H: 1', 1H, t, *J* = 6.9 Hz), 7.27–7.31 (H: 5, 7', 2H, m), 7.62 (H: 8, 1H, t, *J* = 7.3 Hz), 7.70 (H: 2', 2H, s), 7.72 (H: 9, 1H, s), 7.85–7.92 (H: 8', 5', 6, 3H, m), 8.01 (H: 7, 1H, d, *J* = 8.1 Hz), 8.22 (H: 8', 1H, d, *J* = 8.8 Hz), 8.68 (H: 10, 1H, d, *J* = 8.5 Hz) ppm. <sup>13</sup>C NMR (DMSO-*d*<sub>6</sub>): δ 49.9 (C: 1), 81.9 (C: 3), 114.6 (C: 10b), 119.0 (C: 5), 122.6 (C: 6'), 123.3 (C: 4'), 123.5 (C: 3''), 124.4 (C: 10), 124.9 (C: 7'), 126.0 (C: 8), 126.5 (C: 9), 126.7 (C: 1'), 127.8 (C: 3'), 127.9 (C: 2'), 128.2 (C: 8'), 128.6 (C: 7), 128.7 (C: 8a'), 128.8 (C: 5'), 129.2 (C: 6), 131.0 (C: 10a), 131.1 (C: 4a'), 134.0 (C: 6a), 137.8 (C: 2'), 145.8 (C: 4'), 147.4 (C: 1''), 152.5 (C: 4a) ppm. C<sub>28</sub>H<sub>20</sub>N<sub>2</sub>O<sub>3</sub> (432.47): calcd. C 77.76, H 4.66, N 6.48; found C 77.69, H 4.68, N 6.52.

##### 4.6.2. 1-(1-Naphthyl)-3-(4-nitrophenyl)-2,3-dihydro-1H-naphth[1,2-e][1,3]oxazine (28)

White crystals, yield 0.153 g (80%), m.p. 170–173 °C. <sup>1</sup>H NMR (DMSO-*d*<sub>6</sub>): δ 4.74 (H: 2, 1H, dd, *J* = 5.0, 13.6 Hz), 5.76 (H: 3, 1H, d, *J* = 13.6 Hz), 5.84 (H: 1, 1H, d, *J* = 4.9 Hz), 7.29–7.33 (H: 2'', 9', 2H, m), 7.4–7.53 (H: 10, 2', 5', 6', 8', 5H, m), 7.69–7.74 (H: 3', 7', 2H, m), 7.80 (H: 3', 2H, d, *J* = 8.7 Hz), 7.89–7.98 (H: 4', 7, 6, 6', 4H, m), 8.25–8.26 (H: 8, 5, 2H, m). <sup>13</sup>C NMR (DMSO-*d*<sub>6</sub>): δ 54.6 (C: 1), 83.2 (C: 3), 114.6 (C: 10b), 119.1 (C: 5), 123.3 (C: 8), 123.4 (C: 2'), 124.0 (C: 2'), 124.4 (C: 10), 125.4 (C: 8'), 126.0 (C: 6'), 126.1 (C: 9), 126.7 (C: 3'), 127.5 (C: 4', 7'), 127.8 (C: 5'), 127.9 (C: 3''), 128.1 (C: 6), 128.5 (C: 6a), 128.7 (C: 6'), 129.4 (C: 7), 131.3 (C: 8a'), 132.3 (C: 10a), 132.5 (C: 4a'), 140.6 (C: 1'), 145.7 (C: 1'), 147.2 (C: 4''), 152.1 (C: 4a) ppm. C<sub>28</sub>H<sub>20</sub>N<sub>2</sub>O<sub>3</sub> (432.47): calcd. C 77.76, H 4.66, N 6.48; found C 77.82, H 4.68, N 6.44.

##### 4.6.3. 4-(2-Naphthyl)-2-(4-nitrophenyl)-2,3-dihydro-1H-naphth[2,1-e][1,3]oxazine (31)

Light-brown crystals, yield 0.151 g (78%), m.p. 190–192 °C. <sup>1</sup>H NMR (CDCl<sub>3</sub>): δ 5.45 (H: 4, 1H, s), 5.92 (H: 2, 1H, d, *J* = 8.4 Hz), 7.14 (H: 5, 1H, d, *J* = 8.4 Hz), 7.33–7.36 (H: 6', 1H, m), 7.44–7.51 (H: 10, 5, 2H, m), 7.57–7.59 (1', 9, 7, 3H, m), 7.76–7.83 (H: 8', 7', 2H, m), 7.85–7.87 (H: 2', 2H, d, *J* = 7.8 Hz), 7.91 (H: 4', 1H, d, *J* = 8.5 Hz), 8.01 (H: 5', 1H, d, *J* = 8.2 Hz), 8.25 (H: 3'', 2H, d, *J* = 8.7 Hz), 8.32–8.38 (H: 10, 8, 2H, m) ppm. <sup>13</sup>C NMR (CDCl<sub>3</sub>): δ 56.0 (C: 4), 82.2 (C: 2), 116.4 (C: 4a), 120.1 (C: 6), 121.3 (C: 8), 123.6 (C: 3''), 125.3 (C: 7), 125.9 (C: 6'), 126.1 (C: 5), 126.3 (C: 10), 126.6 (7'), 127.0 (C: 1') 127.5 (C: 2'), 127.9 (C: 4'), 128.1 (C: 3'), 128.5 (C: 8'), 128.6 (C: 9), 129.5 (C: 5'), 132.9 (C: 4a'), 133.0 (C: 8a'), 133.9 (C: 6a), 140.3 (C: 2'), 146.2 (C: 1''), 147.9 (C: 4'),

149.1 (C: 10b) ppm. C<sub>28</sub>H<sub>20</sub>N<sub>2</sub>O<sub>3</sub> (432.47): calcd. C 77.76, H 4.66, N 6.48; found C 77.78, H 4.64, N 6.50.

##### 4.6.4. 4-(1-Naphthyl)-2-(4-nitrophenyl)-2,3-dihydro-1H-naphth[2,1-e][1,3]oxazine (32)

Yellow crystals, yield 0.156 g (80%), m.p. 197–200 °C. <sup>1</sup>H NMR (CDCl<sub>3</sub>): δ 2.87 (H: 3, 1H, s), 5.96 (H: 2, 1H, s), 6.05 (H: 4, 1H, s), 7.02–7.07 (H: 5, 8, 2H, m), 7.32 (H: 3', 1H, t, *J* = 8.1 Hz), 7.42 (H: 6, 1H, d, *J* = 8.5 Hz), 7.55–7.61 (H: 6', 8, 9, 3H, m), 7.77 (H: 3'', 2H, *J* = 8.5 Hz), 8.37 (H: 10, 1H, d, *J* = 7.5 Hz), 8.48 (H: 2', 1H, d, *J* = 8.5 Hz) ppm. <sup>13</sup>C NMR (CDCl<sub>3</sub>): δ 53.1 (C: 4), 82.2 (C: 2), 116.6 (C: 4a), 120.2 (C: 6), 121.3 (C: 2''), 124.1 (C: 2'), 124.8 (C: 3'), 125.2 (C: 10a), 125.9 (C: 8, 5), 126.1 (C: 8'), 126.5 (C: 6'), 126.6 (C: 6'), 126.5 (C: 3''), 127.7 (C: 7'), 127.8 (C: 7), 128.8 (C: 5', 9), 128.9 (C: 4') ppm. C<sub>28</sub>H<sub>20</sub>N<sub>2</sub>O<sub>3</sub> (432.47): calcd. C 77.76, H 4.66, N 6.48; found C 77.80, H 4.69, N 6.45.

#### Acknowledgement

The authors' thanks are due to the Hungarian Research Foundation (OTKA No. K 75433) for financial support.

#### References

- [1] M. Betti, *Gazz. Chim. Ital.* 30 II (1900) 310.
- [2] M. Betti, *Org. Synth. Coll.* 1 (1941) 381.
- [3] C. Cardellaccio, G. Ciccarella, F. Naso, E. Schingaro, F. Scordari, *Tetrahedron: Asymmetry* 9 (1998) 3667.
- [4] C. Cimarelli, A. Mazzanti, G. Palmieri, E. Volpini, *J. Org. Chem.* 66 (2001) 4759.
- [5] C. Cimarelli, G. Palmieri, E. Volpini, *Tetrahedron: Asymmetry* 13 (2002) 2417.
- [6] J.-X. Ji, L.-Q. Qiu, C.W. Yip, A.S.C. Chan, *J. Org. Chem.* 68 (2003) 1589.
- [7] J.-X. Ji, J. Wu, T.T.-L. Au-Yeung, C.-W. Yip, R.K. Haynes, A.S.C. Chan, *J. Org. Chem.* 70 (2005) 1093.
- [8] Y. Lu, Z. Nikolovska-Coleska, X. Fang, W. Gao, S. Shangary, S. Qiu, D. Qin, S. Wang, *J. Med. Chem.* 49 (2006) 3758.
- [9] A.Y. Shen, C.T. Tsai, C.L. Chen, *Eur. J. Med. Chem.* 34 (1999) 877.
- [10] H.R. Shaterian, H. Yarahmadi, M. Ghahang, *Bioorg. Med. Chem. Lett.* 18 (2008) 788.
- [11] H.R. Shaterian, H. Yarahmadi, M. Ghahang, *Tetrahedron* 64 (2008) 1263.
- [12] H.R. Shaterian, H. Yarahmadi, *Tetrahedron Lett.* 49 (2008) 1297.
- [13] C. Duff, J.E. Bills, *J. Chem. Soc.* (1934) 1305.
- [14] D. Tóth, I. Szatmári, F. Fülöp, *Eur. J. Org. Chem.* (2006) 4664.
- [15] I. Szatmári, D. Tóth, A. Koch, M. Heydenreich, E. Kleinpeter, F. Fülöp, *Eur. J. Org. Chem.* (2006) 4670.
- [16] Z. Turgut, E. Pelit, A. Köycü, *Molecules* 12 (2007) 345.
- [17] I. Szatmári, T.A. Martinek, L. Lázár, F. Fülöp, *Tetrahedron* 59 (2003) 2877.
- [18] I. Szatmári, T.A. Martinek, L. Lázár, F. Fülöp, *Eur. J. Org. Chem.* (2004) 2231.
- [19] Gaussian 03, Revision C.02, M.J. Frisch, G.W. Trucks, H.B. Schlegel, G.E. Scuseria, M.A. Robb, J.R. Cheeseman, J.A. Montgomery Jr., T. Vreven, K.N. Kudin, J.C. Burant, J.M. Millam, S.S. Iyengar, J. Tomasi, V. Barone, B. Mennucci, M. Cossi, G. Scalmani, N. Rega, G.A. Petersson, H. Nakatsuji, M. Hada, M. Ehara, K. Toyota, R. Fukuda, J. Hasegawa, M. Ishida, T. Nakajima, Y. Honda, O. Kitao, H. Nakai, M. Klene, X. Li, J.E. Knox, H.P. Hratchian, J.B. Cross, C. Adamo, J. Jaramillo, R. Gomperts, R. E. Stratmann, O. Yazyev, A.J. Austin, R. Cammi, C. Pomelli, J.W. Ochterski, P.Y. Ayala, K. Morokuma, G.A. Voth, P. Salvador, J.J. Dannenberg, V.G. Zakrzewski, S.A. Dapprich, D. Daniels, M.C. Strain, O. Farkas, D.K. Malick, A.D. Rabuck, K. Raghavachari, J.B. Foresman, J.V. Ortiz, Q. Cui, A.G. Baboul, S. Clifford, J. Cioslowski, B.B. Stefanov, G. Liu, A. Liashenko, P. Piskorz, I. Komaromi, R.L. Martin, D.J. Fox, T. Keith, M.A. Al-Laham, C.Y. Peng, A. Nanayakkara, M. Challacombe, P.M.W. Gill, B. Johnson, W. Chen, M.W. Wong, C. Gonzalez, J.A. Pople, Gaussian, Inc., Wallingford, CT, 2004.
- [20] J.P. Stewart, *Comp. Chem.* 10 (1989) 209.
- [21] J.P. Stewart, *Comp. Chem.* 10 (1989) 221.
- [22] W.J. Hehre, L. Radom, P.v.R. Schleyer, J.A. Pople, *Ab Initio Molecular Orbital Theory*, Wiley, New York, 1986.
- [23] A.D. Becke, *J. Chem. Phys.* 98 (1993) 1372.
- [24] T. Helgaker, M. Watson, N.C. Handy, *J. Chem. Phys.* 113 (2000) 9402.
- [25] V. Barone, J.E. Peralta, R.H. Contreras, J.P. Snyder, *J. Phys. Chem. A* 106 (2002) 5607.
- [26] SYBYL 7.3, Tripos Inc., 1699 South Hanley Rd. St. Louis, MO 63144, USA, 2006.
- [27] GaussView 2.0, Gaussian Inc., Carnegie Office Park, Building 6, Pittsburgh, PA 15106, USA.